UC Irvine

UC Irvine Electronic Theses and Dissertations

Title

Dynamic dispatch and control of hydrogen energy storage from solar power in microgrids

Permalink

https://escholarship.org/uc/item/988727cd

Author

YLL PROUS, RAMON

Publication Date

2015

Copyright Information

This work is made available under the terms of a Creative Commons Attribution License, availalbe at https://creativecommons.org/licenses/by/4.0/

Peer reviewed|Thesis/dissertation

eScholarship.org Powered by the California Digital Library
University of California

UNIVERSITY OF CALIFORNIA,
IRVINE

Dynamic dispatch and control of hydrogen energy storage from solar power in microgrids

THESIS

submitted in partial satisfaction of the requirements
for the degree of

MASTER OF SCIENCE

in Mechanical and Aerospace Engineering

by

Ramon Yll Prous

Thesis Committee:
Professor Jacob Brouwer, Chair
Professor Scott Samuelsen
Professor Faryar Jabbari

2015

© 2015 Ramon Yll Prous

DEDICATION

To my parents, Mª Teresa Prous Martí and Ramon Yll Felis, for their unconditional emotional support. Their advices have guided me and given me strength whenever I have needed it. They are the ones who encouraged and financially allowed me to study abroad and I will always be grateful for it. To my siblings, Laia and Jordi, for their cheerfulness. To my grandparents, Conxita Felis Reñé and Josep Yll Bertrán, for their optimism, modesty, and understanding. It was not until I got to live on my own that I realize how important the education I have received from them was. They are such an example to me. Also, to the rest of my family for having made me feel loved at every moment. I feel proud to be a part of them.

You can't connect the dots looking forward; you can only connect them looking backwards. So you have to trust that the dots will somehow connect in your future. You have to trust in something: your gut, destiny, life, karma, whatever. This approach has never let me down, and it has made all the difference in my life.

Steve Jobs
"Stanford Commencement Address", 2005

TABLE OF CONTENTS

LIST OF FIGURES ..... **V**

LIST OF TABLES ..... **XI**

ACKNOWLEDGEMENTS ..... **XIII**

ABSTRACT OF THE THESIS ..... **XV**

1. INTRODUCTION **1**

1.1. Overview **1**

1.2. Goals and Objectives **5**
1.2.1. Goal 5
1.2.2. Objectives 5

2. BACKGROUND **6**

2.1. Hybrid Energy Storage Systems **6**

2.2. Hydrogen Storage **17**
2.2.1. Ways to Store Hydrogen 17
2.2.1.1. Liquid Hydrogen 17
2.2.1.2. Metal Hydrides 19
2.2.1.3. Compressed Gas 21

2.3. Power-to-Gas **26**
2.3.1. Natural Gas Pipeline System 30

2.4. Literature Gaps Addressed **33**

3. APPROACH **34**

4. MODEL OVERVIEW **37**

5. MODEL IMPLEMENTATION **42**

5.1. Control Strategies **47**
5.1.1. Chiller Plant Power Manipulation 47
5.1.2. NGCC Power Manipulation 52
5.1.2.1. NGCC Turndown Efficiency Analysis 54
5.1.3. Chiller Plant Operation Manipulated (1) and NGCC Turndown (2) 56
5.1.4. NGCC Turndown (1) and Chiller Plant Operation Manipulated (2) 59

5.2. Energy Otherwise-Curtailed Assessment **62**

5.2.1. Use of RFC 62
5.2.2. Power-to-Gas 65

5.3. Maximum Amounts of Renewable Integration 67

6. RESULTS 70

6.1. Feasibility of Introducing 2 MW of Extra Solar Power to the UCI Microgrid 73
6.1.1. Best Control Strategy 75
6.1.1.1. Control Strategies Analysis 75
6.1.1.2. GHG Emissions Analysis 91
6.1.1.3. Economic Analysis 96

6.2. Renewable Integration Summary 98

7. SUMMARY AND CONCLUSIONS 109

7.1. Summary 109

7.2. Conclusions 109

8. RECOMMENDATIONS 112

9. BIBLIOGRAPHY 113

LIST OF FIGURES

Figure 1: Schematic of a PbA battery operation..... 9
Figure 2: Schematic of an ultra-capacitor concept.....11
Figure 3: Schematic of a H_2 FC concept. 13
Figure 4: Schematic of an electrolyzer concept.....14
Figure 5: Schematic of a reversible fuel cell (RFC) concept with the same cathode-electrolyte-anode materials set operating in each mode. 16
Figure 6: Absorption and desorption of hydrogen. Source: Energie Speicher.....20
Figure 7: United States Natural Gas Pipeline Network. Source: Energy Information Administration Office of Oil & Gas, Natural Gas Division, Gas Transportation Information System. 31
Figure 8: University of California, Irvine microgrid power management.....38
Figure 9: Schematic of Hydrogen Energy Storage System (HESS) model. 41
Figure 10: Dispatch of power for the month of January. Data of the year 2014 are used. 43
Figure 11: Dispatch of power for the month of June. Data of the year 2014 are used. 44
Figure 12: Dispatch of power for the month of January with all the photovoltaic being installed in 2015 available. 2014 data are used. 46
Figure 13: Dispatch of power for the month of June with all the PV being installed in 2015 available. Data of the year 2014 data are used.....46
Figure 14: Schematic of the strategy the HESS model follows in order to manipulate the chiller plant operation so as to utilize the otherwise-curtailed solar power.....48
Figure 15: Hypothetical case of the month of January where 2 times the amount of solar PV existent at UCI. The chiller plant operation is manipulated. Data of the year 2014 are used.....50
Figure 16: Hypothetical scenario where 2 times the amount of solar PV existent at UCI are installed and just the normal operation of the chiller plant is modified on January 10 and 11, 2015. Data of the year 2014 are used. 51
Figure 17: Comparison of the chiller plant operation before and after manipulating them for a hypothetical scenario with 2 times the amount of solar PV existent at UCI on January 10 and 11, 2015. Data of the year 2014 are used. 52
Figure 18: Schematic of the strategy the HESS model follows in order to turn down the NGCC operation so as to utilize the otherwise-curtailed solar power. 52
Figure 19: Hypothetical case of the month of January with 2 times the amount of solar PV existent at UCI. The NGCC Power is turned down when required. Data of the year 2014 are used. 53

Figure 20: Hypothetical scenario where 2 times the amount of solar PV existent at UCI are installed and just the NGCC Power is turned down when required on January 6 and 7, 2015. Data of the year 2014 are used. 54

Figure 21: Quadratic regression of the in-field operation efficiency values of the UCI GT [58]. 55

Figure 22: Schematic of the strategy the Hydrogen Energy Storage System model follows in order to first manipulate the chiller plant operation and, second, turn down the NGCC so as to utilize the otherwise-curtailed solar power. 57

Figure 23: Hypothetical scenario where 2 times the amount of solar PV existent at UCI are installed. First the chiller plant operation and second, the NGCC output power, are modified when required on the month of January. Data of the year 2014 are used. 57

Figure 24: Hypothetical scenario where 2 times the amount of solar PV existent at UCI are installed. First the Chiller Plant Operation and second, the NGCC output power, are modified when required on March 27 and 28, 2015. Data of the year 2014 are used. 58

Figure 25: Schematic of the strategy the HESS model follows in order to first turn down the NGCC and, second, manipulate the chiller plant operation so as to utilize the otherwise-curtailed solar power. 59

Figure 26: Hypothetical scenario where 2 times the amount of solar PV existent at UCI are installed. First the NGCC output power and second, the chiller plant operation, are modified when required for the month of January. Data of the year 2014 are used. 60

Figure 27: Hypothetical scenario where 2 times the amount of solar PV existent at UCI are installed. First the NGCC output power and second, the chiller plant operation, are modified when required on January 19 and 20, 2015. Data of the year 2014 are used. 61

Figure 28: Hypothetical scenario where 3 times the amount of solar PV existent at UCI are installed. First the chiller plant operation and second, the NGCC output power, are modified when required on April 1 and 2, 2015. The remaining otherwise-curtailed power coming from solar is converted to H_2 using a 250 KW electrolyzer. This H_2 is afterwards used to run a 180 KW FC to generate electricity again. Data of the year 2014 are used. 63

Figure 29: 2nd April of 2015 zoom of the hypothetical scenario where 3 times the amount of solar PV existent at UCI are installed. First the chiller plant operation, and second the NGCC output power, are modified when required on April 2, 2015. The remaining otherwise-curtailed power coming from solar is converted to H_2 using a 250 KW electrolyzer. This H_2 is afterwards used to run a 180 KW FC to generate electricity again. Data of the year 2014 are used. 64

Figure 30: Hypothetical scenario where 3 times the amount of solar PV existent at UCI are installed. First the chiller plant operation, and second the NGCC output power, are modified when required on January 5 and 6, 2015. The remaining otherwise-curtailed power coming from solar is converted to H_2 and to electricity again when required using a 1,800 KW FC. Data of the year 2014 are used. 65

Figure 31: Hypothetical scenario where 6 times the amount of solar PV existent at UCI are installed. First the chiller plant operation, and second the NGCC output power, are modified when required for the month of January. The remaining otherwise-curtailed power coming from solar is converted to H_2 using a 3,000 KW electrolyzer. This H_2 is blended with NG at the NG pipeline which feeds the GT. Data of the year 2014 are used. 66

Figure 32: Zoom of the hypothetical scenario where 6 times the amount of solar PV existent at UCI are installed. First the chiller plant operation, and second the NGCC output power, are modified when required on January 15 and 16, 2015. The remaining otherwise-curtailed power coming from solar is converted to H_2 using a 3,000 KW electrolyzer. This H_2 is blended with NG at the NG pipeline which feeds the GT. Data of the year 2014 are used. 67

Figure 33: 2015 UCI dispatch of power for the month of January. Neither the NGCC nor the chiller plant operation is modified. 71

Figure 34: 2015 UCI dispatch of power for the month of June. Neither the NGCC nor the chiller plant operation is modified. 72

Figure 35: June 25, 2015 daily loads. Neither the NGCC nor the Chiller Plant Operation is modified. 73

Figure 36: UCI dispatch of power for the month of January with all the PV being installed in 2015 available. Neither the NGCC nor the chiller plant operation is modified. 2015 data is used. 74

Figure 37: UCI dispatch of power for the month of June with all the PV being installed in 2015 available. Neither the NGCC nor the chiller pant operation is modified. 2015 data is used. 74

Figure 38: Hypothetical scenario where 2 extra MW are added to the 3.575 MW of solar power existent at the UCI microgrid for the month of January. Just the chiller plant operation is manipulated. Data of the year 2015 are used. 75

Figure 39: Bar graph of the increased chiller plant capacity vs. number of hours they need to do so when following the strategy of just manipulating the chiller plant operation. Data of the year 2015 are used. 76

Figure 40: Typical day (i.e. day with normal TES storage) of the year for the hypothetical scenario where 2 extra MW are added to the 3.575 MW of solar power existent at the UCI microgrid. Just the chiller plant operation is manipulated. Data of the year 2015 are used. 77

Figure 41: Worst day (i.e. day with higher TES storage) of the year for the hypothetical scenario where 2 extra MW are added to the 3.575 MW of solar power existent at the UCI microgrid. Just the chiller plant operation is manipulated. Data of the year 2015 are used. 77

Figure 42: Hypothetical scenario where 2 extra MW are added to the 3.575 MW of solar power existent at the UCI microgrid for the month of January. Just the NGCC operation is turned down when required. Data of the year 2015 are used....78

Figure 43: Bar graph of the NGCC power before and after manipulating its operation vs. number of hours the NGCC operates at each of the power outputs when following the strategy of just turning down the NGCC. Data of the year 2015 are used. 79

Figure 44: Bar graph of the NGCC turndown power vs. number of hours it is needed to do so when following the strategy of just turning down the NGCC. Data of the year 2015 are used....80

Figure 45: Typical day of the year for the hypothetical scenario where 2 extra MW are added to the 3.575 MW of solar power existent at the UCI microgrid. Just the NGCC is turned down when required. Data of the year 2015 are used. 81

Figure 46: Worst day of the year for the hypothetical scenario where 2 extra MW are added to the 3.575 MW of solar power existent at the UCI microgrid. Just the NGCC is turned down when required. Data of the year 2015 are used. 81

Figure 47: Hypothetical scenario where 2 extra MW are added to the 3.575 MW of solar power existent at the UCI microgrid for the month of March. First, the chiller plant operation is manipulated and, second, the NGCC operation is turned down when required. Data of the year 2015 are used. 82

Figure 48: Bar graph of the increased chiller plant capacity vs. number of hours they need to do so when following the strategy of manipulating the chiller plant operation first and then turning down the NGCC when required. Data of the year 2015 are used....83

Figure 49: Bar graph of the NGCC power before and after manipulating its operation vs. number of hours the NGCC operates at each of the power outputs when following the strategy of manipulating first the chiller plant operation and then turning down the NGCC when required. Data of the year 2015 are used. 84

Figure 50: Bar graph of the NGCC turndown power vs. number of hours it is needed to do so when following the strategy of manipulating first the chiller plant operation and then turning down the NGCC when required. Data of the year 2015 are used....84

Figure 51: 2 typical days of the year for the hypothetical scenario where 2 extra MW are added to the 3.575 MW of solar power existent at the UCI microgrid. First, the chiller plant operation is manipulated and, second, the NGCC operation is turned down when required. Data of the year 2015 are used. 85

Figure 52: Worst day (i.e. day with higher NGCC turndown) of the year for the hypothetical scenario where 2 extra MW are added to the 3.575 MW of solar power existent at the UCI microgrid. First, the chiller plant operation is manipulated and, second, the NGCC operation is turned down when required. Data of the year 2015 are used. 86

Figure 53: Hypothetical scenario where 2 extra MW are added to the 3.575 MW of solar power existent at the UCI microgrid for the month of January. First, the chiller plant operation is manipulated and, second, the NGCC operation is turned down when required. Data of the year 2015 are used. 87

Figure 54: Bar graph of the NGCC power before and after manipulating its operation vs. number of hours the NGCC operates at each of the power outputs when following the strategy turning down the NGCC first, and then manipulating the chiller plant operation when required. Data of the year 2015 are used. 88

Figure 55: Bar graph of the NGCC turndown power vs. number of hours it is needed to do so when following the strategy of turning down the NGCC first, and then manipulating the chiller plant operation when required. Data of the year 2015 are used. 88

Figure 56: Bar graph of the increased chiller power capacity vs. number of hours they need to do so when following the strategy of turning down the NGCC first, and then manipulating the chiller plant operation when required. Data of the year 2015 are used. 89

Figure 57: Typical day of the year for the hypothetical scenario where 2 extra MW are added to the 3.575 MW of solar power existent at the UCI microgrid. First, the NGCC operation is turned down when required and, second, the chiller plant operation is manipulated. Data of the year 2015 are used. 90

Figure 58: Worst day of the year for the hypothetical scenario where 2 extra MW are added to the 3.575 MW of solar power existent at the UCI microgrid. First, the NGCC operation is turned down when required and, second, the chiller plant operation is manipulated. Data of the year 2015 are used. 90

Figure 59: Hypothetical scenario where 30.585 MW extra are added to the 3.575 MW of solar power existent at the UCI microgrid for the month of February. The chillers store as much energy as possible and the NGCC is turned up to MO the whole time. Data of the year 2015 are used. 99

Figure 60: Hypothetical scenario where 30.585 MW extra are added to the 3.575 MW of solar power existent at the UCI microgrid for the month of February. The chillers store as much energy as possible and the NGCC is turned up to MO the whole time. The otherwise-curtailed power is converted into H_2 so as to be used afterwards to run a 2 MW PEM FC when required. Data of the year 2015 are used. 100

Figure 61: Amount of H_2 that can be blended with Natural Gas into the NG pipeline. 104

Figure 62: Hypothetical scenario where 30.585 MW extra are added to the 3.575 MW of solar power existent at the UCI microgrid for the month of February. The chillers store as much energy as possible and the NGCC is turned down up to MO the whole time. The otherwise-curtailed power is converted into H_2 and injected intoto the NG pipeline that feeds the GT. Data of the year 2015 are used. 106

Figure 63: 11th of February of the hypothetical scenario where 30.585 MW extra are added to the 3.575 MW of solar power existent at the UCI microgrid. The chillers store as much energy as possible and the NGCC is turned down up to MO the whole time. The otherwise-curtailed power is converted into H_2 and injected into the NG pipeline that feeds the GT. Data of the year 2015 are used. 106

Figure 64: Hypothetical scenario where 30.585 MW extra are added to the 3.575 MW of solar power existent at the UCI microgrid for the month of February. The chillers store as much energy as possible and the NGCC is turned down up to MO the whole time. The otherwise-curtailed power is converted into H_2 and used afterwards to run a PEM FC and smooth the imported electricity. The remaining H_2 is injected into the NG pipeline that feeds the GT. Data of the year 2015 are used. 107

Figure 65: 11th of February of the hypothetical scenario where 30.585 MW extra are added to the 3.575 MW of solar power existent at the UCI microgrid. The chillers store as much energy as possible and the NGCC is turned down up to MO the whole time. The otherwise-curtailed power is converted into H_2 and used afterwards to run a PEM FC and smooth the imported electricity. The remaining H_2 is injected into the NG pipeline that feeds the GT. Data of the year 2015 are used. 108

LIST OF TABLES

Table 1: Volumetric and gravimetric efficiencies of liquefied hydrogen, compressed hydrogen, and hydrogen stored in solid structures at specific ranges of pressures and temperatures [31]. 17

Table 2: Energy Density of several fuels [36]. 21

Table 3: Principal Natural Gas Pipeline Companies Serving the Western Region. 32

Table 4: UCI plant chillers sizes and efficiencies. 39

Table 5: Current Solar Generation sites and capacities of all the UCI solar photovoltaic installations. 45

Table 6: Individual and overall UCI Central Plant electric chillers characteristics. 49

Table 7: GHG emissions from solar photovoltaic power for each of the different strategies proposed for the hypothetical case where 2 MW of extra solar power are added to the 3.575 MW currently existing in the microgrid. Data of the year 2015 are used. 91

Table 8: GHG emissions from the Gas Turbine for each of the different strategies proposed for the hypothetical case where 2 MW of extra solar power are added to the 3.575 MW currently existing in the microgrid. Data of the year 2015 are used. 92

Table 9: Number of pounds of CO_2 produced from different fuels, the average heat rates for steam-electric generators in 2013 using those fuels, and the resulting amount of CO_2 produced per kW [66]. 93

Table 10: GHG emissions from SCE Import for each of the different strategies proposed for the hypothetical case where 2 MW of extra solar power are added to the 3.575 MW already installed in 2015. Data of the year 2015 are used. 94

Table 11: Total GHG emissions for each of the different strategies proposed for the hypothetical case where 2 MW of extra solar power are added to the 3.575 MW already installed in 2015. Data of the year 2015 are used. 95

Table 12: Economic difference between operating the NGCC at current levels and with 2 MW of extra solar PV power. Data of the year 2015 are used. 96

Table 13: Economic difference between operating the NGCC at current levels and with 2 MW of solar power extra. Data of the year 2015 are used. 97

Table 14: Maximum renewable integration with and without ES systems. The two strategies proposed are analyzed individually and together. Data of the year 2015 are used. 98

Table 15: Amount of hydrogen that can be blended with Natural Gas into the NG pipeline every month from January to June, 2015 supposing concentrations of

0.2, 5, 10, and 15% of hydrogen by volume. The maximum and minimum amounts of H_2 are presented. Data of the year 2015 are used. 103

Table 16: Overall demand renewable energy contribution when blending a 0.2, 5, 10, and 15% of hydrogen by volume into the natural gas pipeline system. Data of the year 2015 are used. 105

ACKNOWLEDGEMENTS

First and foremost, I would like to express my sincere gratitude to the Advanced Power and Energy Program (APEP) at the University of California, Irvine for letting me fulfill my desire to study in the United States of America. Specially, I would like to thank both Professor Jacob Brouwer and Professor Scott Samuelsen for their guidance. The success and final outcome of this MS Thesis required a lot of direction and assistance from them. On one hand, Professor Brouwer's strong leadership, consistent desire for perfection, organization, intelligence, good sense of humor, and outstanding professional and social skills create an environment in which one feels comfortable and willing to work. I feel fortunate to have had him as my advisor. As one of his students, I have learnt more than just the theoretical concepts he has taught me throughout the two years I have known him. He has served and will keep serving as a model and inspiration to me. On the other hand, Professor Samuelsen, director of APEP, creates a unique atmosphere wherein diverse research topics can be pursued simultaneously. His pragmatic and experienced opinions have always been a valuable input to me.

Special thanks to Professor Faryar Jabbari for all the knowledge he imparted on me and for kindly agreeing to review this work as part of my thesis committee. Moreover, thanks to all of those who have shared the EG3111 laboratory with me: Siavash Ebrahimi, Ali Hatamizadeh, Ali Azizi, Adrià Carmona, Lorenzo Menghini, Alessio Coracci, and Àlex Peracaula. All of them are part of my success, too. I do also recognize the support I have received from the rest of APEP students and staff. Without them, the goals accomplished by the department would not be possible.

Thanks to my family for their unconditional encouragement, support, and love. This work would not be possible without them either.

Furthermore, I am grateful to all the friends and people I have met while studying at the University of California, Irvine. Everyone needs to disconnect from time to time from working and I have been able to do so by sharing great moments with all of them. Also, I want to thank for their valuable suggestions all the friends I have in Catalunya, with whom I have kept contact with.

Finally, I greatly acknowledge the funding of the Balsells-Generalitat de Catalunya fellowship program.

ABSTRACT OF THE THESIS

Dynamic dispatch and control of hydrogen energy storage from solar power in microgrids

by

Ramon Yll Prous

Master of Science in Mechanical and Aerospace Engineering

University of California, Irvine, 2015

Professor Jacob Brouwer, Chair

To evaluate the impacts and capabilities of deploying a combination of reversible fuel cells and hydrogen storage in a microgrid as a community energy storage option for mitigating power intermittency associated with a high-penetration of renewable photovoltaic resources, dynamic system models for compressed hydrogen energy storage have been developed and applied. The option of hydrogen storage tanks or injection and mixing of the hydrogen into the natural gas pipeline is presented and considered in the simulations as a means of storing the otherwise-curtailed solar power. With 15-minute resolution experimental data from the operating microgrid of the University of California, Irvine, control strategies that would facilitate the dynamic operation of existing generation, load and storage resources (e.g., a gas turbine, steam turbine, chillers, thermal energy storage) are used to project the utility and applicability of hydrogen energy storage. Results show that, by turning down the co-gen cycle as much as possible and manipulating the operation

of the chiller plant in order to thermally store the otherwise-curtailed solar energy during the day, the renewable integration of the microgrid could be increased from the current 3.48% to a total of 8.52%.

Special attention is given to those scenarios were the procurement from eligible renewable energy resources is increased in order to meet the future energy goals for the State of California. It is demonstrated how this goal can be easier to accomplish by dynamically dispatching the chiller plant, the co-gen cycle, and using Power-to-Gas techniques.

1. Introduction

1.1. Overview

Energy, which is present in transportation fuels, electricity, heating, etc., is central to enabling increased quality of life since it has historically become progressively more reliant on goods and services which require more and more energy. An increase of the energy consumption is afterwards translated into more greenhouse gas (GHG) emissions since most of the energy consumed nowadays comes from fossil fuel combustion. This leads to increased globally average temperatures, more intense localized temperature extremes, sea level rise, more intense storm and drought events, and other significant changes in earth system climate. Also, although regulations have caused significant progress, combustion of fossil fuels still produces a lot of criteria pollutant emissions which degrade air quality and render it unhealthy to breathe. Solutions to these matters exist, but the pathway towards sustainability is not straightforward. Energy efficiency and multitasking has helped slow some of these trends, but per-capita, energy use is still increasing due to population growth occurrence in previously low-energy intensity areas.

It is necessary to understand the current workings of the electric infrastructure to determine how it must evolve to accommodate low-carbon electric power sources. Internet technology and the reality of renewable energy are creating a new type of electrical grid, one in which energy is stored and distributed on an individual basis. As well as at the present time human beings create their own information and share it on the internet, soon they will be generating and sharing all the green energy they require in their homes, offices, and factories. In just a few years, millions of buildings and even cities will become

energy self-sufficient since the electrical distribution system will be undergoing a major evolution. Yinger et al. [1] pointed out that federal and state policy makers have recognized the need for a smarter, more robust to microgrids electricity infrastructure to accommodate greater amounts of renewable generation, electricity used as a fuel for vehicles, and technologies and programs that enable consumers to become active participants in the energy supply chain. To achieve this, the way to further the knowledge in this area is none other than throughout research and signaling the end of our reliance on fossil fuels, which is getting closer since they are starting to run out and people are getting more conscious about the consequences their use have in our environment.

United States today's electrical system is complex, fragile, and must rapidly raise and lower its outputs to meet changing demand for electricity. This means that rarely, if ever, operates at maximum efficiency. As a result, a huge amount of energy is wasted by the grid and this hurts the competitiveness and economy of the country. Moreover, by some estimates, the nation will need somewhere between 4 and 5 tera kilowatt-hours of electricity annually by 2050 [2]. It is easy to see that the problem is not easy to solve in a nation where the average population density is six or seven times smaller than the population density of the nowadays considered world leader countries for energy efficiency, such as Germany. That is to say that replacing the USA current electrical grid, even if it is necessary (in some places is about fifty years old), is extremely expensive and will not solve the problem the country is facing. It will just blur it since it will appear again sooner or later. Therefore, it is worth spending money in investigating alternative solutions to obtain many electrical benefits to utilities and consumers and an overall greater

efficiency. A greater efficiency translates afterwards into less pollution, lower prices, and more reliable power.

Smart grid is based on a modernized electrical grid computer-based remote control and automation that gathers and acts on information about the behaviors of suppliers and consumers. It is made possible by the integration of high-technological devices that allow a two-way communication technology and computer processing that has been used for decades in other industries. These devices optimize the electrical service and help customers taking the appropriate energy decisions. Thus, smart grid goal is to develop and deploy a more reliable, secure economic, efficient, safe, and environmentally friendly electric system. This vision covers all facets of energy, from its production to its efficient use in homes, businesses, and vehicles.

A microgrid is the indispensable infrastructure of nowadays smart grid. It is a semiautonomous grouping of generating sources that are placed and operated for the benefit of its customers. It can also be defined as a local energy grid with control capability, which means that it can disconnect from the traditional grid and operate on its own using local energy generation in times of crisis like storms or power outages, or for other reasons. This backup provided for the grid can be very useful in some critical facilities, such as in hospitals or military forts, where energy supply has to be guaranteed so as to have a thriving performance of the center. Moreover, a microgrid allows communities to be more energy independent and, in most of the cases, more environmentally friendly.

The most important feature of a microgrid is that the generating sources that constitute it are interconnected by micro-source controllers to the electrical distribution network.

Therefore, the main requirement of the generation sources used in microgrids is centered in its interconnection by means of power electronic devices. These devices maintain energy balance and power quality through passive plug and play power electronic features that allow operation without tight central active control or fast communication. Moreover they can be connected and disconnected without reconfiguring the equipment.

However, fluctuation and intermittence resulted from unstable micro-sources and nonlinear loads will execute considerable impacts on normal operation of a microgrid [3]. Energy storage technology is the solution to that issue as it provides energy when it is needed just as transmission provides energy where it is needed. Furthermore, energy storage decouples generation from demand and stabilizes load curves, distribution, and the transmission of electricity. Energy storage allows the integration of renewable energies, which derive in a demand and cost reduction. A microgrid can be powered by distributed generators, batteries, capacitors, fuel cells, and other renewable resources like solar panels. That is the reason why the global revenue for energy storage in microgrids will grow from $662 million in 2014 to more than $4 billion in 2024, according to Navigant Research [4].

1.2. Goals and Objectives

1.2.1. Goal

The goal of this thesis is to evaluate the impacts and capabilities of deploying a combination of reversible fuel cells and hydrogen storage in a microgrid as a community energy storage option for mitigating power intermittency associated with a high-penetration of renewable photovoltaic resources.

1.2.2. Objectives

The following objectives have been established to achieve the goal:

1. Accomplish a literature review that thoroughly examines reversible fuel cells and hydrogen energy storage technology for use with high renewable use.
2. Obtain 15-minute resolution experimental data from the operating microgrid of the University of California, Irvine.
3. Develop a dynamical physical model of the University of California, Irvine microgrid operation control.
4. Apply the model to parametric variations according to specific case scenarios.
5. Include compressed Hydrogen Energy Storage System (HESS) in the model.
6. Analyze results and propose new ways of operating the microgrid in order to increase its renewable energy penetration.

2. Background

2.1. Hybrid Energy Storage Systems

Sunlight is by far the predominant source, and it contains a surprisingly large amount of energy. On average, solar radiation reaches Earth with more than enough energy in a single square meter to illuminate five 60-watt light bulbs if all the sunlight could be captured and converted to electricity [5]. As the sun warms the planet's surface, the atmosphere warms too. Some parts of the Earth receive direct rays from the sun all year and are always warm. Other places receive indirect rays, so the climate is colder. Warm air rises because it weighs less than cold air, causing a movement of air that makes the wind blow and therefore, that allows us to obtain energy from wind turbines. Solar energy also evaporates water that falls as rain and builds up behind dams, where its motion is used to generate electricity via hydropower. Moreover, the sun is what allows the existence of fossil fuels. When sunlight strikes a plant, some of the energy is trapped through photosynthesis and is stored in chemical bonds as the plant grows. This energy can be recovered months or years later by breaking the chemical bonds (burning wood is an example). More often, though, the stored energy is used in the much more concentrated forms that result when organic matter, after millions of years of geological and chemical activity underground, turns into fossil fuels, such as coal, oil, or natural gas. Either way, we are reclaiming the power of sunlight.

Nevertheless, since sunlight is intermittent we cannot rely on it when wanting to completely meet the demand using only the energy it releases. Neither can we waste all the energy coming from the sun that exceeds the amount needed in every moment. Thus, it has

to be converted into another type of energy so as to be used when required (i.e., when there is not enough energy coming from the sun). As the amount of power produced from renewable resources increases, storing it for later use is a worldwide challenge. Energy storage systems are widely used and known. They can provide frequency regulation, alleviate transmission congestion, defer costs of new construction, provide load shifting, and/or reduce "time of use" and demand charges [6]. There are two different types of energy storage systems; those that have energy and power decoupled one from another (e.g., Hydrogen and the fuels cells or natural gas and gas turbines) and those that have energy and power coupled (e.g., batteries or ultra-capacitors). On one hand, when energy and power are decoupled a large storage capacity to accommodate massive energy storage for not only daily load shifting but also for seasonal shifting can be obtained. On the other hand, when energy and power are coupled the system can just give response to small amounts of power. As a result, the power quality is poor.

In addition to the environmental and sustainable benefits renewable energies provide, they constitute an ancillary support to electrical networks. Nevertheless, any time a reliance on renewable energy or intermittent energy without a grid tie appears, some sort of storage is required. Energy storage systems that have energy and power coupled are classified in two major groups depending on their discharge timescale (long, such as batteries, or short, such as ultra-capacitors or super-capacitors) [7]. The ones that have a long discharge timescales (up to 24h) are employed for energy management purposes, whereas the ones with short discharge timescales (seconds to hours) are practical for bridging power applications. Since the different energy storage systems technologies that are currently available are not enough to satisfy the wide frequency spectrum of the generated energy, the use of a hybrid

energy storage systems is necessary in order to make the overall system more immune to perturbations [8]. Hybrid energy storage systems are characterized by containing more than one electrical generation technology that contributes in increasing the overall efficiency of the system up to 90% [9]. Batteries and ultra-capacitors are the main devices developed at the moment to store energy.

A battery is a device that is able to store electrical energy in the form of chemical energy, and convert that energy into electricity. They are rechargeable; they are designed so that electrical energy from an outside source can be applied to the chemical system, and reverse its operation, restoring the battery's charge. As shown in Figure 1, batteries basically have three parts: a negative (-) electrode, a positive (+) electrode, and an electrolyte that separates chemically these two terminals. The electrolyte is a chemical medium that allows the flow of electrical charge between the cathode and anode. Even though the electrolyte represented is aqueous, it can be different depending on the type of battery. When a device is connected to a battery chemical reactions occur at the double layer that create a flow of electrical energy to the device. The double-layer region is where the truncation of the metal's electronic structure is compensated for in the electrolyte [10]. It can also be understood as the region where the electrode and electrolyte interact and therefore, where all the electrochemical reactions occur. So, the current produced, is directly proportional to the area of the interface and that is the reason why current density is more fundamental than current. Thus, it makes more sense to know the current per unit area than the current itself

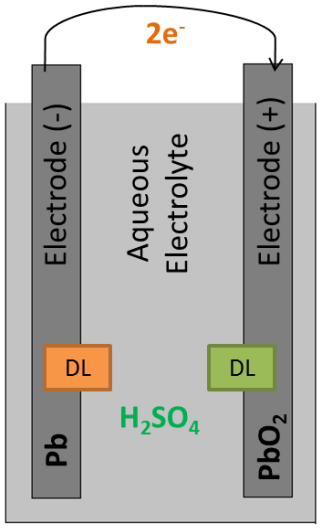

Figure 1: Schematic of a PbA battery operation.

Lead acid (PbA) batteries are extremely well-known and used in microgrids, but they do have issues. They are toxic and very heavy, and they require maintenance. Lithium-based batteries offer many advantages to answer these performance issues. Lower weight and volume ratios compared to power output are additional benefits. Lithium-titanate battery technology offers high power, fast charge and discharge rates, and long life, plus a superior power to weight ratio over the conventional lithium-ion batteries [11]. Nevertheless, they are approximately five times more expensive than PbA batteries. Hittinger et al. [12], who evaluated the value of batteries in microgrid electricity systems, showed that the Aqueous Hybrid Ion (AHI) battery chemistry appears to be a better complement to solar PV, and scenarios that do not require constant cycling of the batteries strongly favor PbA. They also said that in order to reduce the levelized cost of the electricity microgrids have to be designed differently according to whether they use AHI or PbA batteries. However, the type of battery used in a microgrid depends on the design of it and on what is preferred.

On the other hand, ultra-capacitors have become the best choice for dynamic power compensation to improve the stability of microgrids [13]. The electric double-layer capacitor effect was first noticed in 1957 by General Electric engineers experimenting with devices using porous carbon electrode. However, it was not until 1966 that the modern version of the devices was eventually developed by researchers at Standard Oil of Ohio [14]. They work in a similar way than capacitors but instead of having a solid dielectric between the two electrodes they consist of two electrodes separated by an ion permeable membrane (separator), and an electrolyte electrically connecting both electrodes. When the electrodes are polarized with an applied voltage, ions in the electrolyte form electric double layers of opposite polarity to the electrode's polarity. The charged ions and the electrodes act as two conventional capacitors with an effective thickness exceedingly thin (double layer), and because of the porous nature of the carbon the surface area is extremely high, which translates to a very high capacitance [14]. Figure 2 shows it all graphically.

Additional, depending on electrode material and surface shape, more or less ions may permeate the double layer becoming specifically adsorbed ions and contribute with pseudo-capacitance to the total capacitance of the ultra-capacitor. Consequently, although capacitors have the ability to store energy at a very fast rate, they have a low energy density. In order to keep taking advantages of their rapid charge and discharge cycles rather than long term compact energy storage while solving the low energy per unit volume or mass they have, super-capacitors or ultra-capacitors are required. Nevertheless, their energy density is still lower than that of lead-acid battery [15, 16].

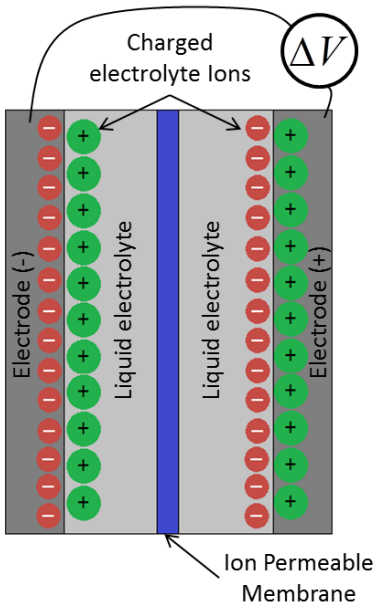

Figure 2: Schematic of an ultra-capacitor concept.

Hydrogen's use has been rising constantly throughout the last years. It can be produced using diverse, domestic resources, using a wide range of processes. As an energy carrier, primarily derived from water, it can address issues of sustainability, environmental emissions, and energy security [17]. It can also be used for other purposes, such as a fuel for transportation, as well as a medium to long term energy storage. In microgrids hydrogen subsystems are adopted. These consist of a fuel cell, a water electrolyzer, and hydrogen storage capability, among others. A refueling system is added if hydrogen is to be used for transportation. Some of the advantages observed when using hydrogen subsystems are: low noise level, potential for high energy density storage, seasonal energy storage without energy loss over time, ability to handle power fluctuations and therefore ideal for integration with renewable energy storage systems, potential for low and predictable operation and maintenance costs, and reduced environmental impact compared to conventional energy sources [18].

Hydrogen fuel cells are the ultimate power generation devices which technology offers a unique potential for efficient energy conversion with low pollutant emissions [19]. Unlike batteries, which must be thrown away or plugged in for a time-consuming recharge, fuel cells allow easy independent scaling between power and capacity and can be quickly recharged by refueling. But fuel cells not only provide a cleaner and more resilient power production. They also are a highly efficient and suitable alternative for a large number of applications. For this reason, universities, energy companies such as *Bloom Energy*, and independent power producers have been and are researching and advancing the fuel cell systems. At the present time several governments, the military, and top companies such as *Walmart*, which has 500 fuel cell units in operation at several warehouses, have already adopted this innovative technology.

Figure 3 shows how a FC works. It can be observed how the anode of a FC is fed with fuel (i.e., H_2), while the cathode electrode is fed with oxidant (i.e., O_2). Oxidation, which takes part at the anode, refers to a process in which electrons are removed from a species and delivered to the electric circuit. On the other hand, reduction, which occurs at the cathode, refers to a process in which electrons provided by the electric circuit are added to a species. A catalyst is often used to speed up the reactions at both electrodes. Every fuel cell also has an electrolyte layer as shown in the figure debajo de which spatially separates the electrodes and permits the appropriate ions to pass between them.

The current (electricity) produced by a fuel cell scales with the size of the triple phase boundary (TPB), the reaction area where the reactants, the electrode, and the electrolyte meet. The TPB is where all the electrochemical reactions occur. Larger TPB surface areas

translate into larger currents. As in the double layer of the batteries, the current produced, is directly proportional to the area of the interface.

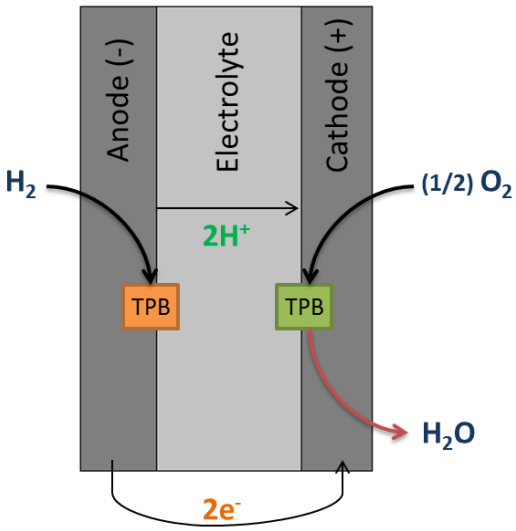

Figure 3: Schematic of a H_2 FC concept.

There are five major types of fuel cells, differentiated from one another according to the 2 nature of the electrolyte they use. Each type requires different materials and fuels and is suitable for different applications. The most important ones are the Polymer Electrolyte Membrane Fuel Cell (PEMFC) and the Solid Oxide Fuel Cell (SOFC). However, due to low working temperature, fast startup, extremely low emission, and very low noise among different type of fuel cells, PEM fuel cell are the best candidates for microgrid applications [20, 21].

Pike Research, one of the market research and consulting firms that provides in-depth analysis of global clean technology markets, has estimated that the stationary fuel cell market will reach 50 GW by 2020 [22]. Thus, as retail electricity prices creep up and many renewable sources of power decline in cost, fuel cells are inching closer to being a realistic

power option, particularly at the microgrid level. Phosphoric acid cells are commercially available in the 200 kW range, and high temperature solid-oxide fuel cells (SOFC) and molten-carbonate fuel cells (MCFC), as well as low temperatures ones such as proton exchange membrane (PEMFC), have been demonstrated and are particularly promising for microgrid applications. Actually though, all types of fuel cells could play a role. It all depends on what is preferred in the microgrid. High temperature fuel cells are used if a high efficiency is desired. Instead, if a quick start or fast dynamics are wanted, low temperature fuel cells are more suitable.

There exist different ways to obtain hydrogen using power. The overall process of electrolysis is the reverse process of a fuel cell. In electrolysis, an electric current applied to water (for example) produces hydrogen and oxygen. The reaction that takes part in an electrolytic cell is not spontaneous, whereas the one that takes part in a galvanic cell, such as a fuel cell, is. An electrolyzer, represented in Figure 4, is an electrochemical energy conversion device designed to perform electrolysis.

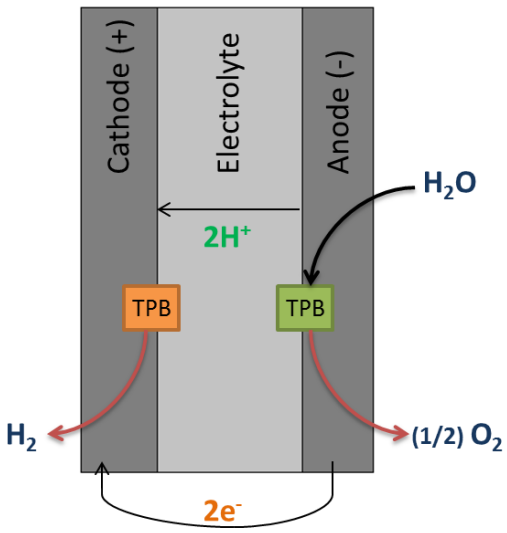

Figure 4: Schematic of an electrolyzer concept.

Reversible fuel cells (RFC) combine voltaic and electrolytic capabilities by utilizing a single bi-functional electrode-electrolyte set that can alternate between the two different modes of operation as Figure 5 shows debajo de. If for example a RFC is used to store the otherwise-curtailed power from a given solar PV installation, during the day it will operate in the electrolyzer mode, converting solar energy into chemical energy in the form of H_2. At night it will switch into its fuel cell mode and will convert the chemical energy stored in hydrogen back into electricity. Compared with batteries, there is the disadvantage of lower turnaround efficiency with hydrogen production through water electrolysis as the first step and subsequent reconversion to electric power or the use of the hydrogen as fuel. On the other hand, gas storage provides capacities that are out of reach of battery storage. Furthermore, it is suitable for weekly and even seasonal storage [23].

Maclay et al. [24], who assessed the viability of employing a RFC as an energy storage device to be used with photovoltaics (PV) electrical generation in renewable residential applications, concluded that employing a RFC with batteries in a hybrid configuration increased PV utilization and both battery efficiency and power density.

Hydrogen is stored in gas or metal tanks. Metal hydride tanks are more expensive, but offer high safety against accidents [18]. Salt caverns made by hydraulic underground mining are also used as the literature shows [25]. Although fuel cells and electrolyzers are usually used and designed separately, they can be combined as what is known as reversible fuel cells (RFC). Therefore, RFC combine voltaic and electrolytic capabilities by utilizing a single bi-functional electrode set that can alternate between the two different modes of operation.

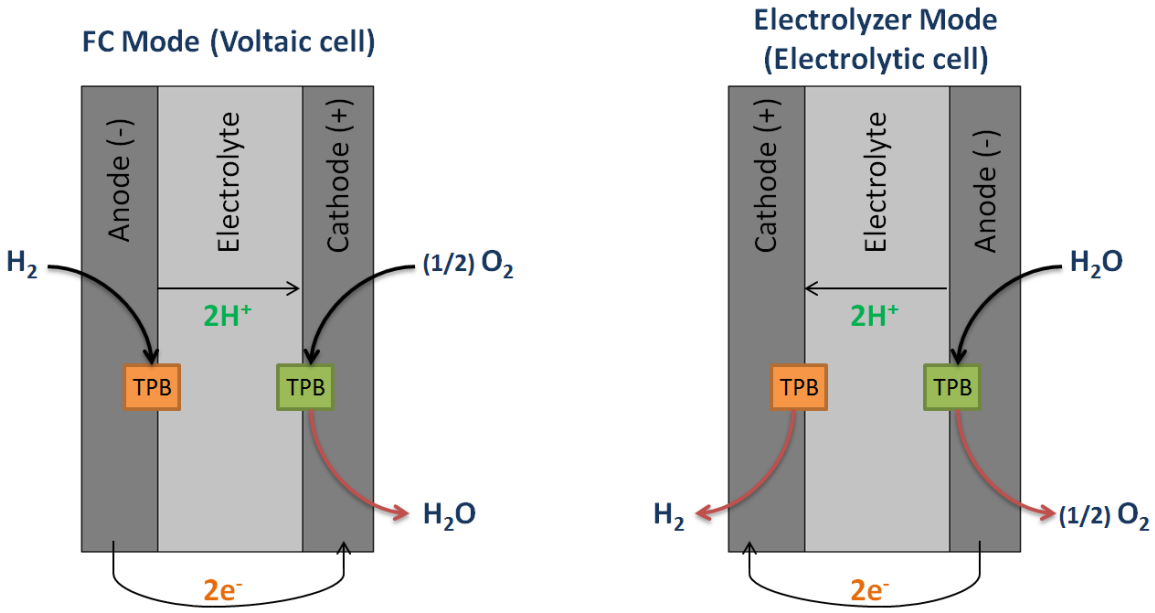

Figure 5: Schematic of a reversible fuel cell (RFC) concept with the same cathode-electrolyte-anode materials set operating in each mode.

Solar-hydrogen production can be accomplished via a number of different technologies including photovoltaic-electrolysis systems, direct solar thermal splitting of water, methane or hydrogen sulphide, photo-electrochemical processes, photo-enzymatic processes using hydrogenases, and photo-biological processes [26]. Production of hydrogen from water electrolysis becomes an interesting option when combined with renewable electricity in markets with high solar and wind penetration [27, 28]. Even though the cost to operate these devices is still challenging nowadays -which is one of the reasons why they are not more used- Gibson et al. [29] said that based on the increase in efficiency and the decreasing future PV system costs (a doubling of cumulative production and 20% price decrease has occurred every 2.5 years) that have been forecast based on trends in photovoltaic technology, the cost to generate a given amount of hydrogen could decrease by a factor of 5 or more within the next 15 years.

2.2. Hydrogen Storage

2.2.1. Ways to Store Hydrogen

About the current worldwide hydrogen production, 77% is produced from oil and gas, 18% comes from coal and the other 4% via electrolysis [30]. However, the electrolysis hydrogen production approach is gaining importance and has been attracting more attention in recent years, primarily because of its potential use with renewable power input.

There are basically three different ways of storing hydrogen: liquid hydrogen, metal hydrates storage, and compressed gas storage [31]. Table 1 shows how the volumetric and gravimetric efficiencies of these three methods vary under specific conditions of pressure and temperature.

Table 1: Volumetric and gravimetric efficiencies of liquefied hydrogen, compressed hydrogen, and hydrogen stored in solid structures at specific ranges of pressures and temperatures [31].

	$\rho\ \left[\frac{kg}{m^3}\right]$	x [%]	Pressure [bar]	Temperature [K]
Compressed Gas	57	4 – 6	700	Standard Temp. (298)
Liquid Hydrogen	71	14	Standard P. (1)	20 – 21
Metal Hydrides	150 – 200	2 – 10	Standard P. (1)	Standard Temp. (298)

2.2.1.1. Liquid Hydrogen

To exist as a liquid, H_2 must be cooled below hydrogen's critical point of 33 K. However, for hydrogen to be in a full liquid state without evaporating at atmospheric pressure, it needs

to be cooled to 20.28 K. Liquefaction processes use a combination of compressors, heat exchangers, expansion engines, and throttle valves to achieve the desired cooling. The simplest liquefaction process is the Linde cycle or Joule-Thompson expansion cycle. In this process, the gas is compressed at ambient pressure. Then is cooled in a heat exchanger, before passing through a throttle valve where it undergoes an isenthalpic Joule-Thompson expansion, producing some liquid. This liquid is removed and the cool gas is returned to the compressor via the heat exchanger [32].

Hydrogen molecules exist in two forms, para and ortho, depending on the electron configurations in the two individual hydrogen atoms [33]. At hydrogen's boiling point of 20 K the equilibrium concentration is almost all para-hydrogen, but at room temperature or higher, the equilibrium concentration is 25% para-hydrogen and 75% ortho-hydrogen. The uncatalyzed conversion from ortho to para-hydrogen proceeds very slowly, so without a catalyzed conversion step, the hydrogen may be liquefied, but may still contain significant quantities of ortho-hydrogen. This ortho-hydrogen will eventually be converted into the para-form in an exothermic reaction, releasing a significant amount of heat (527 KJ/Kg) [33]. If ortho-hydrogen remains after liquefaction, this heat of transformation will slowly be released as the conversion proceeds, resulting in the evaporation of as much as 50% of the liquid hydrogen over about 10 days. This means long-term storage of hydrogen requires that the hydrogen be converted from its ortho form to its para form to minimize boil-off losses, which can be accomplished using a number of catalysts. The heat released in the conversion is usually removed by cooling the reaction with liquid nitrogen because it requires less energy to liquefy than hydrogen and still cools the hydrogen enough to achieve an equilibrium concentration of roughly 60% para-hydrogen [34].

A major concern in liquid hydrogen storage is minimizing hydrogen losses from liquid boil-off. Because liquid hydrogen is stored as a cryogenic liquid that is at its boiling point, any heat transfer to the liquid causes some hydrogen to evaporate, which results in a net loss of efficiency. Hence, a part of performing an ortho-to-para conversion of the hydrogen during the liquefaction step, another important step in preventing boil-off is to use insulated cryogenic containers. These are designed to minimize conductive, convective, and radiant heat transfer from the outer container wall to the liquid [35]. Most liquid hydrogen tanks are spherical, because this shape has the lowest surface area for heat transfer per unit volume [34, 35]. Therefore, the bigger the diameter of the tank, the less heat transfer area in proportion is. Another option if the hydrogen is stored on the same site where it is liquefied is to pull the hydrogen gas out of the liquid hydrogen vessel and re-liquefy it. This way no hydrogen is lost, and because the hydrogen gas is still cold, it is easier to compress [36].

Medium-sized liquefaction plants have production rates of 380-2,300 kg/h [37]. However, plants built during the past few years have been smaller (110-450 kg/h).

2.2.1.2. Metal Hydrides

Many metals have the property to absorb reversibly a huge quantity of hydrogen. As Figure 6 shows, metal hydrides store hydrogen by chemically bonding the hydrogen to metal or metalloid elements and alloys [33]. Hydrides are unique because some can adsorb hydrogen at or below atmospheric pressure, and then release the hydrogen at significantly higher pressures when heated. Heat released during hydride formation must be

continuously removed to prevent the hydride from heating up. If the temperature is allowed to increase the equilibrium pressure will increase until no more bonding occurs. To recover the hydrogen from the metal hydride, heat must be added to break the bonds between the hydrogen and the metal. The higher the temperature is, the higher the release pressure.

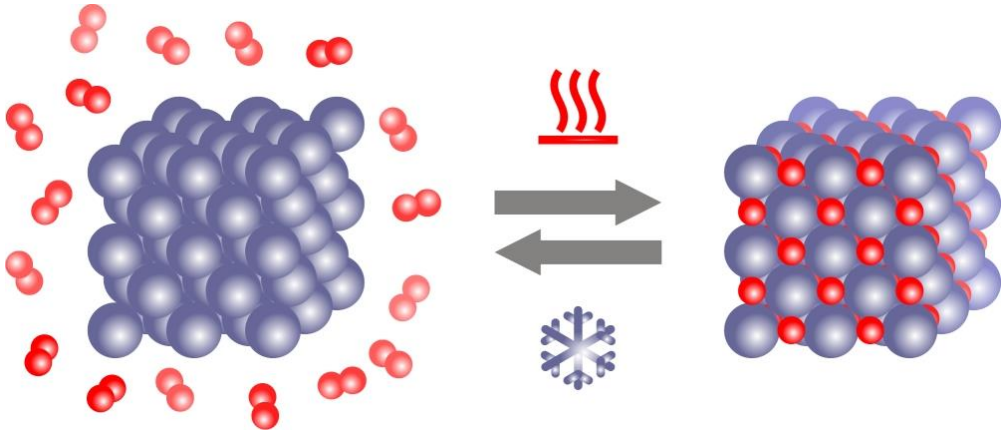

Figure 6: Absorption and desorption of hydrogen. Source: Energie Speicher[1].

There is a wide operating range of temperatures and pressures for hydrides depending on the alloy chosen [38]. That is the reason why the construction of the storage unit becomes a challenge.

In terms of safety, metal hydrides appear to be the safest storage option because the storage unit is at low pressure. If there is a leak in the container, very little hydrogen will leak out because a source of continuous heat is required to release the bond between the metal and the hydrogen [35]. A serious damage to a hydride tank (e.g. collision) would not pose fire hazard, since hydrogen would remain in the metal structure [39].

[1] http://forschung-energiespeicher.info/en/project-showcase/industrial-processes/project-single-view//Metallhydride_speichern_schneller_mit_Graphit/

2.2.1.3. Compressed Gas

There are several factors that need to be analyzed in the selection of the storage to use [36], such as the application, the required energy density, the storage period and the quantity of hydrogen to be stored, the geology of the area, the maintenance requirements, and the capital costs. As it has been commented liquefying hydrogen is very expensive because a lot of equipment is required. Thus, if the objective is to store hydrogen so as to use it in a micr-grid is not worth building such a plant. Same problem happens with using metal hydrates. That is why the most feasible option for a microgrid is to compress the H_2.

Even though, as Table 2 presents, hydrogen has the best gravimetric energy density in comparison to other fuels energy density, it has a very low volumetric energy density due to its low density ($0.089 \frac{kg}{m^3}$ at standard conditions). That is the main reason why the H_2 gas needs to be compressed.

Table 2: Energy Density of several fuels [36].

	H_2 fraction	**State in Normal Conditions**	**Energy Density $\left[\frac{MJ}{Kg}\right]$**	**Energy Density $\left[\frac{MJ}{m^3}\right]$**
Hydrogen	1	Gas	120	4 ÷ 6
Methane	0.25	Gas	50	36
Ethane	0.2	Gas	47.5	23.7
Propane	0.18	Gas	46.4	22.8
Gasoline	0.16	Liquid	44.4	31.1
Ethanol	0.13	Liquid	26.8	21.2
Methanol	0.2	Liquid	19.9	15.8

Compressed gas storage of hydrogen is the simplest storage solution since the only equipment required is a compressor and a pressure vessel [40]. It is the one used in hydrogen pipeline transport, in compressed hydrogen tube trailer transport, and in above-the-ground storage tanks. The main concern with compressed gas storage is the low storage density, which depends on the storage pressure that is proportional to the cost of compressing hydrogen. Hence, higher storage pressures result in higher operating costs.

Two approaches are being pursued to increase the gravimetric and volumetric storage capacities of compressed gas tanks from their current levels. The first approach involves cryo-compressed tanks. This is based on the fact that, at fixed pressure and volume, gas tank volumetric capacity increases as the tank temperature decreases. Thus, by cooling a tank its volumetric capacity will increase. The second approach involves the development of conformable tanks.

At low-pressure spherical tanks can hold as much as 1,300 kg of hydrogen at 1.2-1.6 MPa [35]. On the other hand, high-pressure storage vessels have maximum operating pressures of 20-30 MPa [37]. However, one of the problems that large storage vessels present (especially underground storage) is the cushion gas that remains in the empty vessel at the end of the discharge cycle. In small containers this may not be a concern, but in larger containers this may represent a large quantity of cushion gas [35, 41]. One option is to use a liquid such as brine to fill the volume of the container and displace the remaining hydrogen gas [41].

The cost of high-pressure compressed gas tanks is essentially dictated by the cost of the carbon fibers used for lightweight structural reinforcement. Thus, lowering costs without

compromising weight and volume is a key challenge. Carbon fiber-reinforced 5000-psi and 10,000-psi compressed hydrogen gas tanks are under development by Quantum Technologies and others. Such tanks are already in use in prototype hydrogen-powered vehicles.

Three different options can be approached to store the compressed H_2. These are: (1) Underground storage; (2) Storage in Pipelines; (3) Above-the-ground storage in tanks.

Underground Storage

Throughout the years, various types of underground geologies have been exploited for geologic storage of compressed gas. Depleted oil and natural gas wells, aquifers, mined hard rock caverns, and solution mined salt caverns have all been utilized. Recent studies have been conducted to evaluate various types of geology for storage, and the results show that salt caverns provide the lowest risk of gas leakage, provide customizable cavern sizes, can be cycled (charged and discharged) more frequently than depleted oil and gas wells or aquifers, and require a smaller amount of cushion gas for operation [6, 36, 42]. Moreover, lower pressure underground gas storage in bulk quantities is much less expensive than above ground storage in high pressure containers [36]. This storage option is economically the best, since it allows the user to store huge amounts of hydrogen by using natural geographic sites. Nevertheless, so as to take advantage of it the microgrid needs to be located near the cavern.

A great example of underground storage is the Chevron Phillips Clemens Terminal in Texas, which has stored hydrogen since the 1980s in a solution-mined salt cavern. The cavern is a

cylinder with a diameter of 49 m, a height of 300 m and a usable hydrogen capacity of $30.2 \cdot 10^6$ m^3. Its roof is about 850m underground. Other examples of salt caverns are one located in Huntorf, Germany, which has a usable hydrogen capacity of $3.1 \cdot 10^6$ m^3, and another one located in Manosque, France, which has a usable hydrogen capacity of $496 \cdot 10^6$ m^3.

Above-the-Ground Storage in Tanks

Above-ground storage of hydrogen typically employs high-pressure spherical or cylindrical tanks with pressure ratings as high as 30 MPa, but low-pressure spherical tanks with large diameters are also used [35, 37]. Carpetis et al. [43] and Oy et al. [44] said that above-ground compressed gas storage is the second best option to consider for storage times of several hours to several days. They all coincided and agreed that the best strategy is the underground storage. However, equipping, monitoring or repairing underground vessels to be environmentally safe. As a consequence, above-ground storage vessels are becoming more frequently used. By using an above-ground storage tanks it is possible to more closely monitor leaks, primarily because the tank is fully visible. Further, the tank is less likely to leak in the first instance because it may be maintained with paint and the like [45].

It can be inferred from Table 2 that a large hydrogen tank will be heavier than the small hydrocarbon tank used to store the same amount of energy, all other factors remaining equal.

Storage in Pipelines

The movement of fuel by pipeline is one of the cheapest methods of energy transmission and the hydrogen pipeline would be no exception [46]. Hydrogen pipeline transport is a transportation of hydrogen through a pipe as part of the hydrogen infrastructure. Piping systems are usually several miles long, and in some cases may be hundreds of miles long. Because of the great length, and therefore great volume, of these piping systems, a slight change in the operating pressure of a pipeline system can result in a large change in the amount of gas contained within the piping network [36]. However, hydrogen has problems with both hydrogen embrittlement and corrosion. Hydrogen has an active electron, and therefore behaves somewhat like a halogen. For this reason, hydrogen pipes have to resist corrosion. The problem is compounded because hydrogen can easily migrate into the crystal structure of most metals.

2.3. Power-to-Gas

There is no doubt that the share of renewable energy to the total power supply is going to increase. This increase will lead to bigger intermittencies and increased fluctuation of the power input into the grid. In the case of predominant power supply by renewables, temporary excess and insufficient power generation, which can last for either very short periods or over weeks, are the consequences. The storage of large amount of energy will become mandatory [23].

Power-to-Gas (P2G) is a concept to describe deploying excess renewable electricity to produce renewable gas (i.e., hydrogen) and introduce this one to the gas pipelines. This is undertaken to handle grid challenges around supply and demand. Hence, integrating storage capacity into the natural gas pipeline network design can increase average-day utilization rates. This integration involves moving not only natural gas currently being produced but natural gas that has been produced earlier and kept in temporary storage facilities. Consequently, blending hydrogen into the existing natural gas pipeline network increases the output of renewable energy systems such as large wind farms providing a way to store energy produced at times of slack demand.

For the transport of hydrogen, there are basically two options: first, direct admixing of hydrogen into the existing natural gas grid, and second, the construction and use of a dedicated hydrogen pipeline system [23]. By following the first approach of using the existing NG infrastructure no further processing steps are required, which saves costs and ensures the maximum energetic efficiency.

Schiebahn et al. [23] said that the drawback of the P2G concept when using the existing NG pipelines can be found in the limited amount of injectable gas. They announced that the maximum proportion is not yet fully known and depends on the particular component. Hüttenrauch et al. [47], who studied the pipeline network of Germany, suggested that just a maximum of 5% hydrogen by volume can be fed as additional gas into the gas grid. Other research proved that if implemented with relatively low concentrations, less than 5%–15% hydrogen by volume, this strategy of storing and delivering renewable energy to markets appears to be viable without significantly increasing risks associated with utilization of the gas blend in end-use devices overall public safety, or the durability and integrity of the existing natural gas pipeline network [48]. End-use requirements are generally the most restrictive conditions on increasing hydrogen blend levels in natural gas. Ranges noted as being acceptable generally for end-use systems fall within 5%–20% hydrogen, and most discussions note types of changes, precautions, or costs associated with higher blends [49].

The percentages regarding the maximum hydrogen blending into the NG pipeline are very dissimilar because one of the most important parameters is the characteristics of the pipeline studied, which usually diverse depending from one research study to another. The impact of hydrogen blends on industrial facilities is also important and must be addressed on a case-by-case basis [50]. Therefore, the capability of the NG pipeline to introduce more or less hydrogen must be studied in each different scenario. In the present work, up to a maximum of 15% of H_2 by volume blended into the NG pipeline is studied.

The durability of some metal pipes can degrade when they are exposed to hydrogen over long periods, particularly with hydrogen in high concentrations and at high pressures. The

effect is highly dependent on the type of steel and must be assessed on a case-by-case basis. However, metallic pipes in U.S. distribution systems are primarily made of low-strength steel, typically API 5L A, B, X42, and X46, and these are generally not susceptible to hydrogen-induced embrittlement under normal operating conditions [48]. However, pipeline steels that are subject to hydrogen-induced cracking are generally insignificant with concentrations up to 50% hydrogen, but a detailed investigation for every case is again mandatory and could result in the upper limitation on hydrogen concentration being reduced [48]. Also, estimate of gas loss is almost twice the total gas loss for leakage for systems delivering natural gas only.

Hart et al. [35] said that if hydrogen is being delivered continuously by pipeline, little if any hydrogen storage may be required, and it would not make sense to liquefy the hydrogen, then deliver it to a pipeline as a gas. In pipelines with large variation in flow, hydrogen may need to be stored to meet peak demand. The method of storage in that case would depend on the quantity to be stored and the storage time. Hence, even for this scenario where the hydrogen is directed to the pipelines, hydrogen storage is still required.

An example of how feasible this option is can be found in some urban areas, such as Honolulu, Hawaii, where manufactured gas continues to be delivered with significant hydrogen blends and is used in heating and lighting applications as an economic alternative to natural gas [51]. Having a specified blend content of renewable hydrogen into the pipelines would therefore increase the renewable energy credit system used in the electricity sector. If properly crafted, this credit system could provide an economic incentive for converting otherwise-curtailed renewable energy to hydrogen, increasing the

energy provided from existing renewable energy production facilities, and enhancing the sustainability of the natural gas supply system. However, while conventional means of producing and delivering hydrogen are relatively well understood, blending as a means of storing or delivering hydrogen is very dependent on specific characteristics of the natural gas pipeline system. Öney et al. [52] challenged the conventionally held belief that hydrogen can only be transmitted over relatively short distances (because of its low volumetric energy content). One of their conclusions was that concluded that these concerns were exaggerated since for a given transmission distance of 500 km and an energy delivery rate of 1.0 GW, 100% hydrogen can be transported at an approximately equal cost of 100% natural gas, if its production pressure is increased from 1 atm to a level of 6.4 times the atmospheric pressure (i.e., 6.4 atm).

Hence, it can be confirmed that blending hydrogen into natural gas pipelines could be a worthwhile strategy to pursue, both now to help take advantage of intermittent renewable energy production and down the road as a means of distributing hydrogen for use in fuel cells. A blending strategy allows suppliers to deliver hydrogen fuel to markets for use in stationary fuel cell systems for buildings, backup power, or distributed generation. It has also been proposed as a means of delivering pure hydrogen to markets. As a hydrogen delivery method, blending can defray the cost of building dedicated hydrogen pipelines or other costly delivery infrastructure during the early market development phase. This hydrogen delivery strategy also incurs additional costs, associated with blending and extraction, as well as modifications to existing pipeline integrity management systems, and these must be weighed against alternative means of bringing more sustainable and low-carbon energy to consumers [48].

Another aspect that must be taken into account when analyzing the feasibility of blending hydrogen and natural gas into the natural gas pipelines is the safety. Since hydrogen will ignite under a broader range of conditions, a main concern is the potential for increased probability of ignition and resulting damage compared to the risk posed by natural gas without a hydrogen blend component. Melaina et al. [48] said that the overall risks posed by the existing natural gas pipeline system can be quantified, and these results are used as a baseline for comparing risks associated with hydrogen blends. Moreover, in instances where natural gas leaks result in explosions, inclusion of 20% or less hydrogen would result in minor increases in the severity of the explosion [48].

2.3.1. Natural Gas Pipeline System

A gas transport system in principle has the task of transporting gas from the source of supply to the demand sink. The major elements of the gas pipeline grid are the pipes, storage facilities, and compressor, measuring, and regulating stations [23].

The U.S. natural gas pipeline network has changed dramatically since the mid-1800s, when just local manufactured gas networks were the ones that served municipalities. Now, it is a highly integrated transmission and distribution grid that can transport natural gas to and from nearly any location in the lower 48 States [49]. The natural gas pipeline grid comprises more than 210 natural gas pipeline systems, 300,000 miles of interstate and intrastate transmission pipelines as Figure 7 shows, and more than 1,400 compressor stations that maintain pressure on the natural gas pipeline network. It encompasses more than 11,000 delivery points, 5,000 receipt points, and 1,400 interconnection points that

provide for the transfer of natural gas throughout the United States. It also has 29 hubs or market centers that provide additional interconnections, 394 underground natural gas storage facilities, 55 locations where natural gas can be imported and exported via pipelines, 5 LNG (liquefied natural gas) import facilities, and 100 LNG peaking facilities [49].

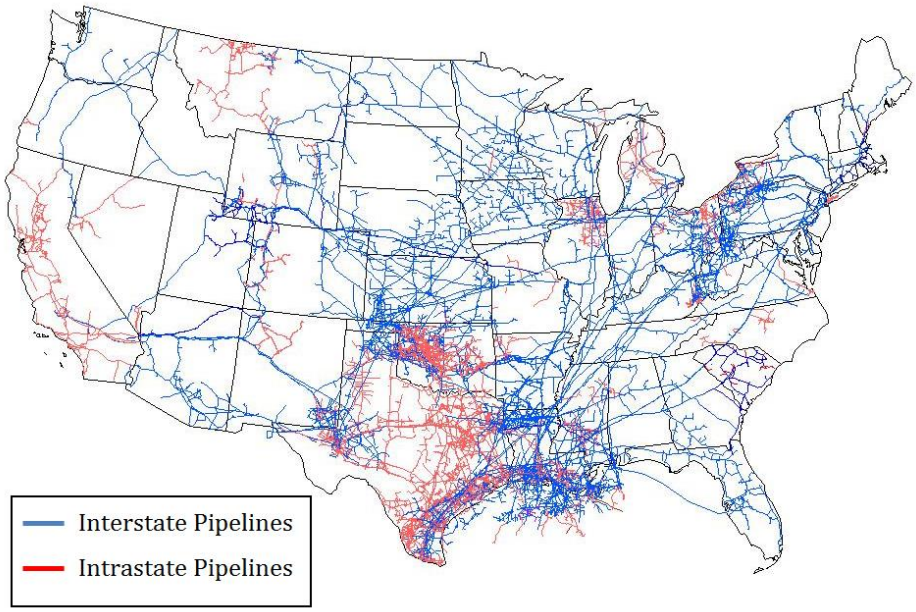

Figure 7: United States Natural Gas Pipeline Network. Source: Energy Information Administration Office of Oil & Gas, Natural Gas Division, Gas Transportation Information System.

The state of California is dependent upon the interstate pipeline system for their supplies of natural gas. On the interstate pipeline grid, the long-distance, wide-diameter (20-42 inch), high capacity trunk lines carry most of the natural gas that is transported throughout the nation. In many instances, natural gas must be routed through several interstate pipeline systems before it reaches its final destination. On the other hand, intrastate natural gas pipelines operate within State borders and link natural gas producers to local markets and to the interstate pipeline network. California is ranked the second largest

natural gas consuming State. Intrastate transportation and distribution are dominated by California Gas Transmission Co. (PG&E) (3,477 miles), Southern California Gas (SoCal) Company (1,887 miles), and the San Diego Gas and Electric Company. SoCal and PG&E are two of the largest distribution companies in the entire United States. Table 3 presents the principal NG companies that serve the Western Region of the United States of America.

Table 3: Principal Natural Gas Pipeline Companies Serving the Western Region.[2]

Pipeline Name	Principal Supply Source(s)	System Configuration* Primary/Secondary
Interstate & importing pipelines		
El Paso Natural Gas Co	San Juan (CO,NM) & Permian Basin (TX)	Trunk/Grid
Gas Transmission Northwest	Canada	Trunk
Kelso-Beaver Pipeline Co	Interstate System	Trunk
Kern River Transmission Co	Wyoming, Utah	Trunk
Mojave Pipeline Co	Southwest (via the Interstate System)	Trunk
North Baja Pipeline Co	Southwest (via the Interstate System)	Trunk
Northwest Pipeline Co[1]	Canada, Green River (WY) & San Juan (CO) Basins	Trunk/Grid
Southern Trails Pipeline (Questar)	San Juan Basin (CO,NM)	Trunk
Transwestern Pipeline Co	San Juan (CO,NM) & Permian Basins (TX)	Trunk
Tuscarora Gas Transmission Co	Canada (via Interstate System)	Trunk
Intrastate Pipelines		
Cascade Natural Gas Co	Interstate System	Grid/Trunk
Ferndale Pipeline Co	Canada	Trunk
Northwest Natural Gas Co	Interstate System	Trunk/Grid
Pauite Pipeline Co (NV)	Interstate System	Trunk
California Gas Transmission Co	Interstate System & California Production	Trunk/Grid
San Diego Gas & Electric Co (CA)	Intrastate System	Trunk/Grid
Southern California Gas Co (CA)	Interstate System & California Production	Trunk/Grid
Southwest Gas Co (CA, NV)	Interstate System	Trunk/Grid

[2] http://www.eia.gov/pub/oil_gas/natural_gas/analysis_publications/ngpipeline/western.html

2.4. Literature Gaps Addressed

Even though, as the previous subsections showed, the hydrogen energy storage systems are widely studied in the literature, just a few of them are used in microgrid applications. Dispatching the chiller plant and the co-gen cycle dynamically, and using Power-to-Gas techniques is the major strategy presented and considered in the present thesis as a means of using as much of the otherwise-curtailed solar power as possible.

3. Approach

In this section, the procedures taken to accomplish each of the tasks mentioned in subsection 1.2.2 are presented.

1. Accomplish a literature review that thoroughly examines reversible fuel cells and hydrogen energy storage technology for use with high renewable use.

   The study and detailed analysis of the fundamental concepts governing the different types of hydrogen energy storage technologies that exist nowadays is performed. Special attention is given to the Power-to-Gas concept, since it represents a complete system solution to the problem of surplus energy reserves.

2. Obtain 15-minute resolution experimental data from the operating microgrid of the University of California, Irvine.

   Data of the power produced by the Gas Turbine, Steam Turbine, and the solar photovoltaic panels installed at the microgrid of study, as well as data of the power imported from SCE, have been collected.

   Personal online accounts that allow direct access to both SunEdison®, and AlsoEnergy® have been provided by the UCI Facilities Management (FM) team [53] to obtain the solar power data needed. Moreover, data from Melrok® have been obtained through the UCI FM team to account for the co-gen cycle and the SCE import power.

3. Develop a dynamical physical model of the University of California, Irvine microgrid operation control.

   Using the 15-minute resolution power data as look-up tables, a Matlab/Simulink® model has been designed and developed. Perfect knowledge is therefore assumed in all the scenarios analyzed.

4. Apply the model to parametric variations according to specific case scenarios.

   Two modifications have been introduced to the operation of the microgrid so as to be able to utilize as much otherwise-curtailed power as possible by means of using the available microgrid technologies. These are the availability of the NGCC to turn down and the availability of the chiller plant operation to be modified when necessary. The four different strategies that can be approached when combining these two are studied. These are: (1) Manipulate the chiller plant operation; (2) Turn down the NGCC; (3) Manipulate the chiller plant operation and, if solar curtailment is still present after doing so, turn down the NGCC; and (4) Turn down the NGCC and, if solar curtailment is still present after doing so, manipulate the chiller plant operation.

5. Include compressed Hydrogen Energy Storage System (HESS) in the model.

   The use of (1) Reversible Fuel Cells (RFC) and (2) Power to Gas (P2G) obtained after blending H_2 with Natural gas (NG) into the existing NG pipelines are studied in the model in order to utilize the otherwise-curtailed power and increase the microgrid procurement from eligible renewable energy resources.

6. Analyze results and propose new ways of operating the microgrid in order to increase its renewable energy penetration.

   Special attention is given to the strategies studied in the model and to other strategies that could be implemented (such as the use of biogas to run the Gas Turbine) to meet the future energy goals for the State of California.

4. Model Overview

Microgrid projects have been undergoing a boom for the last past years after proving their value in critical situations. The complex and integrated University of California, Irvine (UCI) microgrid serves as the case-study for this thesis since the features of the UCI campus are representative of many business, other universities, military forts, and buildings with the integrated infrastructure that defines a microgrid.

The UCI campus has the capacity to self-generate 90% of its annual electricity demand [53]. Hence, it is a perfect example and test of how microgrids operate internally as well as how they interface with the rest of the future smart grid. It is served by the regional electric utility, Southern California Edison (SCE), through the UCI Substation which steps down voltage from 66kV to 12kV using two 15 MVA transformers. It encompasses ten 12kV circuits, is served by a 19MW natural gas fired combined cycle plant, and incorporates centralized chilling including one of the largest thermal energy storage tanks in the country (4.5 million gallons/60,000 ton-hours). The campus central plant includes a 13.5MW gas turbine, a 4.5MW steam turbine generator, seven co-located chillers, of different sizes and performances characteristics as Table 4 shows, and a 175MWh cold-water storage tank [54]. The cold-water storage meets the daily cooling demand during on-peak electric rate hours through the fall, winter and spring seasons, but must be supplemented with daily chiller plant operation during hotter summer days [53].

The microgrid also serves all major buildings with district heating and cooling, and includes 3,575 kW of solar power, 2,569 kW of which were installed from February, 2015

to May, 2015. Even though PV resources provide just 3.5% of campus needs, they cause the gas turbine to be turned down at times of low electric demand and high solar irradiation.

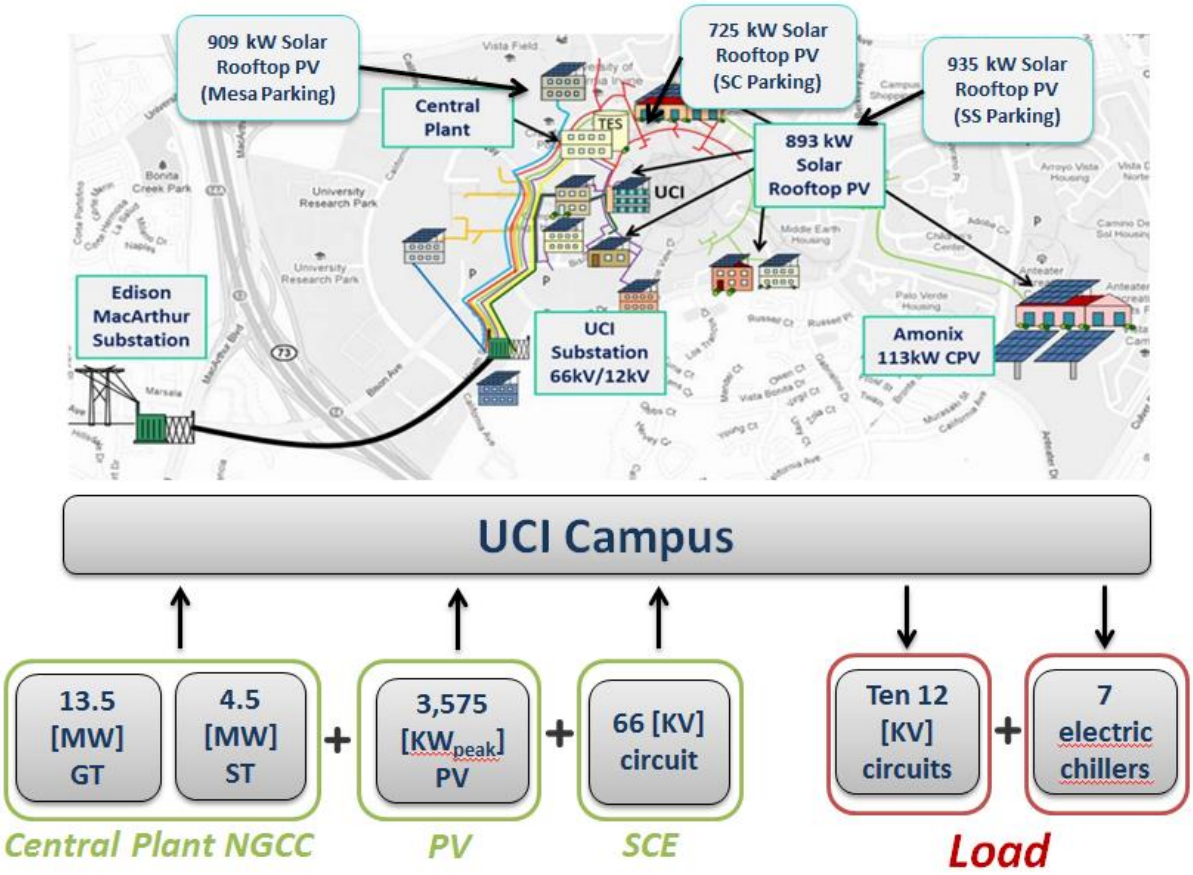

Figure 8: University of California, Irvine microgrid power management.

The electric chillers produce cold water that is circulated throughout the campus. These seven co-located chillers are centrifugal and electric chillers of varying vintage, capacity, and efficiency. There is also a single steam driven centrifugal chiller (chiller number 4). This chiller (4) has not been taken into account in the calculations carried out in the present thesis since it does not work with electricity.

Table 4: UCI plant chillers sizes and efficiencies.

	Ton Capacity	Size (kWe)	COP
CH1	900	600	5.27
CH2	900	651	4.86
CH3	1,000	606	5.8
CH4	2,600	-	1.55
CH5	2,800	2,525	3.9
CH6	2,800	2,140	4.6
CH7	3,250	1,905	6
CH8	3,250	1,905	6

The UCI microgrid also contains a unique set of distributed energy resources that is unparalleled in the world such as hydrogen fueling for fuel cell vehicles, integrated fuel cell absorption chilling, two-axis tracking concentrated solar photovoltaic systems, advanced building energy efficiency measures, advanced building monitoring and control, and advanced power, power quality, and thermal metering [54].

According to form 14-743 [55] of SCE "generating facility interconnection agreement" (inadvertent-export), the UCI campus can have parallel operation of the generating facility, and the occasional, inadvertent, non-compensated, export of power to SCE's distribution system. The agreement states that UCI cannot export more than 5600 kW for more than 2 seconds and not export anything less than that for more than 60 seconds [56]. If the limits agreed to in the agreement are exceeded then the combustion turbine generators are turned off and the demand could increase up to 18MW instantly, which could increase UCI electrical bill up to $300,000/month (due to demand charges) [57].

A dynamic physical model called HESS, which stands for *Hydrogen Energy Storage System*, has been built using Matlab/Simulink® so as to analyze the different strategies that can be followed when looking for the best way to dynamically dispatch the different sources of power generation of an existing microgrid. The microgrid of study is the one present at the University of California, Irvine. Special attention and priority is given to power coming from renewable sources by analyzing how to operate the microgrid when different amounts of solar power capacities are installed. Also, the model simulates the effect and potential benefits of injecting renewable H_2 into the NG pipeline and deploying a combination of reversible fuel cells to mitigate the energy intermittency problem created by solar PV.

A schematic of the system configuration is shown in Figure 9. The model contains nine main components: PV power supply, microgrid power demand, power management, utility grid power supply, electric chillers, a Natural Gas Combined Cycle (NGCC), a Reversible Fuel Cell (RFC), H_2 storage, and the Natural Gas (NG) pipeline. The NGCC (or co-gen cycle) is formed by a 13.5 MW Gas Turbine (GT) and a 4.5 MW Steam Turbine (ST). The solar power supply, the utility grid power supply, and the NGCC are treated as inputs for the model using data provided by Melrok®, SunEdison®, and AlsoEnergy®.

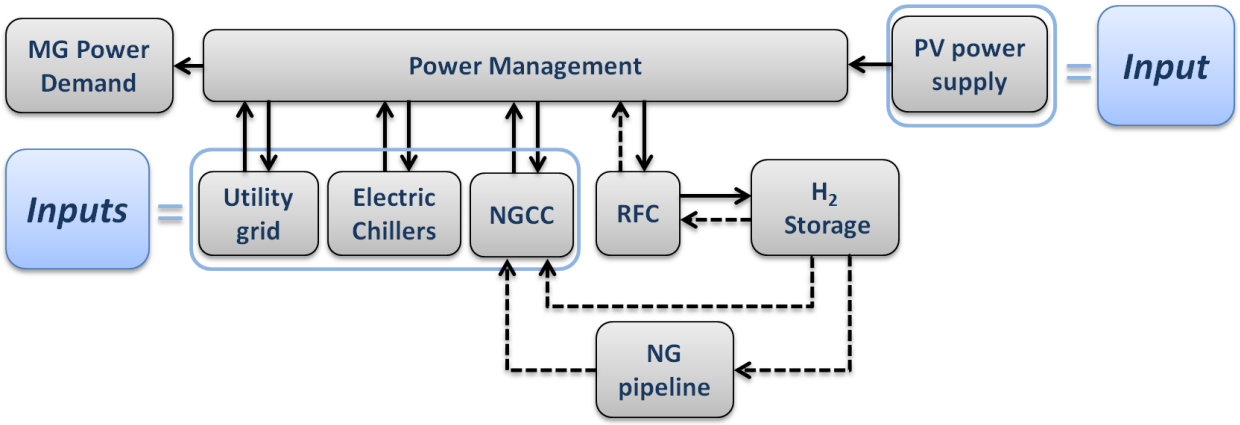

Figure 9: Schematic of Hydrogen Energy Storage System (HESS) model.

Since utility rates are usually determined every fifteen minutes the time resolution used in the model is of fifteen minutes. Therefore, the short-term or fast time-scale microgrid dynamics are not resolved. It is assumed that demand is flexible enough and that both energy storage (e.g., ubiquitous batteries and ultra-capacitors in power supplies) and power generators can operate quickly enough to handle these fast microgrid dynamics properly. Thus, emphasis is primarily given to the design and operation of HESS which can accomplish massive and long-term energy storage, since the energy and power capacities of HESS can be independently sized.

5. Model Implementation

Input data from a specific year is required in order to run simulations using the HESS model. In this section the data use is that which was acquired in 2014. During this year the solar capacity installed on the University of California, Irvine microgrid of study was of 1,006 kW. However, just data from the SunEdison® panels installed in 12 building rooftops is known. These sites have an overall capacity of 893 kW. To account for the rest of the installed solar systems, the 113 kW capacity Amonix® solar panels installed at the Anteater Recreation Center (ARC) fields, the power data from SunEdison® has been scaled multiplying the data points by a constant, K, equal to 1.25. This constant K is obtained using Equation (1).

$$\mathrm{K} = \frac{\text{Total Solar Power Capacity}}{\text{Solar Power Capacity of the data known}} \tag{1}$$

In the HESS model the Demand is computed as Equation (2) shows. The future annual demand of the microgrid is supposed to be the same this had on 2014.

$$\text{Demand} = (\text{NGCC Power})_{2014} + (\text{Solar Power})_{2014} + (\text{SCE Power})_{2014} \tag{2}$$

where $(NGCC\ Power)_{2014}$ is the power the NGCC produced during the whole year 2014; $(Solar\ Power)_{2014}$ is the solar power that was produced during 2014 by the 1.006 MW of solar power that was installed on campus; and $(SCE\ Power)_{2014}$ is the power the campus imported from Southern California Edison in 2014. The chillers load is indirectly included in the total load demand. That is the reason why it does not explicitly appear in Equation

(2). It is straightforward to note that if data from any other year is used, this equation can be used in the same manner.

Annual analyses are carried out but, for the sake of comparison, daily and monthly figures are the ones basically plotted when specific trends are to be shown and discussed. Figure 10 and Figure 11 show the UCI microgrid power dispatch for the year 2014, with just 1,006 KW of solar power available. It was not until 2015 that an extra 2.57 MW of PV power were installed.

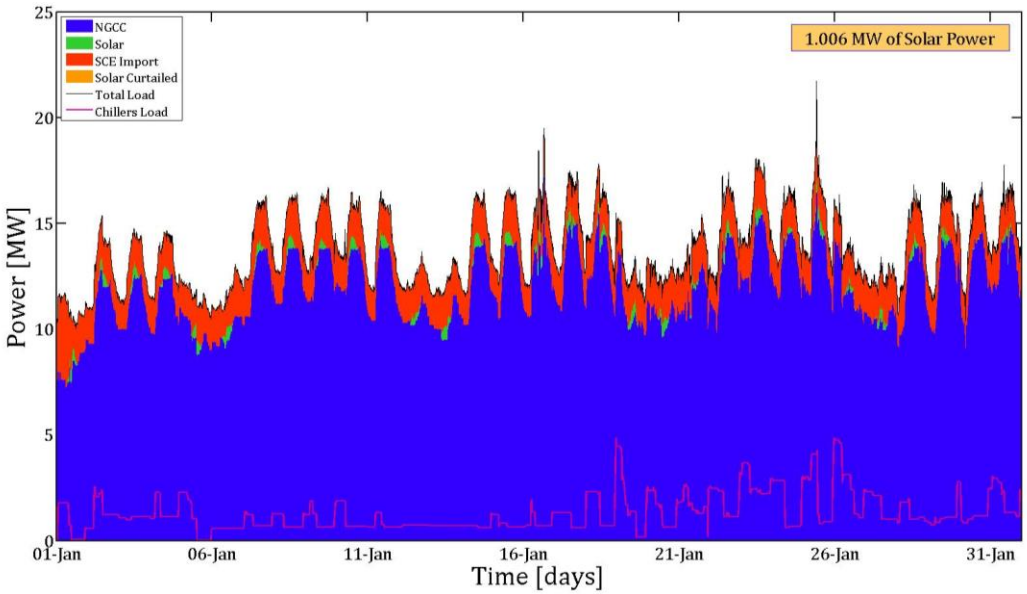

Figure 10: Dispatch of power for the month of January. Data of the year 2014 are used.

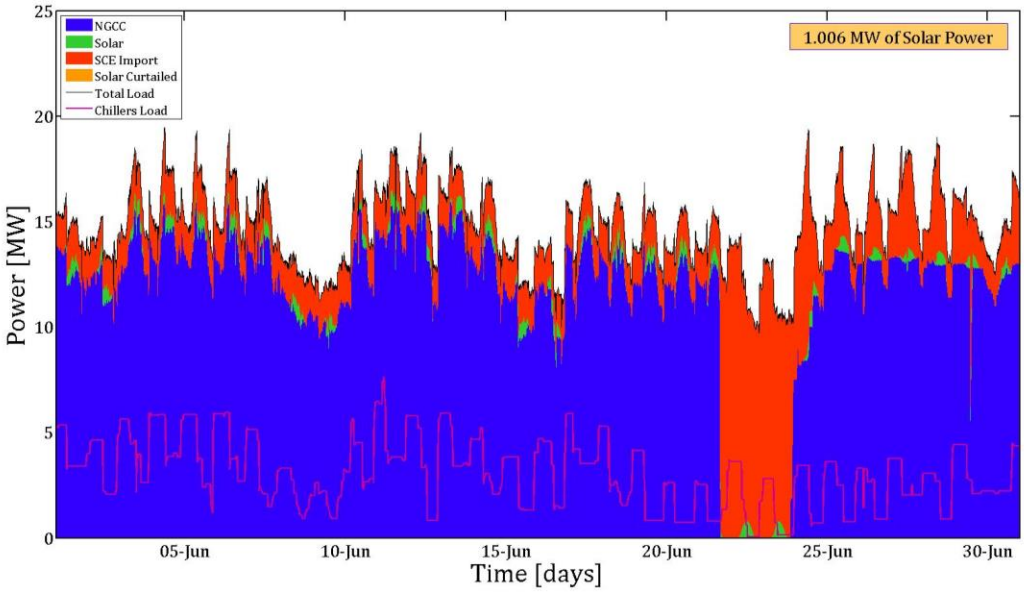

Figure 11: Dispatch of power for the month of June. Data of the year 2014 are used.

The NGCC is the primary source of power of the microgrid as Figure 10 and Figure 11 display and a constant import from the grid is also present the whole time as these two figures also demonstrate. Equation (3) shows how to obtain the Solar Integration (SI), which in case of the UCI campus corresponds to the overall renewable integration.

$$\mathrm{SI} = \frac{\mathrm{SE}}{\mathrm{DE}} \cdot 100 \tag{3}$$

where *DE* is the total Demand of Energy of the microgrid; and *SE* is the Solar Energy used by the microgrid.

The 2014 annual DE of the campus was of 125,519 MWh and only 0.98% of this amount did come from solar PV. Even though this percentage seems very small, it does make sense if is taken into consideration that the Average Campus Load (ACL) for this year was of 14.32 MW. The ACL can be computed using Equation (4) below.

$$\text{ACL} = \frac{\text{Annual Energy Load}}{365\text{days} \cdot 24\ \frac{\text{h}}{\text{day}}} = \frac{125{,}519\ \text{MWh}}{365\text{days} \cdot 24\ \frac{\text{h}}{\text{day}}} = 14.32\ \text{MW} \quad (4)$$

It is important to note how the load demand is increased during the month of June, as Figure 11 presents, due basically to the increase of the chillers load. It is also important to note that the curtailment in summer is bigger than in winter, as expected. Furthermore, Figure 11 shows how the central plant was shut down from June 20, 2014 to June 22, 2014 due to a scheduled maintenance work programmed in advance.

Energy-producing solar panel canopies were installed from February 2015 to May 2015 on the top floors of the Social Science (SS), Student Center (SC), and Mesa Parking Structures. This green energy project provides 2.569 MW of extra solar PV to the campus and increases considerably its sustainable energy production as shown in Table 5.

Table 5: Current Solar Generation sites and capacities of all the UCI solar photovoltaic installations.

Site	**SunEdison**	**Amonix**	**AlsoEnergy**			**TOTAL**
			SS Parking	**SC Parking**	**Mesa Parking**	
Capacity [KWe]	893	113	935	725	909	3,575
Type	Rooftop	Ground-mounted	Rooftop	Rooftop	Rooftop	-

Figure 12 and Figure 13 present how at some point solar curtailment appears at moments of high solar irradiation if the 2014 operation of the microgrid is not modified. These two Figures aim to show how the model works since, as section 6 presents, no curtailment has been present during the year 2015 so far. That is because the UCI Facilities Management

team does already have some control over the microgrid to accommodate the overall 3.575 MW of solar power the campus currently has.

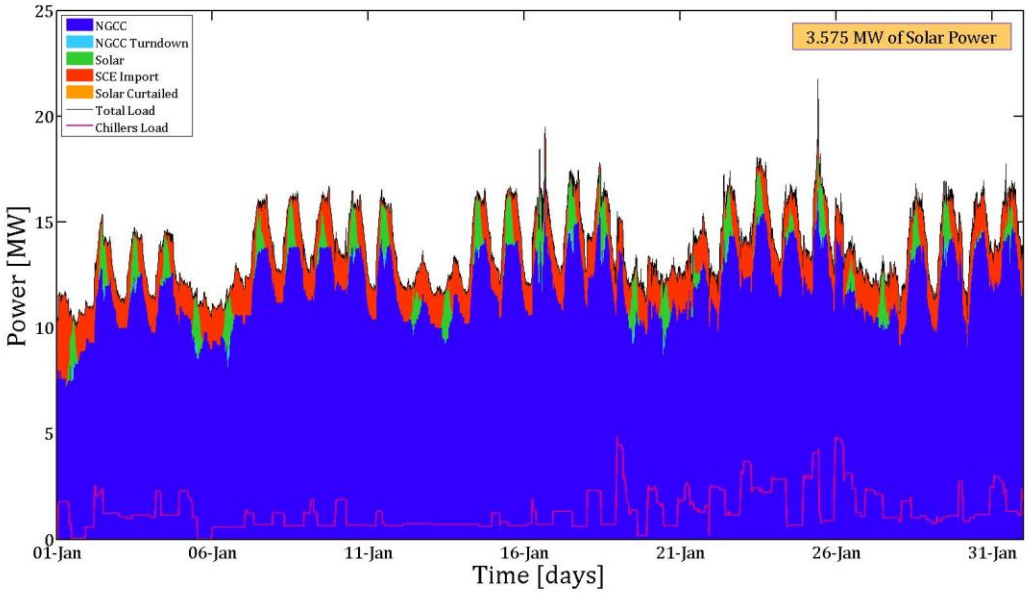

Figure 12: Dispatch of power for the month of January with all the photovoltaic being installed in 2015 available. 2014 data are used.

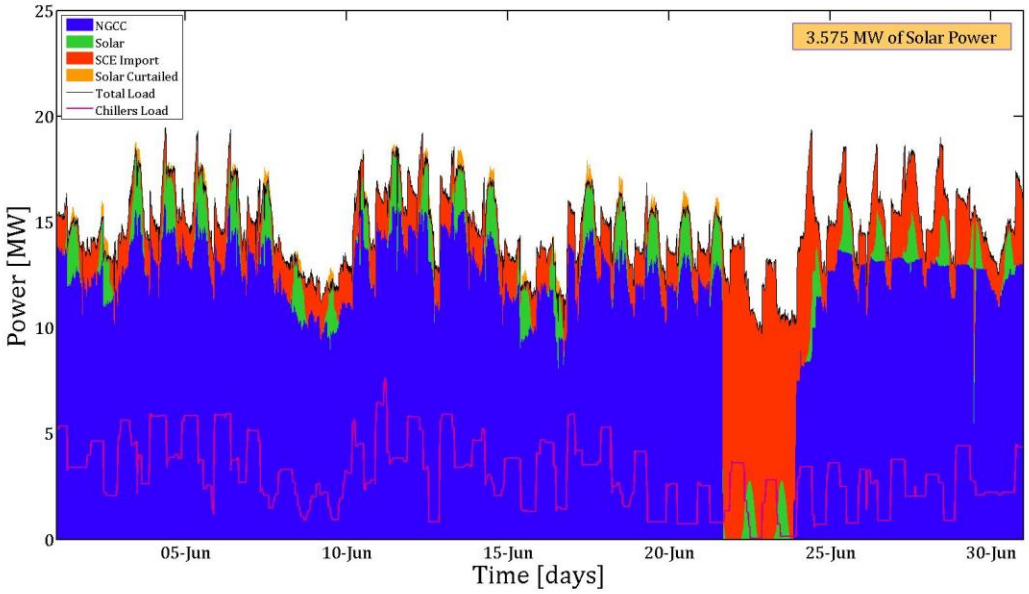

Figure 13: Dispatch of power for the month of June with all the PV being installed in 2015 available. Data of the year 2014 data are used.

5.1. Control Strategies

The following sections present the four different strategies that can be approached when combining the availability of the NGCC to turn down and the availability of the chiller plant operation to be modified when necessary. These are: (1) Manipulate the chiller plant operation; (2) Turn down the NGCC; (3) Manipulate the chiller plant operation and, if solar curtailment is still present after doing so, turn down the NGCC; and (4) Turn down the NGCC and, if solar curtailment is still present after doing so, manipulate the chiller plant operation.

5.1.1. Chiller Plant Power Manipulation

The large capacity of thermal energy storage systems introduces the additional ability to shift energy demand from peak to non-peak demand hours. This forms a more complex problem requiring system optimization with future forecasting and potentially novel methods of solution [53]. This energy shifting is accomplished by operating the electrical chillers at a higher power than the one they require at a specific moment. Thus, thermal energy is stored in them when excess of renewable energy is present and they have not stored enough energy so as to meet their own load demand of the following afternoon and night, when solar power is not available anymore. Then the energy demand decreases at night by the same amount that has been stored previously. Hence, when this approach is followed, the solar power curtailed decreases, too. Figure 14 shows schematically the approach followed.

Figure 14: Schematic of the strategy the HESS model follows in order to manipulate the chiller plant operation so as to utilize the otherwise-curtailed solar power.

Although this project is primarily focused on the UCI microgrid, in most places where solar canopies are installed, chillers are not. In these places the otherwise-curtailed solar energy cannot be thermally stored in chillers, since they are inexistent. As a result, other energy storage techniques need to be implemented so as to benefit from this excess power already generated.

So as to account for the power that the chillers are consuming, since there are a lot of erroneous data points in the set, an alternative approach has been taken. The chiller plant has a maximum capacity which, in the HESS model, has been called Chiller Power Capacity (CPC). The CPC is obtained as shown by Equation (5). The tons delivered are first converted to kW (1 Refrigerated Ton = 3.517 kW). Then, the result is divided by the Coefficient of Performance (COP) of the specific chiller to get an estimated power.

$$\text{CPC [kW]} = \sum_{i} \frac{(\text{Ton Capacity})_i \cdot 3.517}{\text{COP}_i} \tag{5}$$

Table 6 shows the power capacity of each of the electric chillers. Recall that chiller number 4 is not taken into account in the calculations since it is a steam driven chiller. Hence, it is not driven by electricity.

Table 6: Individual and overall UCI Central Plant electric chillers characteristics.

	CH1	CH2	CH3	CH5	CH6	CH7	CH8	TOTAL
Capacity [R.Tons]	1,500	2,000	2,000	3,000	3,000	3,000	3,000	17,500
COP	5.27	4.86	5.8	3.9	4.6	6	6	-
Power Capacity [kWe]	1,001.0	1,447.3	1,212.8	2,705.4	2,293.7	1,758.5	1,758.5	12,177.2

If the chillers load is decreased when no solar power is present by using the solar energy that has been thermally stored during the previous day, the total load of the campus is decreased as well by the same amount. Equation (6) shows how the SCE energy import is reduced if the chillers energy saved during the day is smaller than the SCE energy import of the following afternoon and night in this scenario. It is important to remember that a minimum and constant 100KW of import throughout the night needs to be obtained from SCE.

$$\mathrm{SCE_{FEI}} = \mathrm{SCE_{IEI}} - \mathrm{Chillers_{ES}} \tag{6}$$

where SCE_{FEI} is the final energy import of the campus from SCE after manipulating the chiller plant operation; SCE_{IEI} is the energy import of the campus from SCE before manipulating the chiller plant operation; and $Chillers_{ES}$ is the energy that has been stored thermally in the chillers the previous morning. It can also be understood as the energy no longer imported.

On the other hand, if the chillers energy saved during the day is bigger than the SCE energy import of the following night (minus the energy required to maintain a minimum and constant 100KW of import throughout the night), the SCE_{FEI} is equal to the energy

required to maintain the constant 100 KW of power import. Therefore, the NGCC needs to be turned down afterwards as Equation (7) shows. It can also be understood as a forced NGCC turndown as long as the NGCC operates over its Minimum Operation (MO) of 8MW. In that case, rather than being subjected to a forced turndown, part of the energy produced by the NGCC needs to be curtailed.

$$\mathrm{NGCC_{FT}} = \mathrm{Chillers_{ES}} - \left(\mathrm{SCE_{IEI}} - 100\mathrm{KWh} \cdot \mathrm{Hours_{Night}}\right) \tag{7}$$

where $NGCC_{FT}$ is the difference between the energy the NGCC used to produce before and after manipulating the chiller plant operation. $NGCC_{FT}$ is not represented in the figures because its value is equal to zero or almost insignificant most of the times.

A hypothetical case with 7.150 MW (i.e., 2 times the amount of solar existing on campus) has been simulated so as to show how the excess of solar power is treated when manipulating the chillers as described.

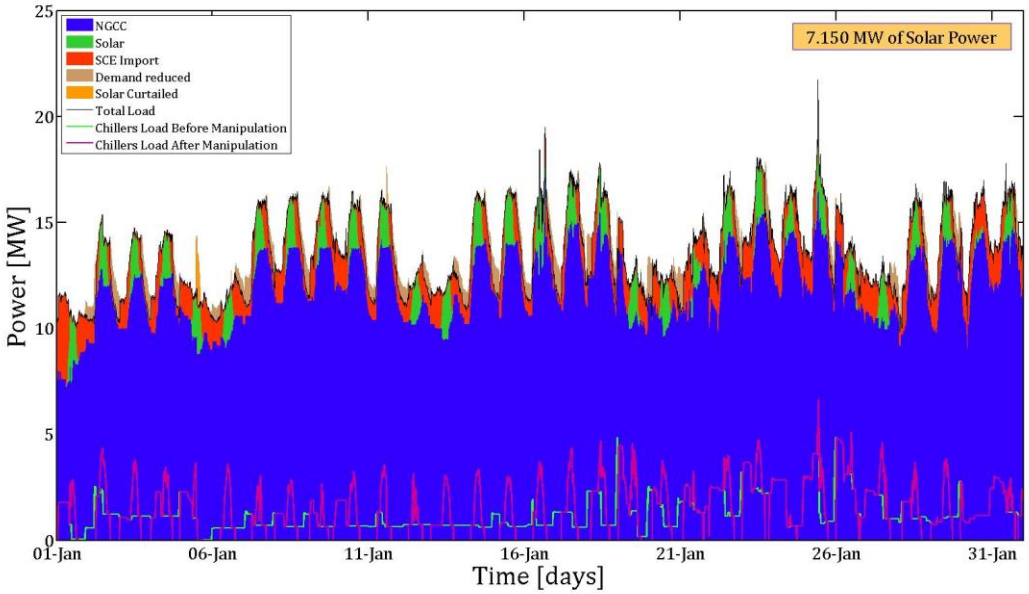

Figure 15: Hypothetical case of the month of January where 2 times the amount of solar PV existent at UCI. The chiller plant operation is manipulated. Data of the year 2014 are used.

Figure 16 shows a simulation of January 10, one of the days where curtailment is still present after manipulating the chiller plant operation, and January 11. In this figure it can be observed how the minimum import of 100 KW is always present. This is used as a constraint in the model because, in real life, it is extremely inefficient and unavailable to turn on and off the import of power when desired, as it has already been commented.

Also, in Figure 16, it can be observed how most of the solar PV is used. It is stored thermally in the chillers during sun hours and used at night. Mathematically speaking, the areas under the curves of the chillers load before and after manipulating their operation are the same. Figure 17 shows that.

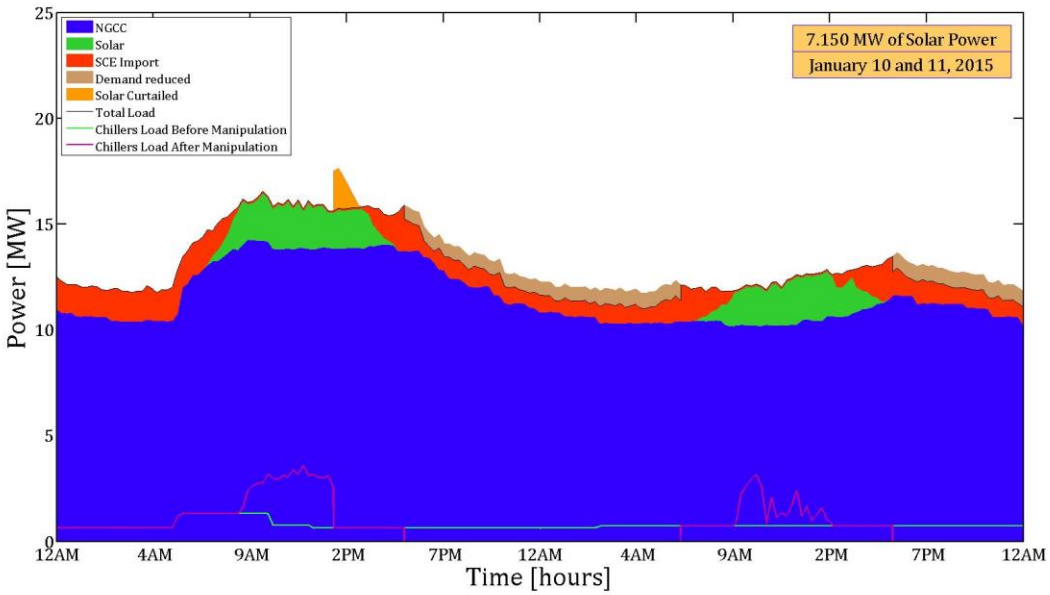

Figure 16: Hypothetical scenario where 2 times the amount of solar PV existent at UCI are installed and just the normal operation of the chiller plant is modified on January 10 and 11, 2015. Data of the year 2014 are used.

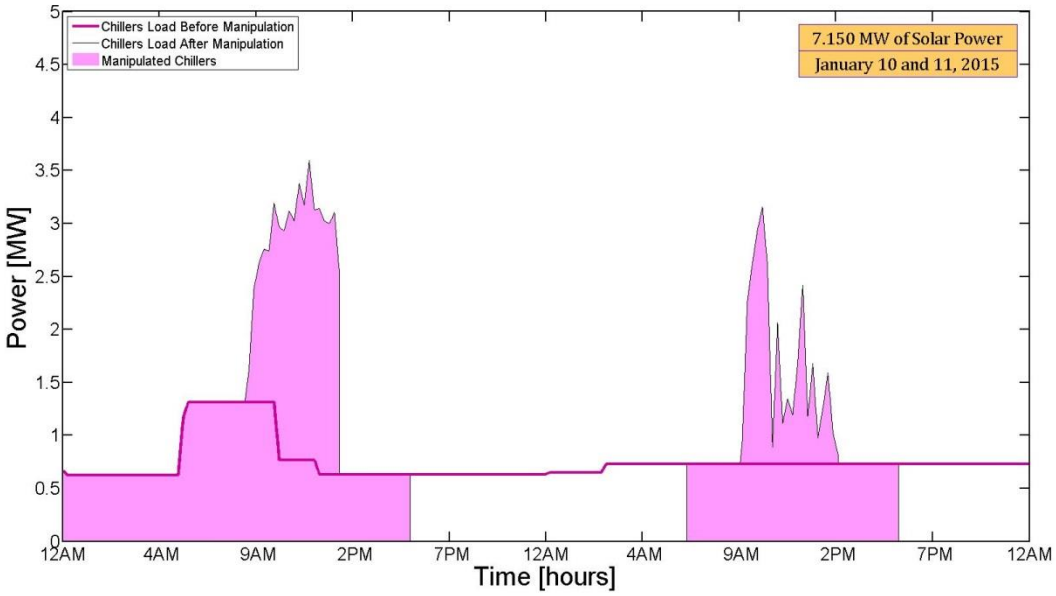

Figure 17: Comparison of the chiller plant operation before and after manipulating them for a hypothetical scenario with 2 times the amount of solar PV existent at UCI on January 10 and 11, 2015. Data of the year 2014 are used.

5.1.2. NGCC Power Manipulation

Central plants are able to regulate their part-load conditions. However, they have limits on how much their power output can be reduced. In other words, they can be turned down as long as a Minimum power Operation (MO) is satisfied. In the UCI microgrid, the NGCC can be turned down up to a minimum operation of 8MW, even though it sometimes operates at a lower output. When the co-gen cycle is working at its lower output the GT is the one working at MO and the ST is turned off and the. In this scenario, all the heat generated by the GT is wasted. Hence, the ST just can work when the NGCC's output is greater than MO.

Figure 18: Schematic of the strategy the HESS model follows in order to turn down the NGCC operation so as to utilize the otherwise-curtailed solar power.

If the NGCC is turned down, the solar power curtailed shown in Figure 12 and Figure 13 will decrease as Figure 18 shows schematically. If just a little bit of power curtailed is present before manipulating the way the NGCC works, most of all of this curtailment disappears. The reason why this happens is because the subtraction of the available NGCC power and the power production (i.e., the solar curtailment that appears when no NGCC turndown is considered) is greater or equal to MO. Hence, by manipulating the NGCC operation more solar power can be used, which is obviously desirable. A higher renewable integration can be therefore achieved in the microgrid by doing so.

Figure 19 represents a hypothetical case with 7.150 MW (i.e., 2 times the amount of solar existing on campus). It has been simulated so as to show how the excess of solar power is treated when manipulating the chillers as explained. It is important to note that the NGCC is turned down basically to allow the system to use more of the solar power generated.

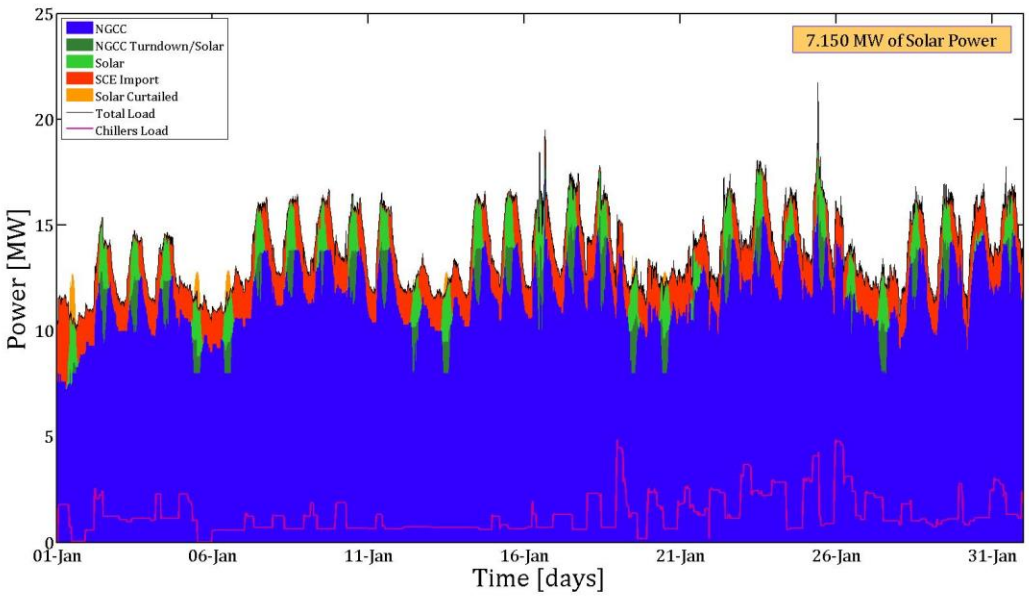

Figure 19: Hypothetical case of the month of January with 2 times the amount of solar PV existent at UCI. The NGCC Power is turned down when required. Data of the year 2014 are used.

Figure 20 displays a simulation of the days 6 and 7 of January, 2015. It can be observed how on January 6 the NGCC is turned down up to MO so as to utilize as much of the otherwise-curtailed power as possible. Once the turndown makes the GT work at this value, no more solar power already generated can be used if no other strategies are approached. So, it needs to be curtailed. Alternatively, on January 7, the amount of solar power existent is not big enough to turn the operation of the NGCC up to MO. Therefore, on this day, all solar power can be utilized and no curtailment is present.

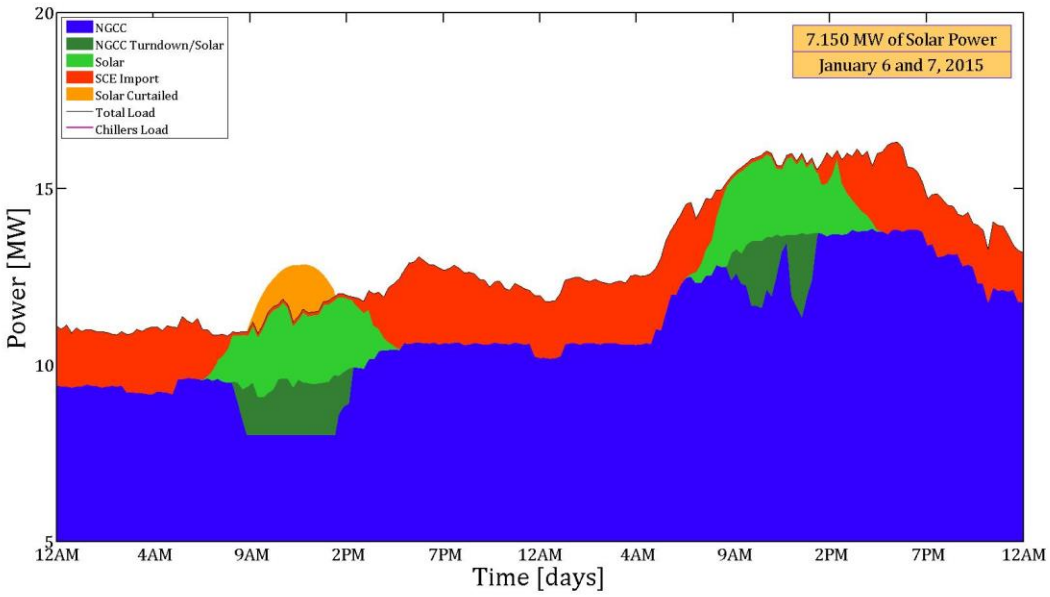

Figure 20: Hypothetical scenario where 2 times the amount of solar PV existent at UCI are installed and just the NGCC Power is turned down when required on January 6 and 7, 2015. Data of the year 2014 are used.

5.1.2.1. NGCC Turndown Efficiency Analysis

The thermodynamic process used by the gas turbine is known as the *Brayton cycle*. The efficiency of this cycle is maximized by increasing the pressure difference across the machine. If the NGCC power output is turned down is because the GT power output is decreased. When doing so, the pressure difference across the machine is also decreased.

This translates into a lower efficiency due to more fuel burnt. Thus, it is necessary to analyze the effect of turning down the NGCC on the overall efficiency of the cycle.

Do et al. [58] developed a model with which they captured the part load performance of the GT used at the UCI Central Plant. The In-Field data points they obtained experimentally have been used and a quadratic approximation to them has been carried out as Figure 21 shows. This quadratic regression, presented by Equation (8), specifies the efficiency of the GT engine in function of its power. Equation (8) is used when comparing the efficiency of the UCI GT before and after manipulating its operation. That is, before and after turning its operation down when the control previously proposed is followed.

$$\eta_{GT}(P) = (-8.9 \cdot 10^{-4}) \cdot P^2 + 0.0299 \cdot P + 0.0833 \tag{8}$$

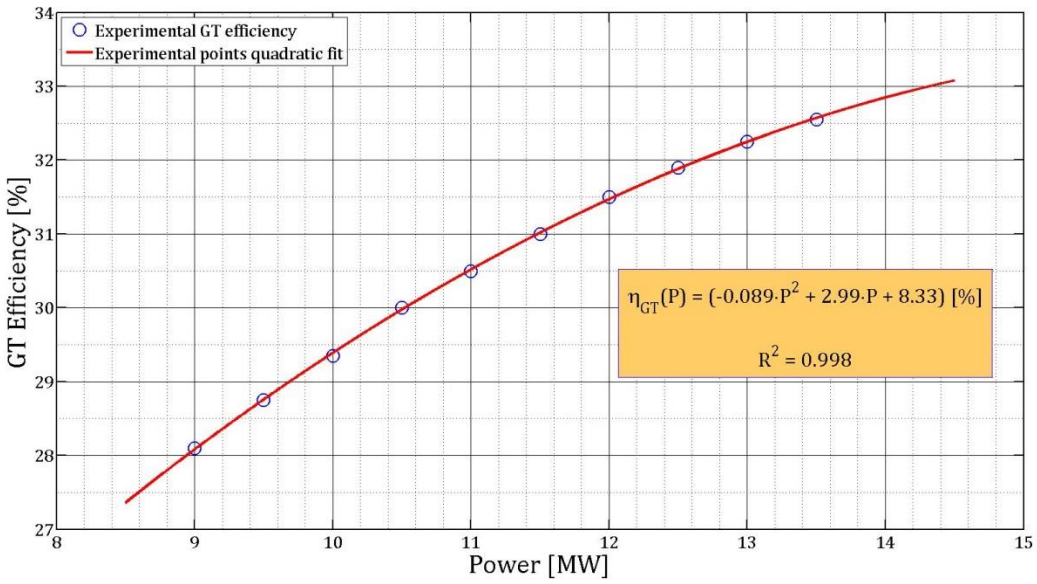

Figure 21: Quadratic regression of the in-field operation efficiency values of the UCI GT [58].

Since no additional fuel is fired to obtain power from the ST, it is assumed that a 100% of the steam power produced is added into the efficiency expression represented by Equation (9) below. The denominator is Power rather than Fuel Input because Equation (8) already accounts for the fuel entering the GT.

$$\eta_{NGCC} = \frac{GT_{Power} \cdot \eta_{GT}(P_{GT}) + ST_{Power}}{GT_{Power} + ST_{Power}} \quad (9)$$

The efficiency of the NGCC when operating at MO (i.e., GT operating at 8MW and ST turned off) is of 26.55%. On the other hand, the efficiency of the NGCC when operating at peak power (15.27MW) is of 39.25%. The NGCC can drop by 12.70 percentage points. That is a decrease of 32.35% in comparison to the efficiency it has at peak power, which obviously happens to be the maximum efficiency of the co-gen cycle. In other words, to operate the NGCC at MO requires 147.83% of the fuel the same system requires to reach this 8MW when working at peak power. Due to this huge decrease in efficiency, it can be inferred that it is preferred to manipulate the operation of the chiller plant as presented in section 5.1.1.

5.1.3. Chiller Plant Operation Manipulated (1) and NGCC Turndown (2)

This third strategy combines the strategies presented in sections 5.1.1 and 5.1.2. First, the chiller plant operation is manipulated in order to utilize as much energy as possible. Then, if solar curtailment is still present the NGCC can be turned down as low as to MO. There will be curtailment only if the chiller plant has stored all the energy it requires the following night and the NGCC is operating at MO in order to use as much solar power as possible. Figure 22 debajo de explains the process approached graphically.

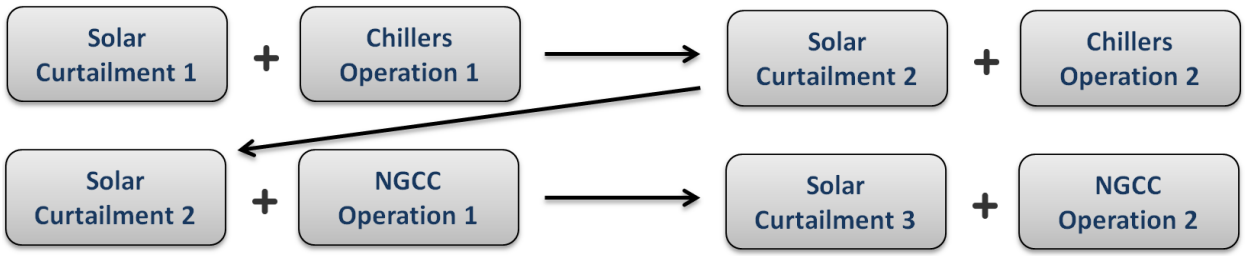

Figure 22: Schematic of the strategy the Hydrogen Energy Storage System model follows in order to first manipulate the chiller plant operation and, second, turn down the NGCC so as to utilize the otherwise-curtailed solar power.

Figure 23 represents a hypothetical case with 7.150 MW (i.e., 2 times the amount of solar existing on campus) has been simulated so as to show how the excess of solar power is treated when manipulating the chiller plant followed by the manipulation of the NGCC is done as explained. It can be observed how the solar curtailment that appeared in the hyphotetical scenarios represented by Figure 15 and Figure 19 is significantly decreased.

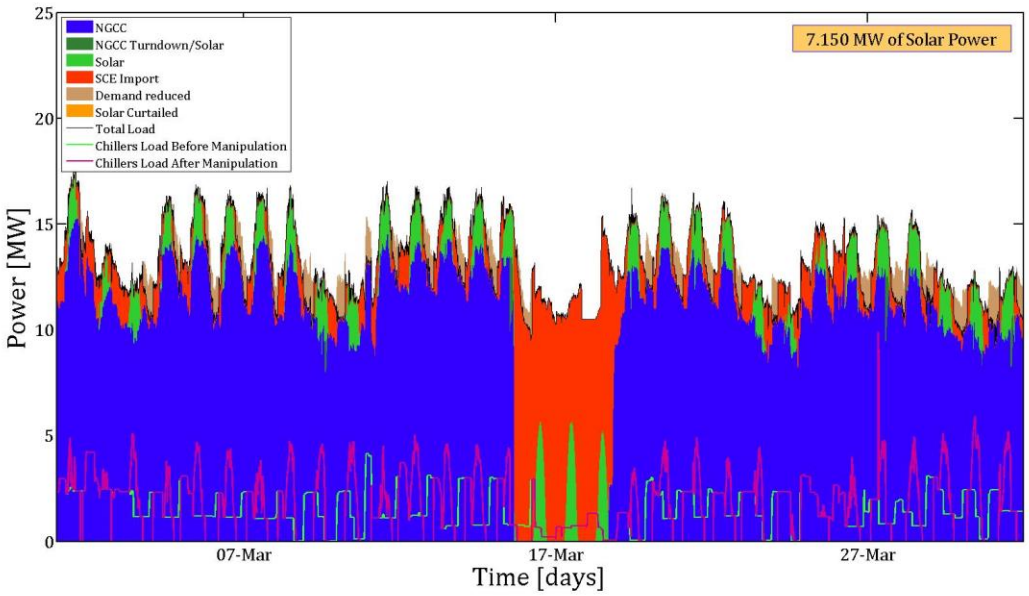

Figure 23: Hypothetical scenario where 2 times the amount of solar PV existent at UCI are installed. First the chiller plant operation and second, the NGCC output power, are modified when required on the month of January. Data of the year 2014 are used.

Figure 24 represents a simulation of the 27th and 28th of March, 2015 rather than a zoom of a day in January like Figure 16, Figure 17, and Figure 20. It does perfectly show how the

chillers store thermally all the energy they will require the following night. Once they have done this, the NGCC is turned down. If after following these two approaches there is still some solar power to utilize, such solar power must be curtailed. This is not the case for 7.150 MW_{peak} of solar used in the UCI Microgrid as shown in Figure 24.

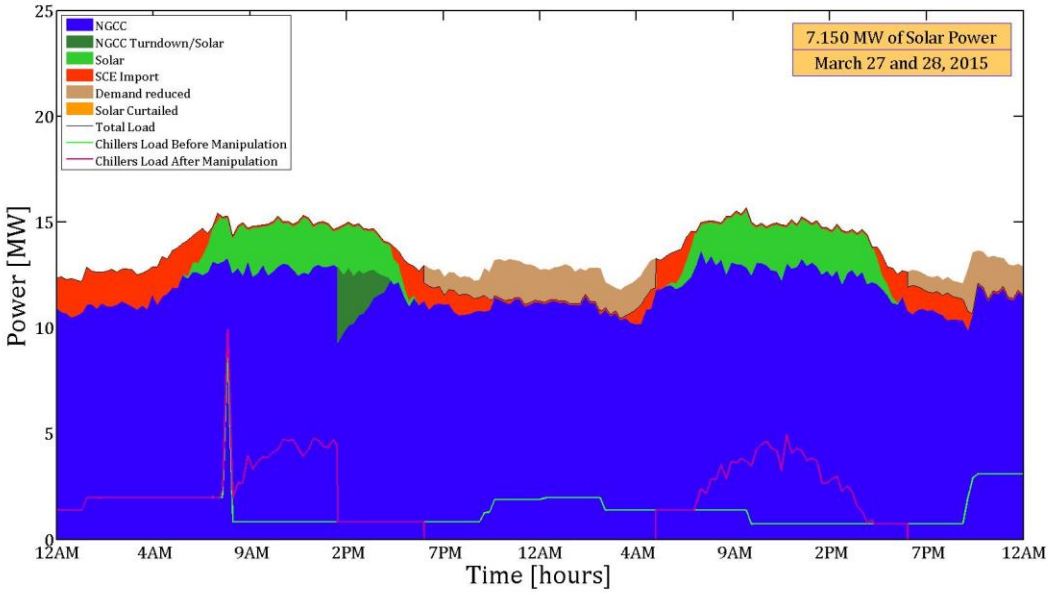

Figure 24: Hypothetical scenario where 2 times the amount of solar PV existent at UCI are installed. First the Chiller Plant Operation and second, the NGCC output power, are modified when required on March 27 and 28, 2015. Data of the year 2014 are used.

This strategy is the best one since it allows a maximum renewable integration using the systems already available at the microgrid (i.e., the chiller plant and the co-gen power plant) and the efficiency of the NGCC is decreased as little as possible since the manipulation of the chiller plant operation is a priority.

5.1.4. NGCC Turndown (1) and Chiller Plant Operation Manipulated (2)

The fourth and last strategy also combines the strategies presented in sections 5.1.1 and 5.1.2. These strategies are approached and used like in section 5.1.3, but in the reverse order. First, the NGCC is turned down so as to utilize as much otherwise-curtailed power as possible. If after doing so, there is still some curtailment present, the chiller plant operation is manipulated in order to utilize as much of this remaining energy as possible, taking always into account the fact that they will have to use it to meet their own demand of the following night. Therefore, solar curtailment is present only if NGCC is operating at its minimum in order to use as much solar power as possible and the chillers have stored all the energy they will require the following night. Figure 25 por encima de explains the process approached graphically.

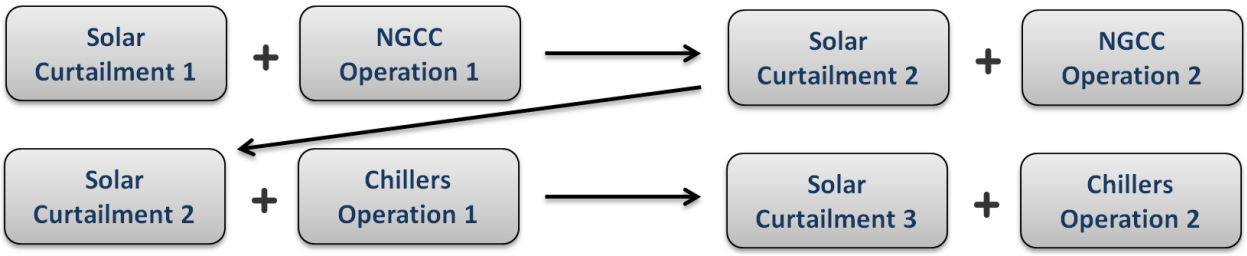

Figure 25: Schematic of the strategy the HESS model follows in order to first turn down the NGCC and, second, manipulate the chiller plant operation so as to utilize the otherwise-curtailed solar power.

Figure 26 represents a hypothetical case with 7.150 MW (i.e., 2 times the amount of solar existing on campus). This scenario has been simulated so as to show how the excess of solar power is treated when manipulating the chiller plant followed by the manipulation of the NGCC.

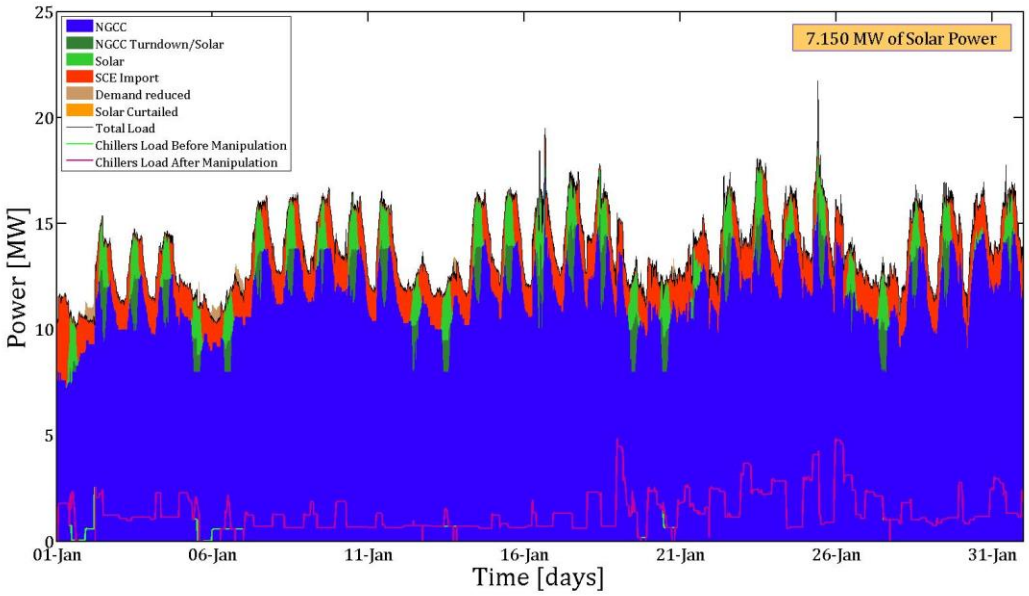

Figure 26: Hypothetical scenario where 2 times the amount of solar PV existent at UCI are installed. First the NGCC output power and second, the chiller plant operation, are modified when required for the month of January. Data of the year 2014 are used.

It can be observed how the days of curtailment and the amount of solar curtailment for these days in the hypothetical scenarios represented in Figure 23 and Figure 26 are the same. It is straightforward to note that this is because the energy the NGCC stops producing in order to accommodate as much of the otherwise-curtailed power plus the energy the chillers store using both strategies is the same. Figure 24 shows a simulation of the 19th and 20th of January, 2015. There is no curtailment at this day due to the fact that all the solar power generated by the canopies installed can be utilized by manipulating the NGCC and chiller plant operations as shown.

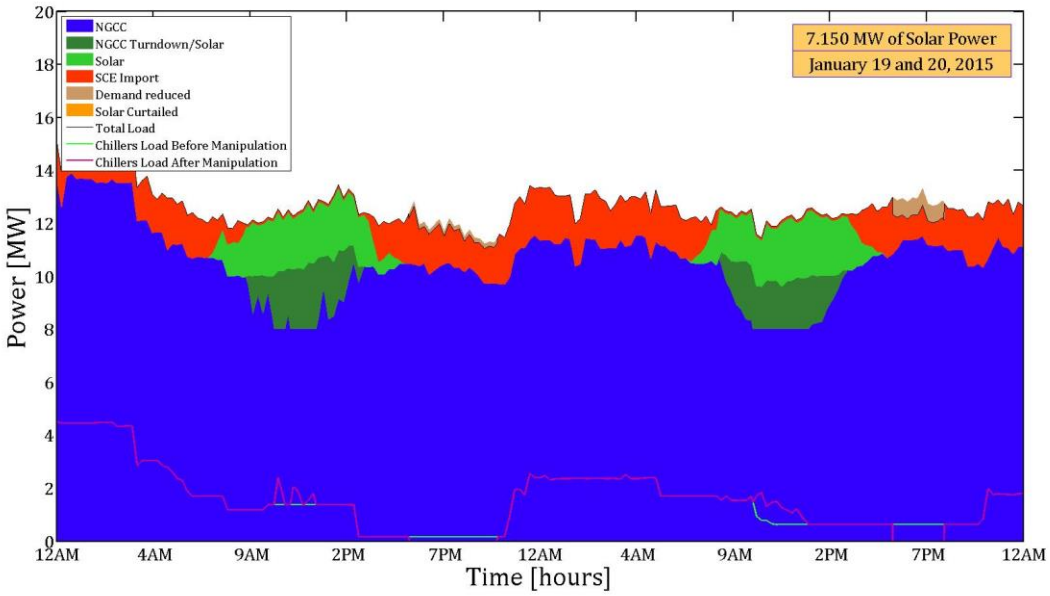

Figure 27: Hypothetical scenario where 2 times the amount of solar PV existent at UCI are installed. First the NGCC output power and second, the chiller plant operation, are modified when required on January 19 and 20, 2015. Data of the year 2014 are used.

5.2. Energy Otherwise-Curtailed Assessment

Different Energy storage strategies can be designed and used in a microgrid so as to utilize the otherwise-curtailed power once the co-gen cycle, the chiller plant, or any other system with an output that can be modified dynamically, are working at their maximum capacities. In this section two different strategies are presented individually and combined with each other. These are: (1) Use of Reversible Fuel Cells (RFC); and (2) Power to Gas (P2G) obtained after blending H_2 with Natural gas (NG) into the existing NG pipelines.

All results presented in this section assume that the chiller plant and the NGCC operations (in this order) have been manipulated as much as possible to absorb otherwise-curtailed solar power.

5.2.1. Use of RFC

In the HESS model excess energy from solar power can be directed to electrolyzers that electrochemically split water into hydrogen and oxygen gas. The use of an electrolyzer prevents the curtailment of renewable energy and allows the smoothing of the net load profile during the hours of high renewable power availability [25]. Hydrogen storage allows the reduction of both renewable energy curtailed and the ramping rate needs. This hydrogen is afterwards stored into an above-the-ground tank. When power is required to meet the demand, the stored hydrogen is converted back to electrical energy in a proton exchange membrane (PEM) fuel cell. PEMFC have the highest power density of all fuel classes, have good start-stop capabilities required for the work it has to do in this project, and do not require high temperatures so as to be operated.

Barbir [59] announced that typical industrial electrolyzers have electricity consumption between 4.5 and 6.0KWh/Nm^3, corresponding to the efficiency of 65–80%. According to O'Hayre et al. [60], the electrical efficiency of PEMFC averages 50%. Barbir et al. [61] also signaled, back in 1997, that in the best case scenario the FC can be produced at $100/KW, operate at 50% efficiency, and generate electricity at <$0.08/KW if hydrogen can be supplied at $10/GJ. Nevertheless, the technology has evolved and nowadays, as Gonzatti et al. [62] stated, the electrical efficiency can go up to 60%.

In the HESS model, the electrical efficiency of the RFC operating in electrolyzer mode is set to 70%. On the other hand, the electrical efficiency of the RFC operating in FC mode is set to 50%. Hence, the round-trip efficiency of the RFC is of 35%. Figure 28 represents a simulation for the 1st and 2nd of April, 2015 where the chiller plant operation is manipulated first, the NGCC is turned down afterwards, and a 250 KW RFC is used if still required.

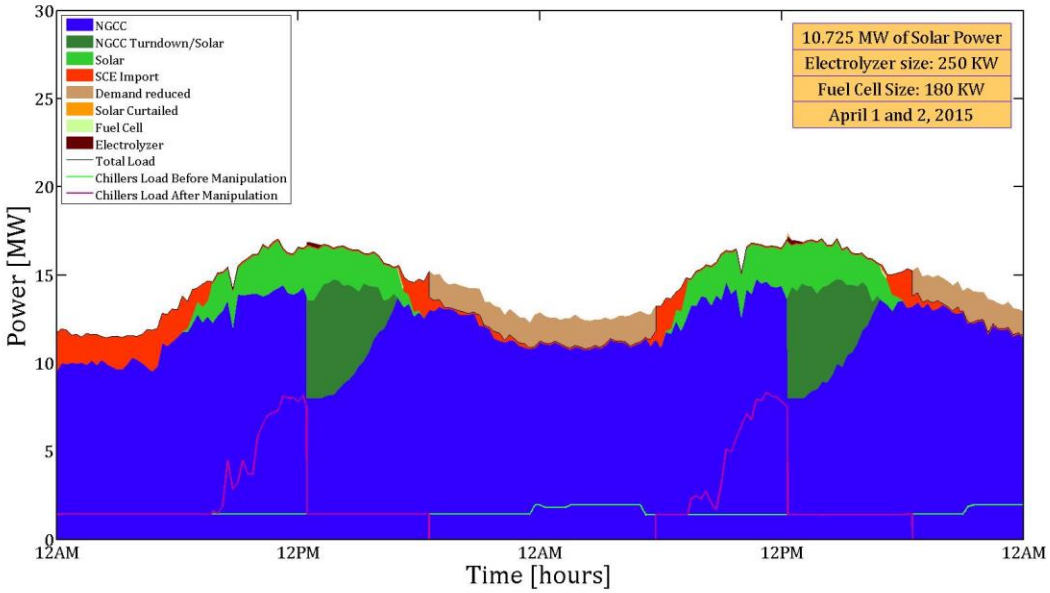

Figure 28: Hypothetical scenario where 3 times the amount of solar PV existent at UCI are installed. First the chiller plant operation and second, the NGCC output power, are modified when required on April 1 and 2,

2015. The remaining otherwise-curtailed power coming from solar is converted to H_2 using a 250 KW electrolyzer. This H_2 is afterwards used to run a 180 KW FC to generate electricity again. Data of the year 2014 are used.

It can be observed how the small amount of power curtailed is significantly reduced when using a 250 KW FC. Figure 29 zooms the area where the electrolyzer and FC power appear so as to better present the way these two function.

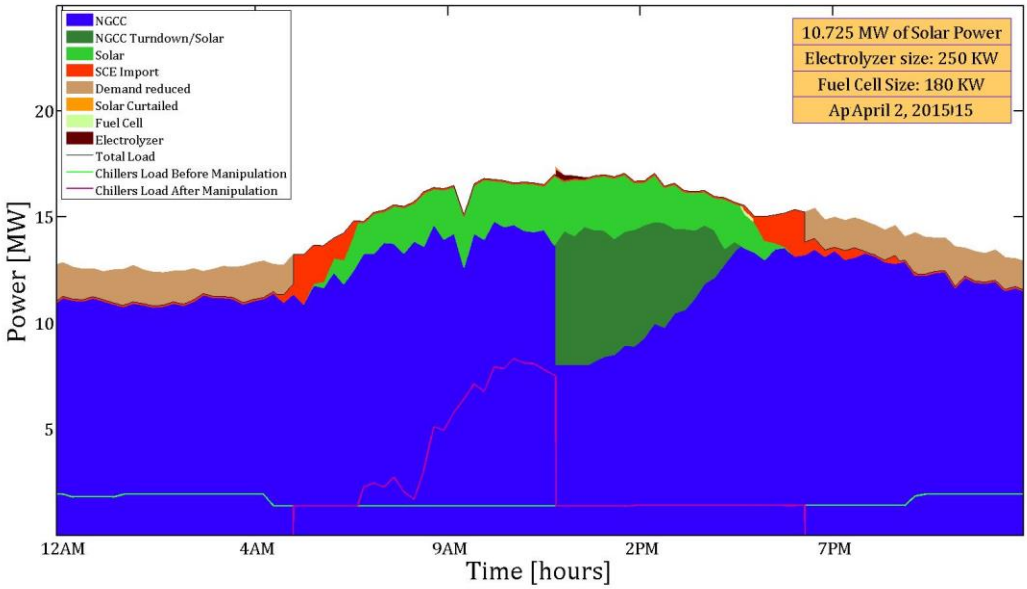

Figure 29: 2nd April of 2015 zoom of the hypothetical scenario where 3 times the amount of solar PV existent at UCI are installed. First the chiller plant operation, and second the NGCC output power, are modified when required on April 2, 2015. The remaining otherwise-curtailed power coming from solar is converted to H_2 using a 250 KW electrolyzer. This H_2 is afterwards used to run a 180 KW FC to generate electricity again. Data of the year 2014 are used.

Installing a 250 KW RFC in a microgrid similar to the one of study is not going to be outstanding since the size of this RFC roughly represents 1 – 1.5% of the total load when working at its maximum capacity. Figure 30 debajo de shows how the RFC effect would be if this one was sized to be 2.5 MW for a couple of days in January where the solar curtailment was still present after manipulating both the chiller plant and the NGCC operations.

From Figure 30 it can be inferred that the bigger the RFC size and the H_2 storage tank capacity, the greater the renewable integration will be and the smoother the SCE import power will be.

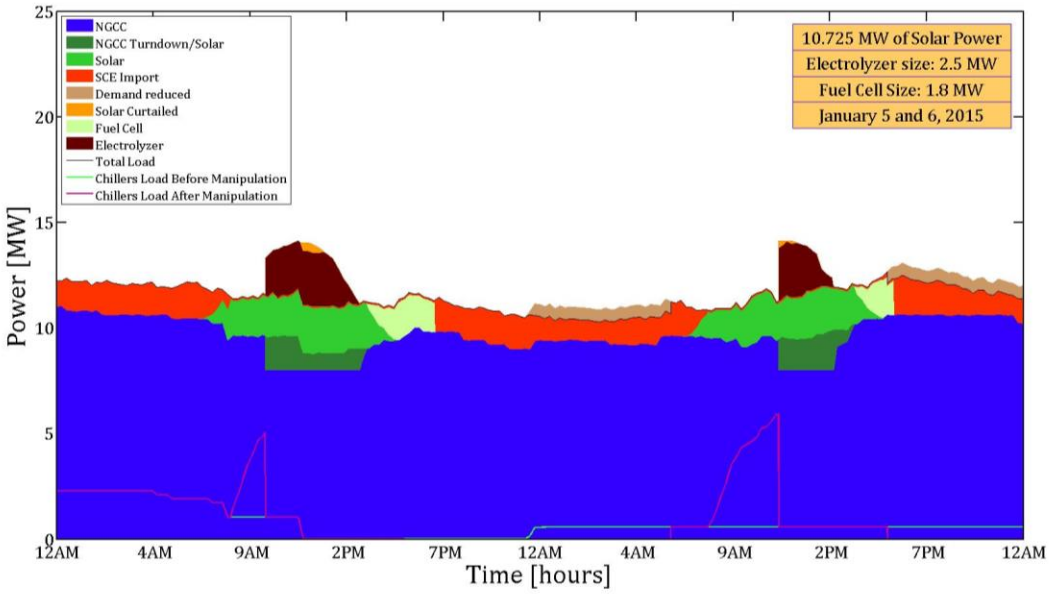

Figure 30: Hypothetical scenario where 3 times the amount of solar PV existent at UCI are installed. First the chiller plant operation, and second the NGCC output power, are modified when required on January 5 and 6, 2015. The remaining otherwise-curtailed power coming from solar is converted to H_2 and to electricity again when required using a 1,800 KW FC. Data of the year 2014 are used.

5.2.2. Power-to-Gas

The introduction of renewable gas into the NG pipeline can increase the overall renewable integration of a microgrid. The HESS model converts the otherwise-curtailed solar power remaining into H_2, after having manipulated the chiller plant and the NGCC operations as explained. This renewable gas obtained is then blended into the NG pipeline that feeds the GT. Figure 31 debajo de represents the hypothetical scenario where the otherwise-curtailed solar power is converted to hydrogen and blended into the NG pipeline. A maximum 5% of blending is allowed in this case scenario.

By looking at the scenario represented in the figure debajo de, it can be observed how the renewable integration is considerably increased. By following the P2G approach not only renewable energy is obtained from solar during the day, but also during the night. Figure 32 shows a zoom to the 15th and 16th of January, 2015.

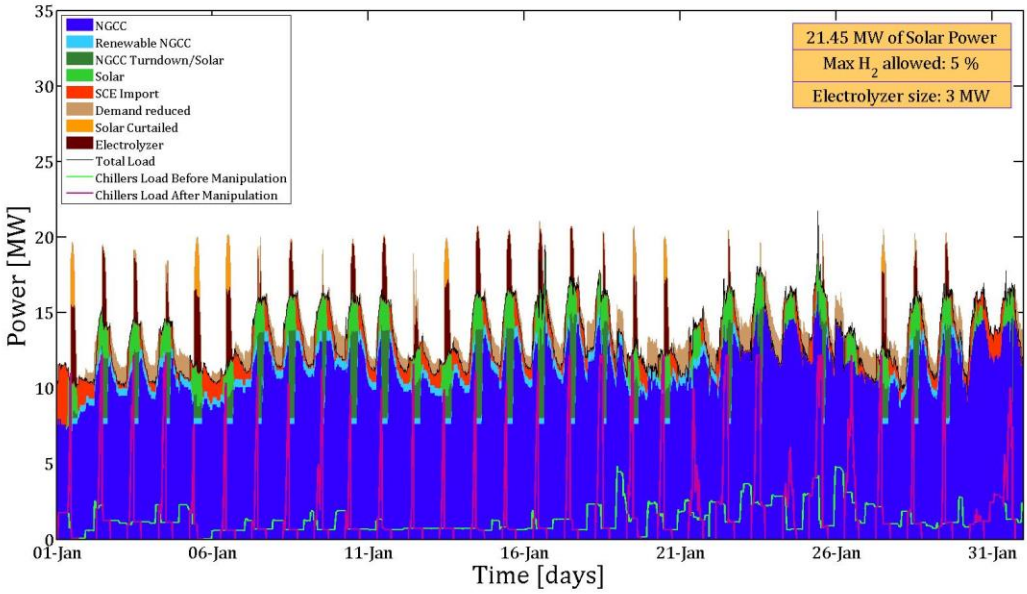

Figure 31: Hypothetical scenario where 6 times the amount of solar PV existent at UCI are installed. First the chiller plant operation, and second the NGCC output power, are modified when required for the month of January. The remaining otherwise-curtailed power coming from solar is converted to H_2 using a 3,000 KW electrolyzer. This H_2 is blended with NG at the NG pipeline which feeds the GT. Data of the year 2014 are used.

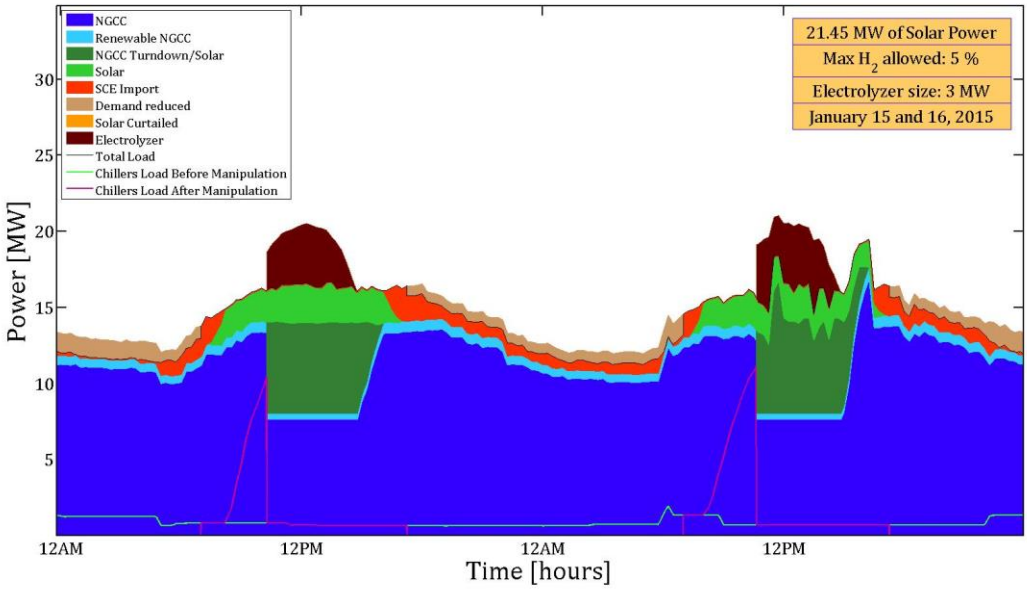

Figure 32: Zoom of the hypothetical scenario where 6 times the amount of solar PV existent at UCI are installed. First the chiller plant operation, and second the NGCC output power, are modified when required on January 15 and 16, 2015. The remaining otherwise-curtailed power coming from solar is converted to H_2 using a 3,000 KW electrolyzer. This H_2 is blended with NG at the NG pipeline which feeds the GT. Data of the year 2014 are used.

5.3. Maximum Amounts of Renewable Integration

The way to dynamically operate a microgrid is as important as the amount of renewable energy that can be installed there. Otherwise, the excess of green energy needs to be curtailed. Both of the strategies presented allow integrating more of the solar power generated. However, so as to choose which one to implement it is also necessary to know which percentage of renewable integration is achieved if they are used without or in combination with energy storage systems.

To account for the amount of solar that can be installed in a microgrid if only the chiller plant operation is modified in order to store the solar power thermally as described in this

thesis when no energy storage systems are used, Equation (10) is used. Basically, the equation supposes that the chiller plant is working at its maximum capacity.

$$\mathrm{MaxRE}_{\mathrm{noES_CH}} = \min_{(>0)}\{[(\mathrm{Load_i}) - (\mathrm{NGCC_i}) + (\mathrm{CPC} - \mathrm{Chillers_i}) - (\mathrm{SCE_{min}})] \cdot (1_{\mathrm{PV}>0} + 0_{\mathrm{PV}=0})]\ \} \qquad (10)$$

where $Load_i$ represents the load demand at each moment in MW; $NGCC_i$ is the NGCC power at each moment; CPC = 12.18MW (i.e., maximum Chillers Power Capacity); $Chillers_i$ symbolizes the chillers load at each moment, and SCE_{min} = 0.1MW. The operation $(\mathrm{CPC} - \mathrm{Chiller_i})$ is done so as to account for the increase in demand it would appear if the chiller plant was operated at its maximum capacity. Recall that the chillers load is included on the total load demand and therefore needs to be subtracted from this one.

On the other hand, if energy storage is available in this scenario, the maximum renewable integration can be computed using Equation (11) below.

$$\mathrm{MaxRE}_{\mathrm{ES_CH}} = \frac{\sum_{\mathrm{i}=1}^{365}\{\left[(\mathrm{Demand_i}) + \left(\mathrm{Chillers_{night}}\right) - (\mathrm{NGCC_i}) - (\mathrm{SCE_i})\right] \cdot (1_{\mathrm{PV}>0} + 0_{\mathrm{PV}=0})\}}{\text{Annual Demand Energy}} \cdot 100\% \qquad (11)$$

where $Demand_i$ is the day i energy demand; $Chillers_{night}$ stands for the maximum amount of energy the chillers can store in day i, which is equivalent to the energy they will require the following night; $NGCC_i$ represents energy produced in day i by the NGCC if its operation is not modified at all; and (SCE_i) is the minimum amount of energy required to be imported from SCE taking into account that a minimum constant import of 100KW is required.

Equation (12) shows the amount of solar power that can be installed in a microgrid if no curtailment is allowed (i.e., all the renewable power is used) and the NGCC is working at MO the whole year.

$$\mathrm{MaxRE}_{\mathrm{noES_NGCC}} = \min_{(>0)}\{[(\mathrm{Load_i}) - (\mathrm{MO}) - (\mathrm{SCE_{min}})] \cdot (1_{\mathrm{PV}>0} + 0_{\mathrm{PV}=0})] \} \quad (12)$$

where $MO = 8$ MW (i.e., minimum operation of the NGCC).

Alternatively, if energy storage systems are included, Equation (12) is used to account for the renewable integration.

$$\mathrm{MaxRE}_{\mathrm{ES_Chiller}} = \frac{\sum_{i=1}^{365}\{[(\mathrm{Demand_i}) + (\mathrm{MO_i}) - (\mathrm{SCE_i})] \cdot (1_{\mathrm{PV}>0} + 0_{\mathrm{PV}=0})\}}{\text{Annual Demand Energy}} \cdot 100\% \quad (13)$$

where (MO_i) stands for the energy required in day i for a constant NGCC output power of 8 MW.

If both the chiller plant and NGCC operations can be manipulated, the maximum amount of solar power that can be utilized without having to curtail (i.e., without energy storage systems) is obtained using Equation (14). In this scenario the NGCC is working the whole time at MO and the chillers are storing as much energy as possible.

$$\mathrm{MaxRE}_{\mathrm{noES}} = \min_{(>0)}\{[(\mathrm{Load_i}) - (\mathrm{MO}) + (\mathrm{CPC} - \mathrm{Chillers_i}) - (\mathrm{SCE_{min}})] \cdot (1_{\mathrm{PV}>0} + 0_{\mathrm{PV}=0})] \} \quad (14)$$

Finally, if not only these two operations can be manipulated but also energy storage systems are used, the maximum amount of renewable penetration can be expressed using Equation (15).

$$\mathrm{MaxRE}_{\mathrm{ES}} = \frac{\sum_{i=1}^{365}\{(\mathrm{Demand_i}) + (\mathrm{Chillers_i}) - (\mathrm{MO_i}) \cdot (1_{\mathrm{Solar}\geq 0} + 0_{\mathrm{Solar}<0})\}}{\text{Annual Demand Energy}} \cdot 100\% \quad (15)$$

6. Results

In section 5 data from 2014 have been used in order to show how the model works. In this section, however, data from January 1, 2015 to June 30, 2015 are used. Equation (2) is therefore modified and expressed as Equation (16) presents.

$$\text{Demand [MW]} = (\text{NGCC Power})_{2015} + (\text{Solar Power})_{2015} + (\text{SCE Power})_{2015} \qquad (16)$$

where $(NGCC\ Power)_{2015}$ is the power the NGCC produced during the whole year 2015; $(Solar\ Power)_{2015}$ is the solar power that was produced during 2015 by the 3.575 MW of solar power that was installed on campus. Since the installation of all the solar panel canopies did not complete until May 2015, the available data at each month has been scaled following the approach presented by Equation (1), For example, if just 1.941 MW out of the 3.575 MW were available, the data is scaled by a factor K of value 1.84; and $(SCE\ Power)_{2015}$ is the power the campus imported from Southern California Edison in 2015. The chillers load is again indirectly included in the total load demand.

The annual results are computed multiplying the half year results obtained by 2.017 when required. This value comes from the ratio of the total number of days of the day 2015 (365) and the number of days from January 1 to June 30 of this same year (181), which are the data points available.

One of the usages of the model is to analyze up to how much solar can the microgrid handle and which strategies are needed to implement this addition. The feasibility of introducing 2 MW of extra solar power to the existing 3.575 MW is studied and presented in the present section as a case example. The work includes an analysis of the Greenhouse Gas emissions

impact, as well as a brief economic analysis of such a solar power penetration. Moreover, results summarizing the renewable strategies proposed and signaling the maximum amounts of renewable integration that can be achieved with and without energy storage are presented and discussed.

As commented in the beginning of section 5, the UCI microgrid campus has not had to curtail any of the power produced by the solar canopies installed on campus. Hence, the renewable integration of the campus is of 3.48%. That is, all the power coming from the existing 3.575 MW is fully utilized. To do so, the central plant facilities management team has been, from time to time, modifying the way the electric chillers operate. Figure 33 and Figure 34 show how the UCI microgrid operates at the moment. Again, the NGCC power gap present in the moment of June is due to one of the scheduled maintenances the Central plant facilities team carries out every year.

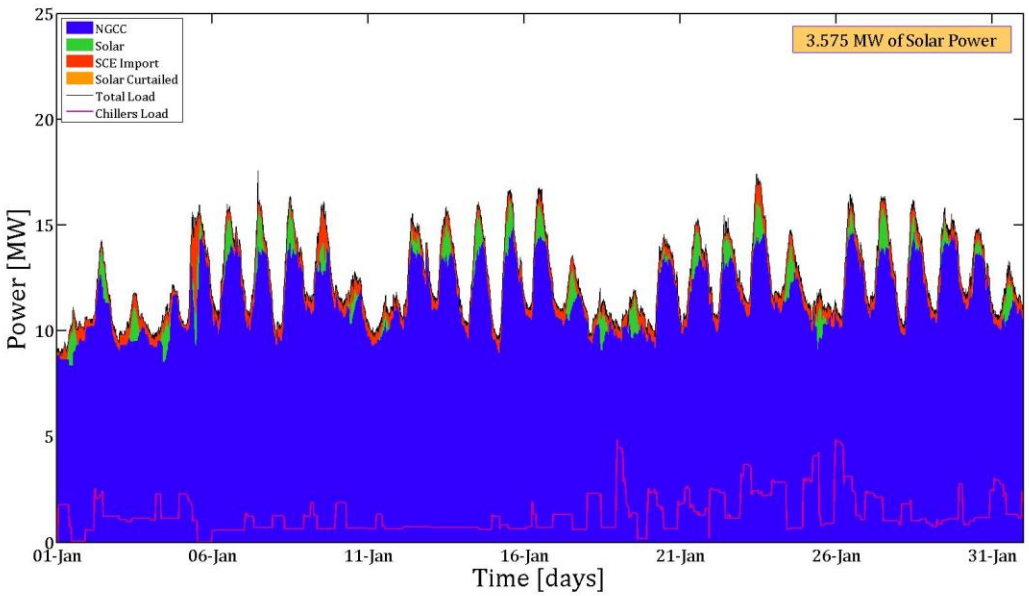

Figure 33: 2015 UCI dispatch of power for the month of January. Neither the NGCC nor the chiller plant operation is modified.

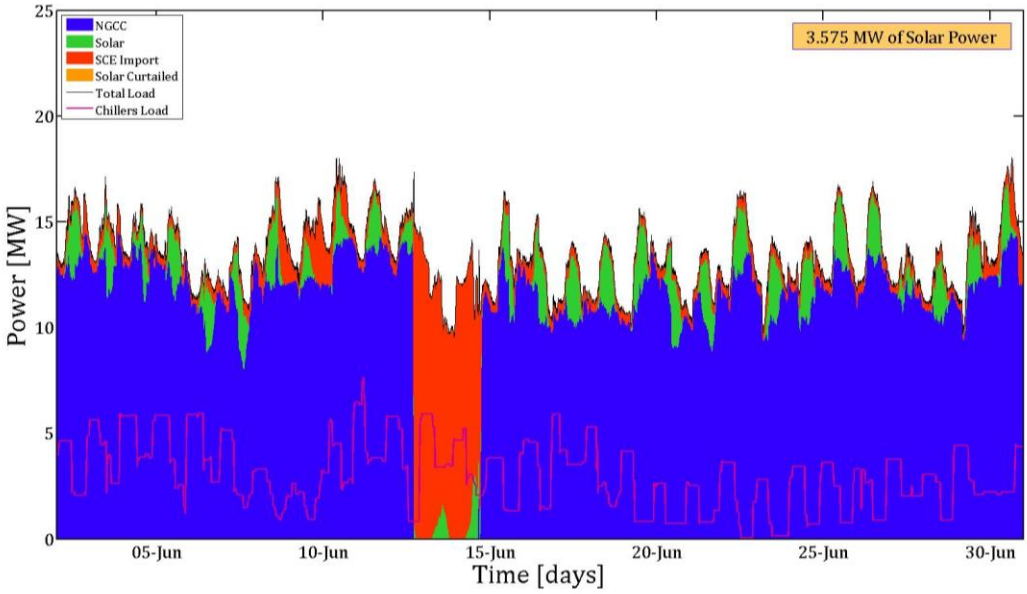

Figure 34: 2015 UCI dispatch of power for the month of June. Neither the NGCC nor the chiller plant operation is modified.

As expected, these two figures por encima de follow the trend presented in Figure 10 and Figure 11, respectively. The main difference to them is that in Figure 33 and Figure 34 the import power has been decreased considerably. However, this import is kept constant because at hours of peak demand, the solar power helps the NGCC meet almost all the load. Figure 35 helps understanding the contribution of each of the power sources existent to the overall microgrid load demand.

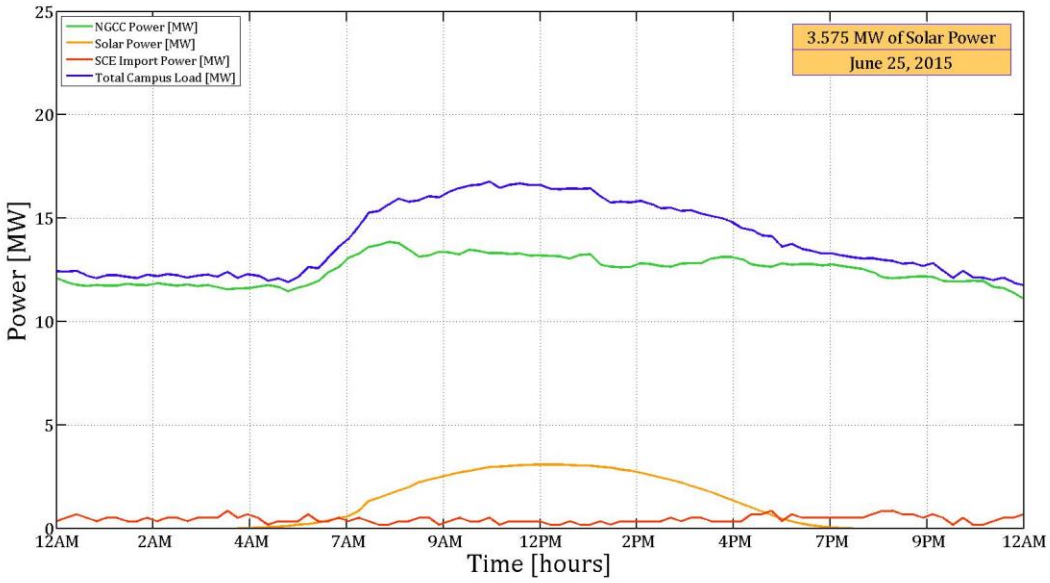

Figure 35: June 25, 2015 daily loads. Neither the NGCC nor the Chiller Plant Operation is modified.

6.1. Feasibility of Introducing 2 MW of Extra Solar Power to the UCI Microgrid

It is evident that if none of the control strategies proposed are approached, solar power curtailed appears when installing these 2 MW of extra solar PV. This occurs due to the fact that during sun hours the SCE Import is kept very low as Figure 33 and Figure 34 show. Coming up next, a hypothetical case where neither the NGCC nor the chiller plant operations are modified is presented by Figure 36 and Figure 37. Curtailment is present 30% of the time of the whole year, 63% of the time the sun is shining. Thus, control strategies must be implemented if all the energy coming from solar wants to be utilized.

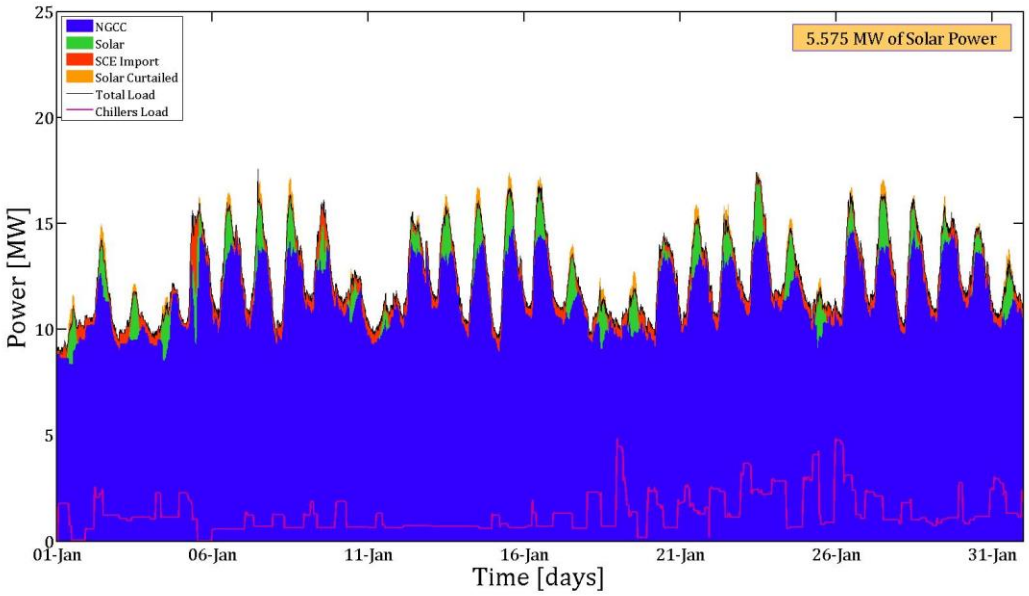

Figure 36: UCI dispatch of power for the month of January with all the PV being installed in 2015 available. Neither the NGCC nor the chiller plant operation is modified. 2015 data is used.

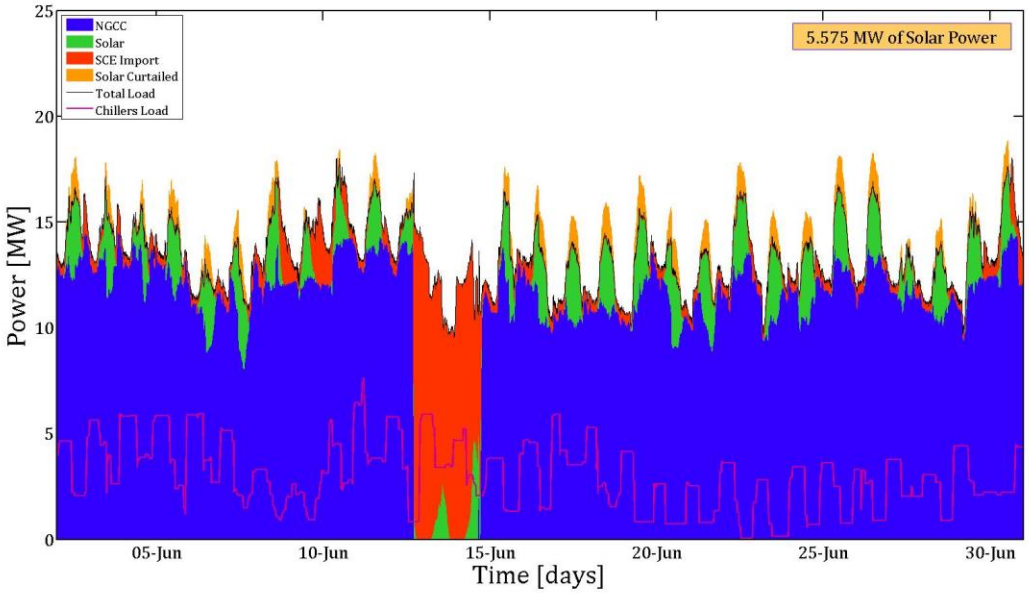

Figure 37: UCI dispatch of power for the month of June with all the PV being installed in 2015 available. Neither the NGCC nor the chiller pant operation is modified. 2015 data is used.

6.1.1. Best Control Strategy

In this subsection the four different control strategies that modify the way the power is dispatched presented in section 5 are studied and presented.

6.1.1.1. Control Strategies Analysis

Chiller Plant Operation Manipulated

By using this strategy most of the solar power is used as Figure 38 shows. It can be observed how the solar curtailment that did appear in Figure 36 is no longer present because the chiller plant operation has been manipulated in order to accommodate it. The remaining otherwise-curtailed energy from solar has been stored and used during the following night.

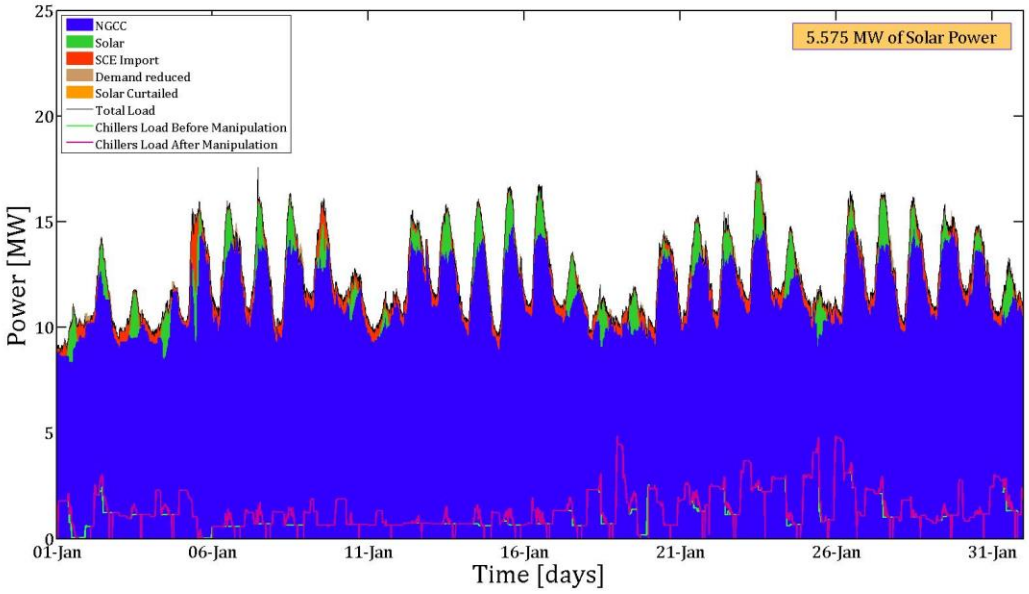

Figure 38: Hypothetical scenario where 2 extra MW are added to the 3.575 MW of solar power existent at the UCI microgrid for the month of January. Just the chiller plant operation is manipulated. Data of the year 2015 are used.

One of the biggest and most difficult concerns when following such a control strategy is to know the amount of time the system operation is required to be modified. By using the most recent data, the HESS model is able to obtain pretty good approximations that solve these questions. Figure 39 shows the increased chiller plant power and the number of hours they need to do so when following the strategy analyzed in this subsection. Even though its capacity needs to be increased a 26.10% of the time, which represents 357 out of 365 days, approximately just 70 hours they need to do so by 1.5 MW. Therefore, the increased capacity required is low but the chiller plant operation must be modified almost every day of the year.

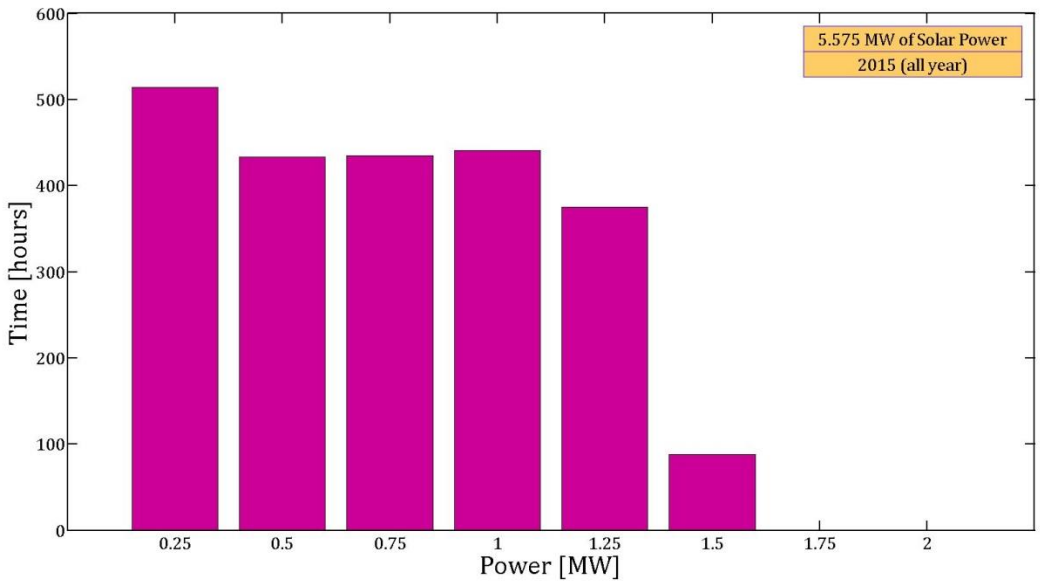

Figure 39: Bar graph of the increased chiller plant capacity vs. number of hours they need to do so when following the strategy of just manipulating the chiller plant operation. Data of the year 2015 are used.

Figure 40 and Figure 41 represent a typical and the worst day of operations when following this strategy, respectively. In the typical day represented the maximum increased chiller plant capacity is of 0.87 MW. However, in May 19 (i.e., the worst day) the maximum increased chiller plant capacity is of 1.73 MW. Either way, both Figures show how the

campus works fine even though the overall system is stressed and curtailment exists at some hours as section 5.3 will present.

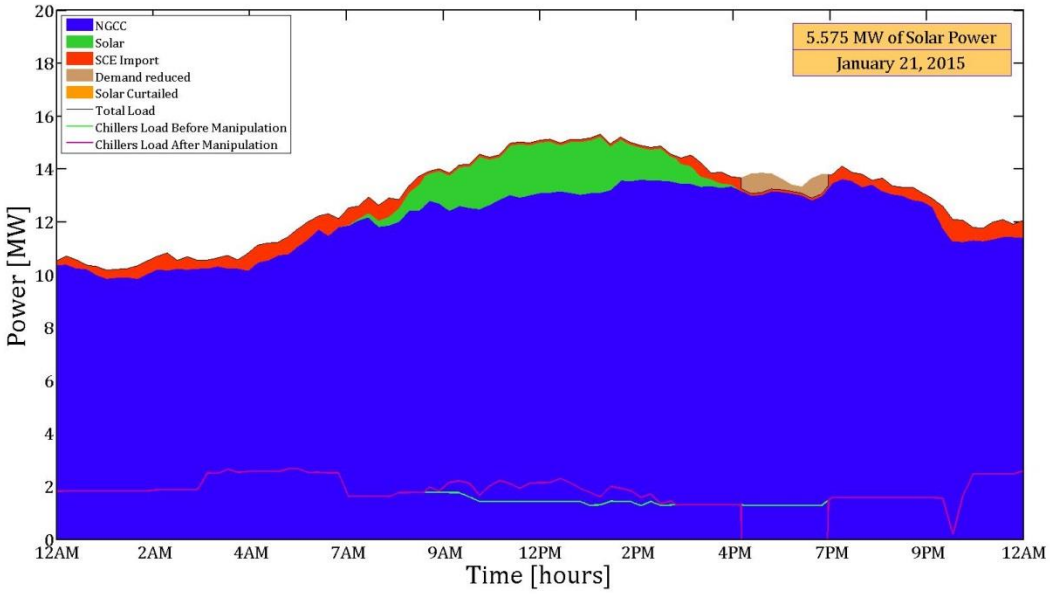

Figure 40: Typical day (i.e. day with normal TES storage) of the year for the hypothetical scenario where 2 extra MW are added to the 3.575 MW of solar power existent at the UCI microgrid. Just the chiller plant operation is manipulated. Data of the year 2015 are used.

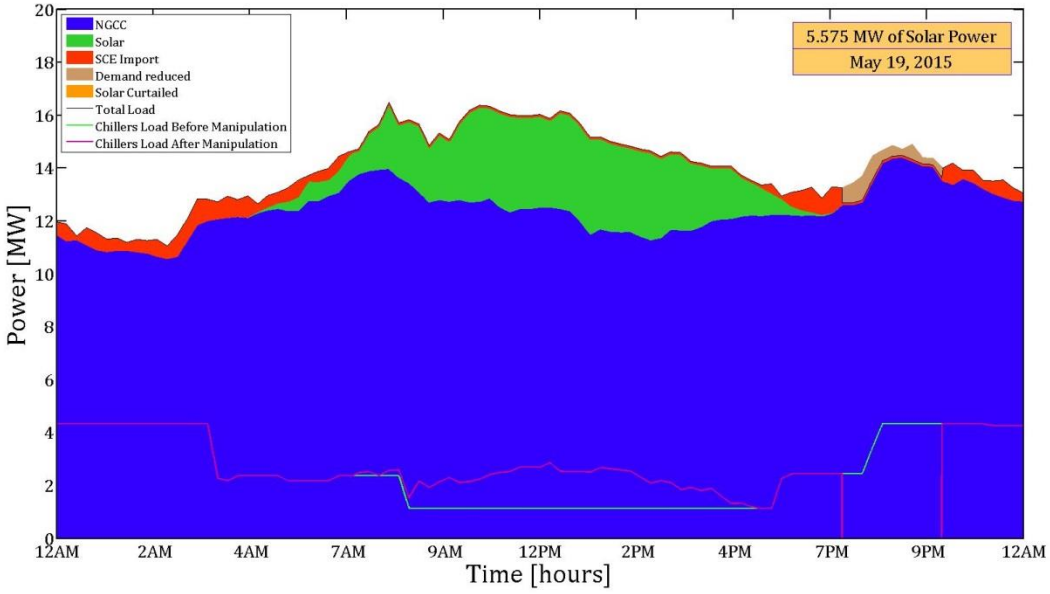

Figure 41: Worst day (i.e. day with higher TES storage) of the year for the hypothetical scenario where 2 extra MW are added to the 3.575 MW of solar power existent at the UCI microgrid. Just the chiller plant operation is manipulated. Data of the year 2015 are used.

NGCC Power Manipulation

As the simulation of the month of January showed debajo de shows, the problem of having to curtail part of the solar generated does no longer hold when following this strategy either.

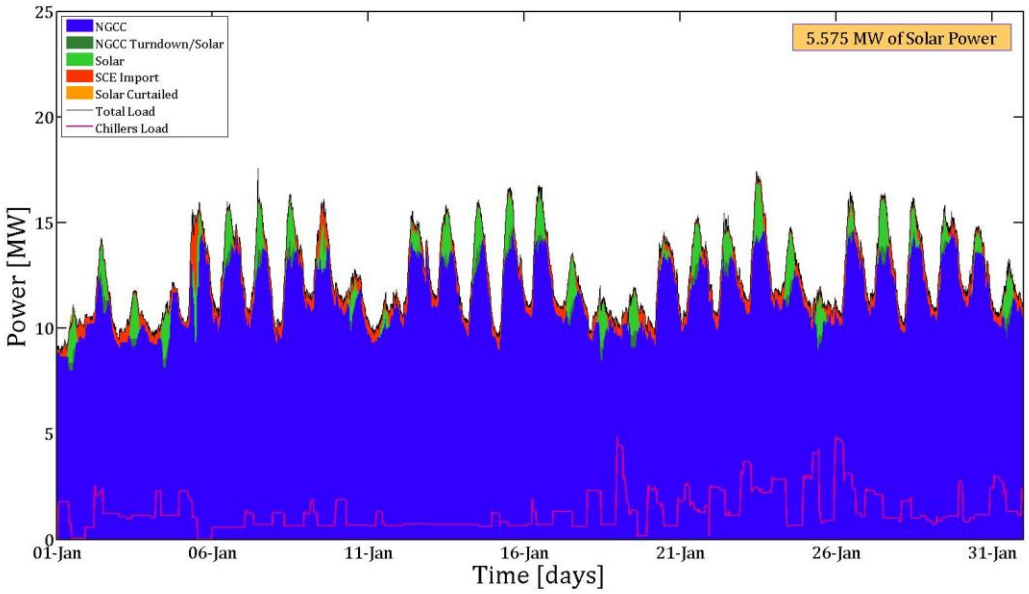

Figure 42: Hypothetical scenario where 2 extra MW are added to the 3.575 MW of solar power existent at the UCI microgrid for the month of January. Just the NGCC operation is turned down when required. Data of the year 2015 are used.

Nevertheless, as in the previous case where just the chiller plant operation was manipulated, when turning down the NGCC is also (and even more) important to account for the number of hours that there is turndown. Also, it is important to account for the amount of power turned down. By doing so not only an idea of how much time it is required to change the way the NGCC currently operates is obtained, but also an idea of by how many efficiency percentage points the system operation decreases.

Figure 43 shows that the operation of the NGCC before and after turning it down so as to utilize the maximum otherwise-curtailed power at each moment is pretty similar. The NGCC operates more at lower outputs and not as much at upper outputs after being turned down, as expected. The biggest consequence of this trend is, as it has already been commented in section 5.1.2.1, the decrease of the NGCC efficiency. The more the NGCC efficiency decreases, the bigger the amount of fuel required to obtain the energy required is. In this scenario the NGCC efficiency decreases by 0.58 percentage points going from 36.65% to 36.07%. In other words, this means that so as to obtain the same power output before and after turning the NGCC down, 1.41% more of fuel needs to be burnt.

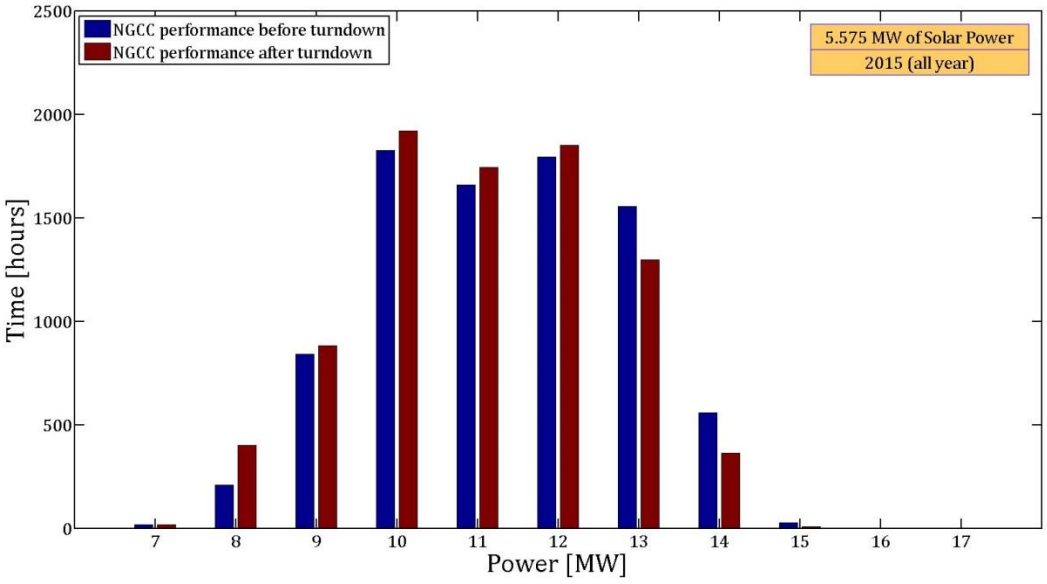

Figure 43: Bar graph of the NGCC power before and after manipulating its operation vs. number of hours the NGCC operates at each of the power outputs when following the strategy of just turning down the NGCC. Data of the year 2015 are used.

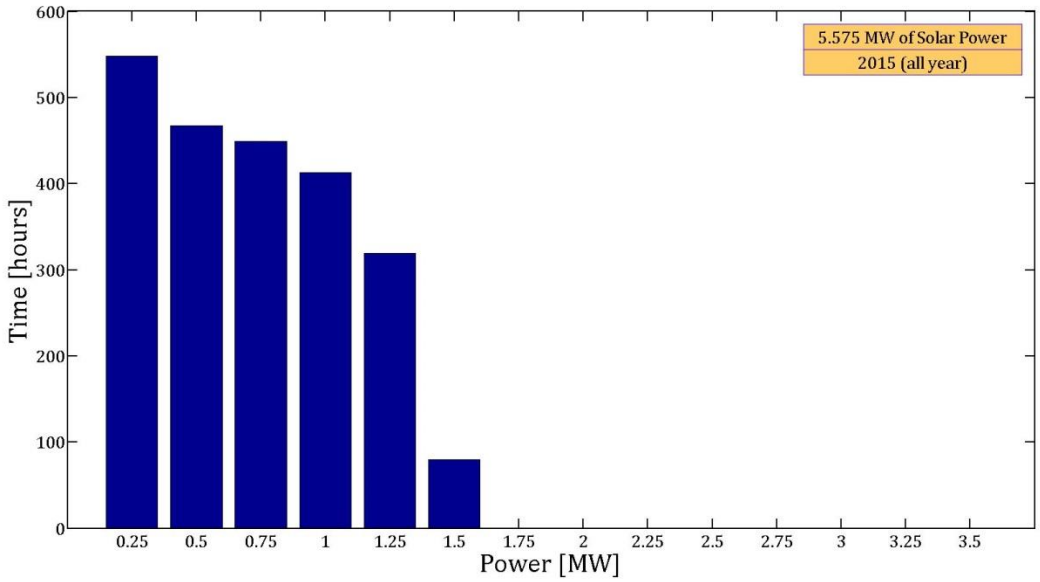

Figure 44: Bar graph of the NGCC turndown power vs. number of hours it is needed to do so when following the strategy of just turning down the NGCC. Data of the year 2015 are used.

Results show that the NGCC needs to be turned down a total of 2,276 hours throughout the whole year. This represents a 25.98% of the time, which is a percentage very similar to the one obtained in the previous case where just the manipulation of the current chiller plant operation was carried out. The average NGCC power before and after the turndown is of 11.53 MW and 11.30 MW, respectively. Thus, not much of a change is observed. Again, the amount of power the NGCC needs to be turned down is not as relevant as the number of days it has to do so, which are 357 out of 365. Hence, the NGCC operation also needs to be manipulated almost every day if this strategy is to be followed.

Figure 45 and Figure 46 represent how a typical day and the worst day, respectively, look like when turning down the NGCC as described. In the typical day represented the maximum NGCC turndown is of 0.87 MW. However, in May 19, 2015 (i.e., the worst day) the maximum NGCC turndown power is of 1.73 MW, too. These results look the same as the

ones obtained in the previous case since when just a total of 5.575 MW of solar power are available on campus, almost never the chillers store all the energy they require for the following night nor the NGCC is turned down up to MO.

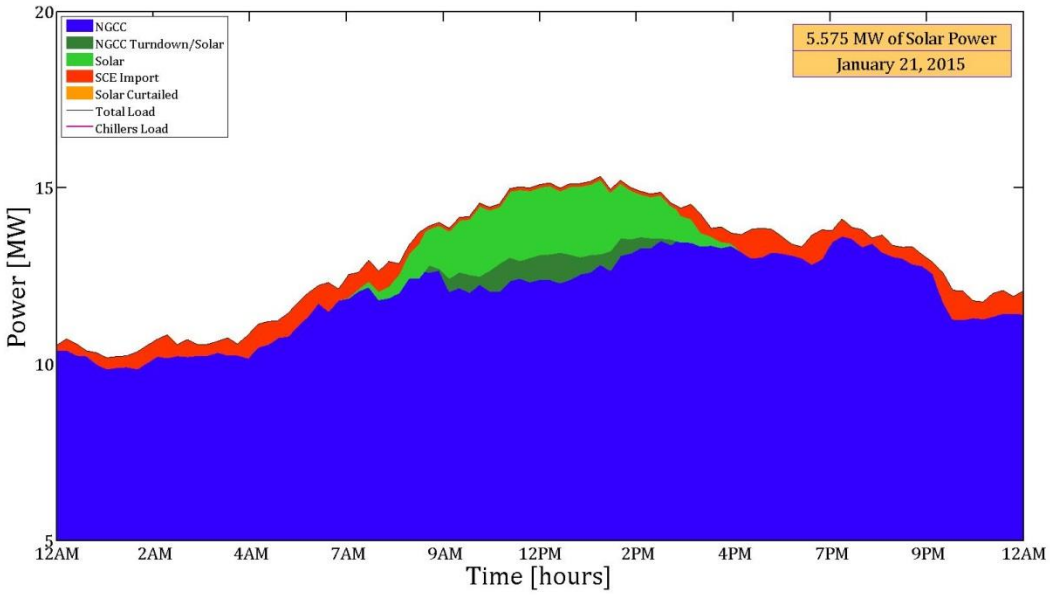

Figure 45: Typical day of the year for the hypothetical scenario where 2 extra MW are added to the 3.575 MW of solar power existent at the UCI microgrid. Just the NGCC is turned down when required. Data of the year 2015 are used.

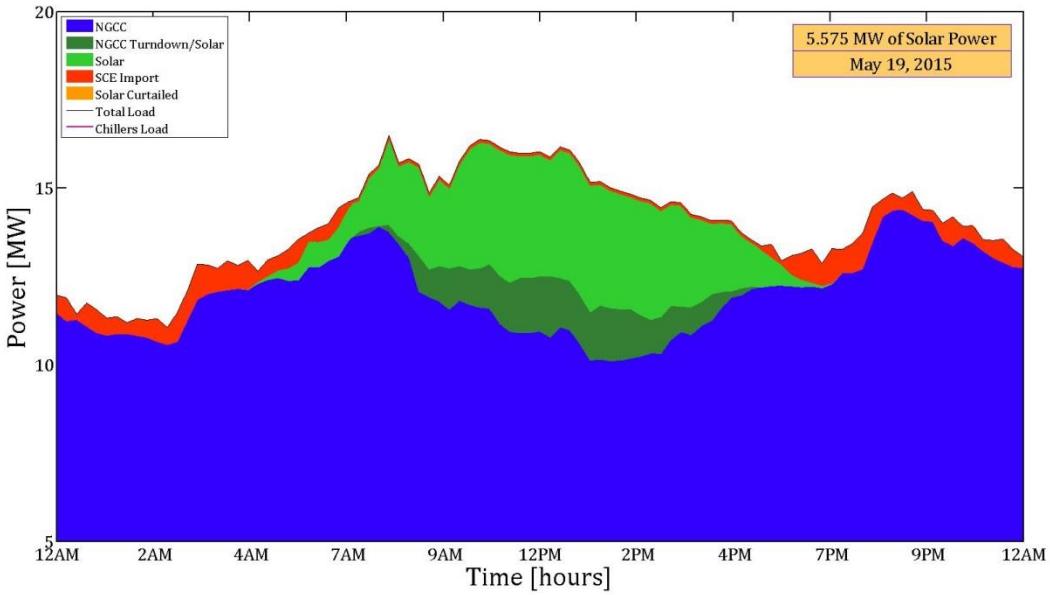

Figure 46: Worst day of the year for the hypothetical scenario where 2 extra MW are added to the 3.575 MW of solar power existent at the UCI microgrid. Just the NGCC is turned down when required. Data of the year 2015 are used.

Chiller Plant Operation Manipulated (1) and NGCC Turndown (2)

When combining both strategies but operating first the chiller plant, no NGCC turndown appears on any day of the month of January as Figure 38 showed. For this reason, the month of March is presented in Figure 47. In this Figure both the chiller plant and the NGCC operations need to be manipulated at some point. The NGCC power gap observed is due to a scheduled maintenance. Also, as it will be announced and explained in section 5.3, when combining both strategies no curtailment appears throughout the whole year.

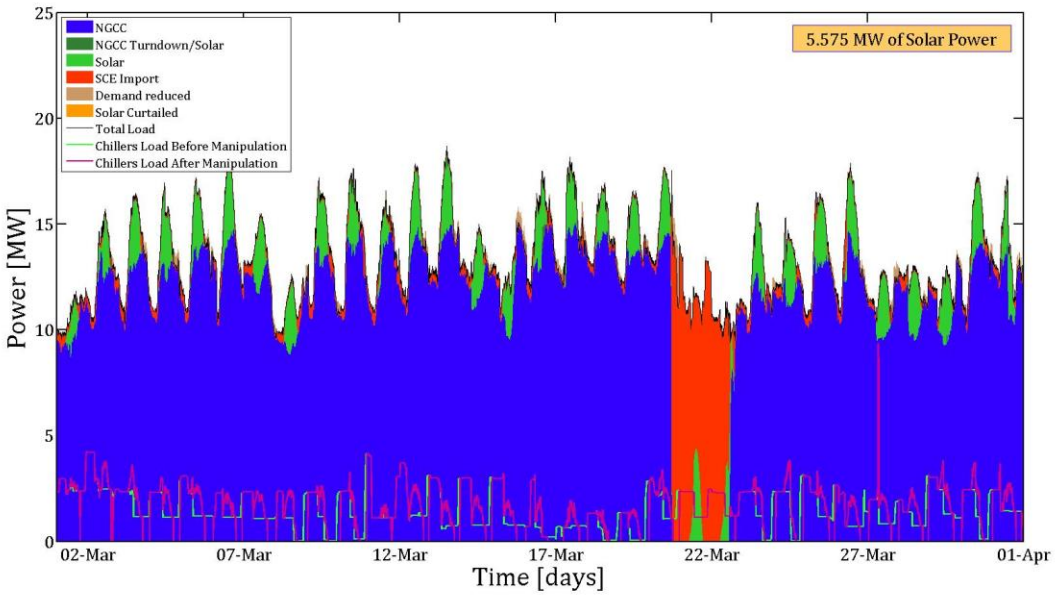

Figure 47: Hypothetical scenario where 2 extra MW are added to the 3.575 MW of solar power existent at the UCI microgrid for the month of March. First, the chiller plant operation is manipulated and, second, the NGCC operation is turned down when required. Data of the year 2015 are used.

In this scenario the chiller plant is operated pretty much the same way than in the case where just the manipulation of the chiller plant operation is present. They can store more energy at some point because the NGCC has the availability to turn down as explained in section 5. However, as Figure 48 shows, in this scenario, the operation of the chiller plant is very similar to the one presented in Figure 39. Thus, its operation is increased 26.11% of

the total year to store the otherwise-curtailed power. Again, this percentage represents 357 days of the whole year.

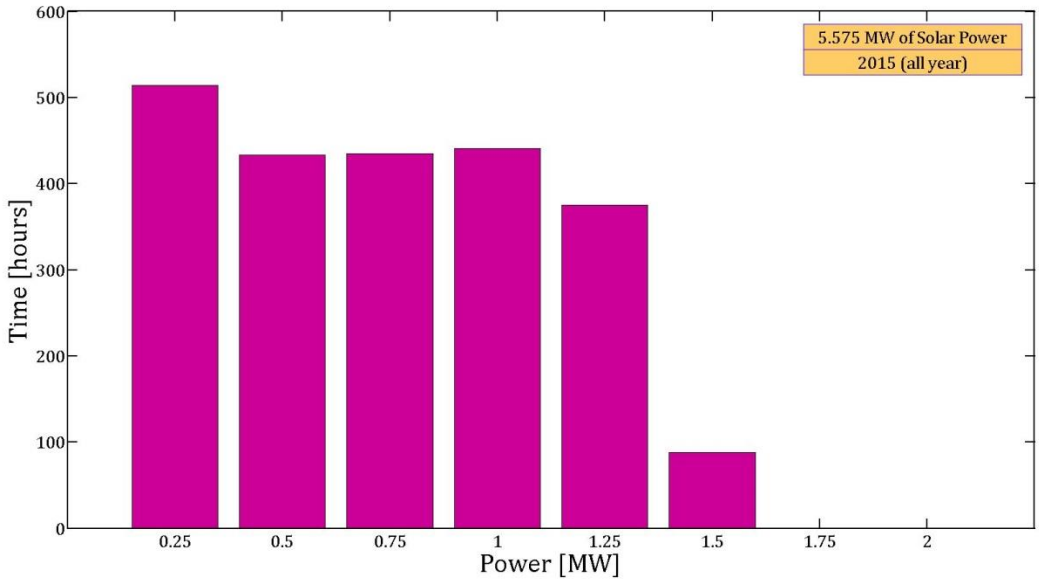

Figure 48: Bar graph of the increased chiller plant capacity vs. number of hours they need to do so when following the strategy of manipulating the chiller plant operation first and then turning down the NGCC when required. Data of the year 2015 are used.

In this 2 MW of extra solar PV scenario, the NGCC power is just required to be turned down 2 days of the whole year for a total of 4.62 hours. That is to say tha just 0.05% of the time this control strategy needs to be approached and added to the manipulation of the chiller plant operation. This small requirement of turning down the NGCC can be easily observed by looking at Figure 49 and Figure 50. Figure 49 shows that the NGCC output power stays pretty much the same before and after the NGCC operation is modified. Figure 50 shows how the number of hours the turndown is required is quite small. The efficiency of the co-gen cycle just decreases by 0.09 percentage points, going from an overall efficiency of 36.65% to an overall efficiency of 36.56%.

The most important conclusion to obtain from this subsection is that the fact of having to turn down the NGCC a little bit indicates that if just the chiller plant operation is manipulated the system will be stressed. Hence, it must be considered combining both strategies.

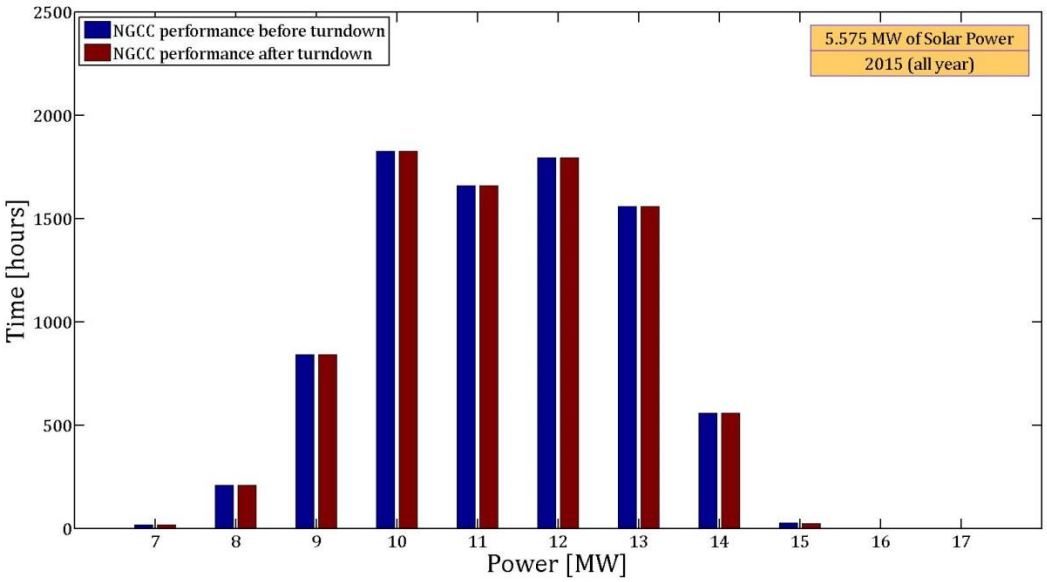

Figure 49: Bar graph of the NGCC power before and after manipulating its operation vs. number of hours the NGCC operates at each of the power outputs when following the strategy of manipulating first the chiller plant operation and then turning down the NGCC when required. Data of the year 2015 are used.

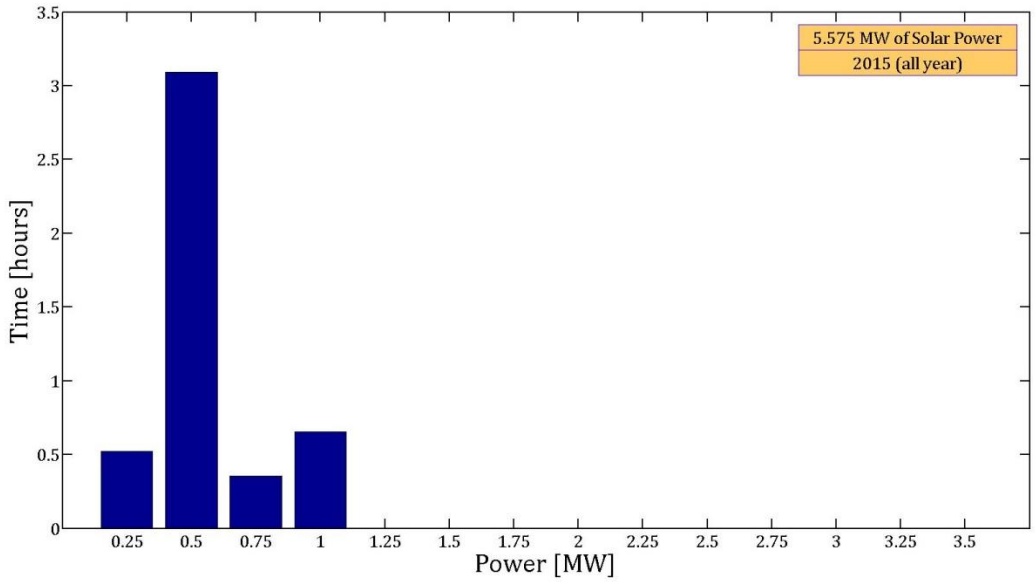

Figure 50: Bar graph of the NGCC turndown power vs. number of hours it is needed to do so when following the strategy of manipulating first the chiller plant operation and then turning down the NGCC when required. Data of the year 2015 are used.

So as to better observe in detail how the system is working, Figure 51 presents a simulation of two typical days of operation. In there the trend described previously can be observed again. The solar energy curtailed is stored in the chillers thermally. However, these can just store up to a certain amount. Hence, at this point, is where the NGCC starts to be turned down. In this figure the NGCC is not turned down because, as commented, it is not typical when having a total of 5.575 MW of solar power available.

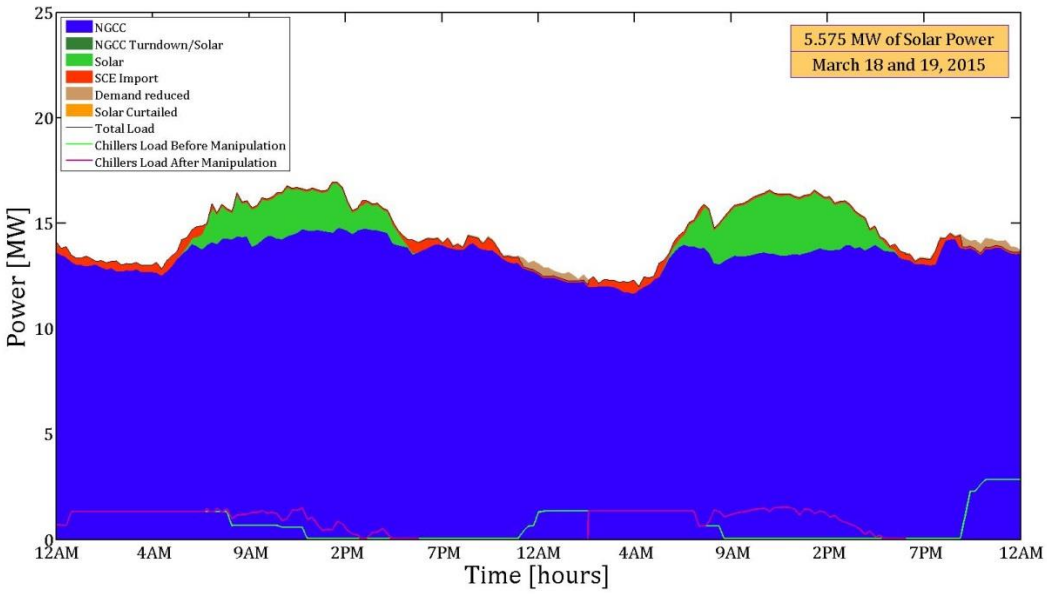

Figure 51: 2 typical days of the year for the hypothetical scenario where 2 extra MW are added to the 3.575 MW of solar power existent at the UCI microgrid. First, the chiller plant operation is manipulated and, second, the NGCC operation is turned down when required. Data of the year 2015 are used.

On the other hand, the worst day for this scenario is represented in Figure 52. There, the NGCC is turned down because the chiller cannot store any more energy. The maximum co-gen turndown power required in this scenario is of 1.14 MW.

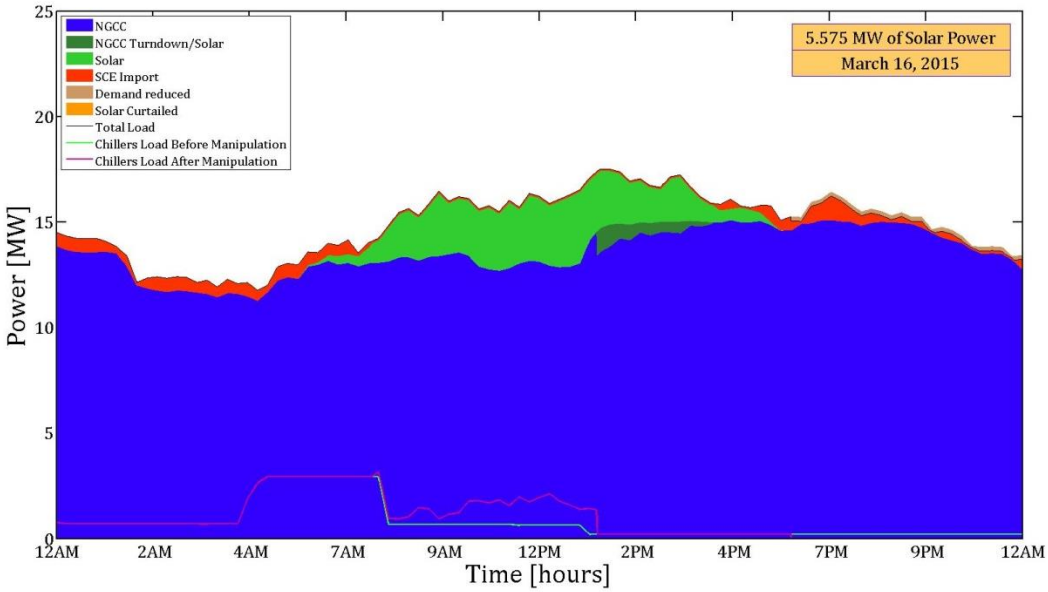

Figure 52: Worst day (i.e. day with higher NGCC turndown) of the year for the hypothetical scenario where 2 extra MW are added to the 3.575 MW of solar power existent at the UCI microgrid. First, the chiller plant operation is manipulated and, second, the NGCC operation is turned down when required. Data of the year 2015 are used.

NGCC Turndown (1) and Chiller Plant Operation Manipulated (2)

By operating the NGCC and chiller pant in this order, the month of January already presents some days where both strategies need to be used so as to utilize all of the otherwise-curtailed power. Figure 53 shows that no curtailment is present when following this strategy.

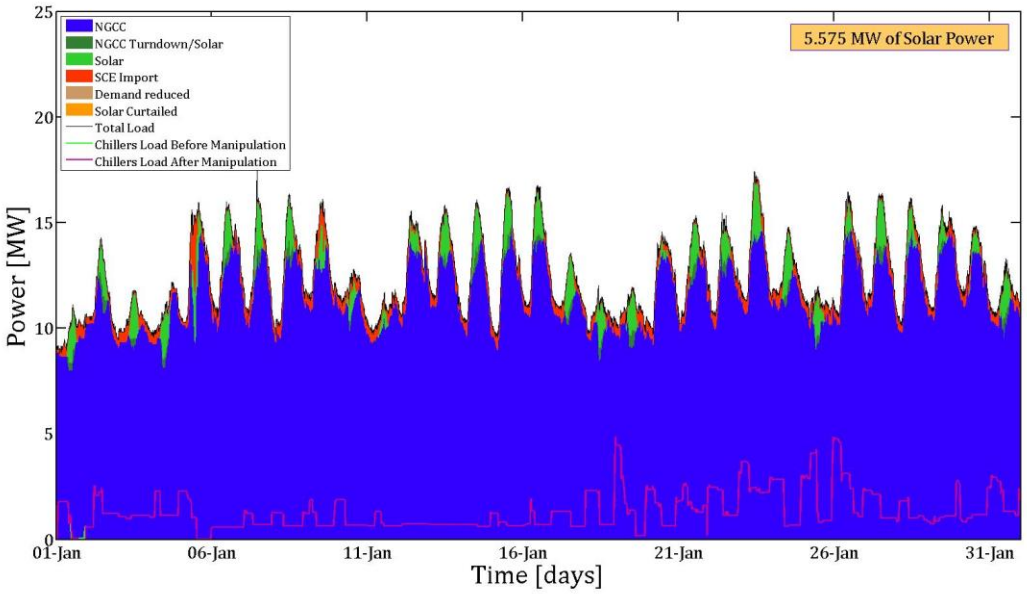

Figure 53: Hypothetical scenario where 2 extra MW are added to the 3.575 MW of solar power existent at the UCI microgrid for the month of January. First, the chiller plant operation is manipulated and, second, the NGCC operation is turned down when required. Data of the year 2015 are used.

On one hand, Figure 54 presents again the power output of the NGCC before and after it is turned down. On the other hand, Figure 55 shows the number of hours and amount of power it is turned down. Results demonstrate that the NGCC needs to be turned down a little bit more in comparison to the case where just the NGCC can be turned down. In this scenario it is turned down 357 days per year. That is, 26.57% of the time. As it has already been commented, the NGCC can be turned down again once the chillers have stored all the energy they will require for the following night (if they need to). The NGCC efficiency when following this strategy is decreased by 0.59 percentage points, going from 36.65% to 36.06%, which translates into 1.65% more fuel in order to obtain the same power output.

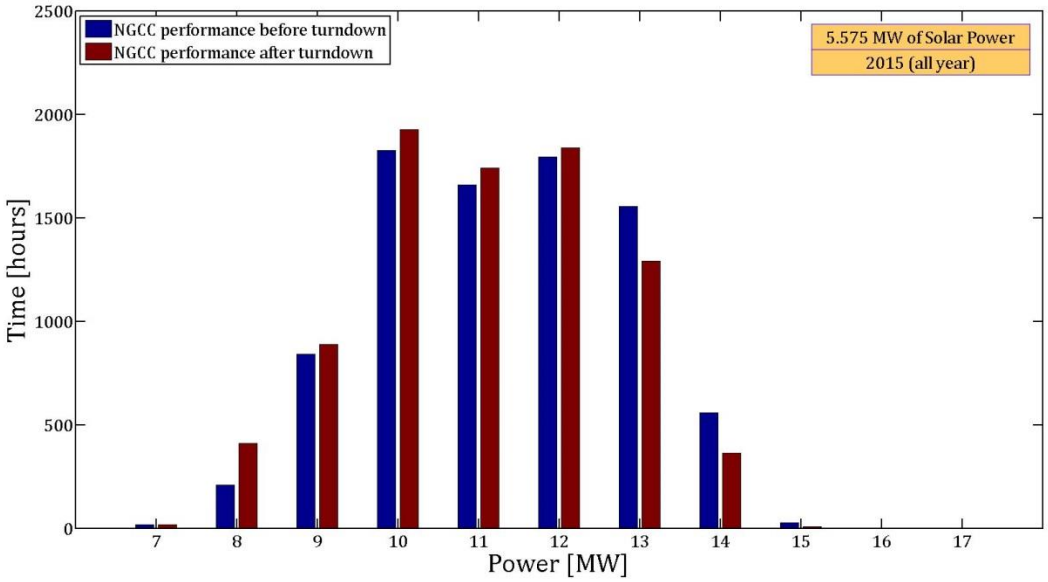

Figure 54: Bar graph of the NGCC power before and after manipulating its operation vs. number of hours the NGCC operates at each of the power outputs when following the strategy turning down the NGCC first, and then manipulating the chiller plant operation when required. Data of the year 2015 are used.

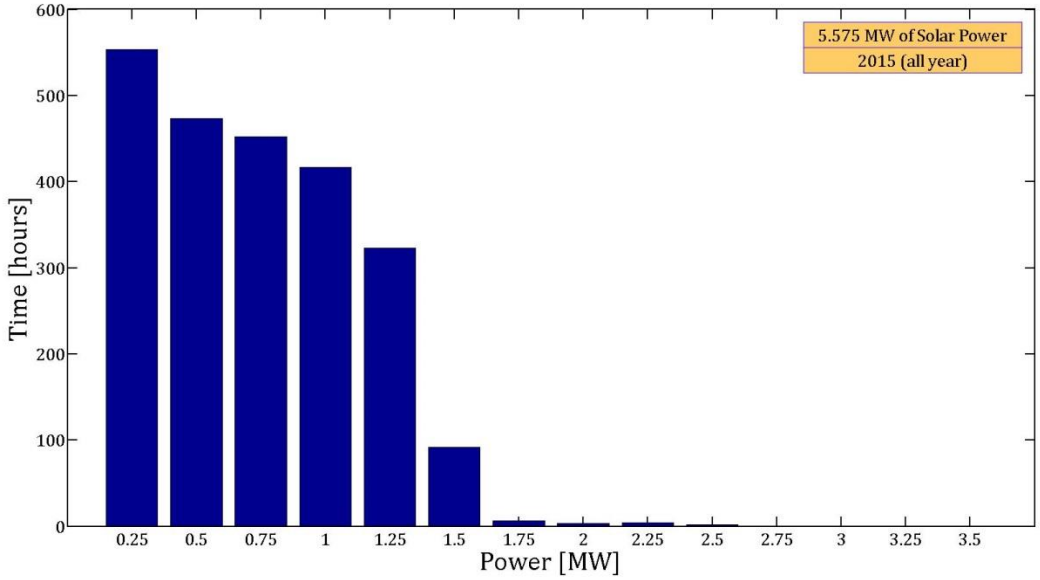

Figure 55: Bar graph of the NGCC turndown power vs. number of hours it is needed to do so when following the strategy of turning down the NGCC first, and then manipulating the chiller plant operation when required. Data of the year 2015 are used.

In this scenario the chiller just need to increase its power capacity 44 days of the whole year for a total of 122.5 hours as Figure 56 suggests. Nevertheless, this number of hours

just represents 1.40% of the time. These results put to forward that if just the NGCC power is turned down, the integration of these 2 MW of extra solar power is not feasible. The chiller plant operation must be modified at some point as well.

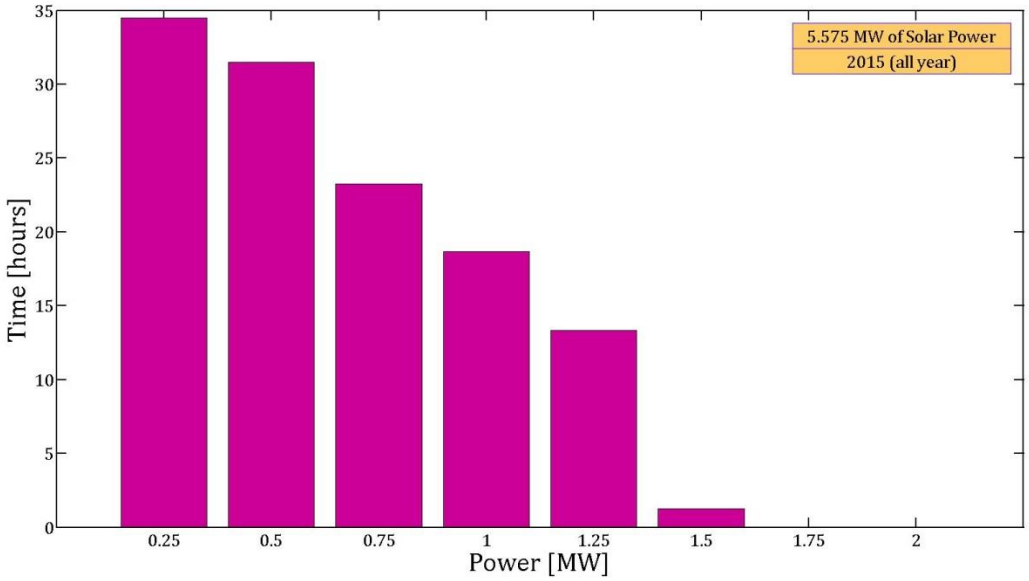

Figure 56: Bar graph of the increased chiller power capacity vs. number of hours they need to do so when following the strategy of turning down the NGCC first, and then manipulating the chiller plant operation when required. Data of the year 2015 are used.

Finally, Figure 57 presents a simulation of two typical days of operation so as to show how the power is dispatched in this scenario. In this graph it is showed how the solar curtailment makes the NGCC turn down up to its maximum capacity (i.e., up to MO). Afterwards, if there is still otherwise-curtailed power remaining, the chillers store it thermally. This figure looks exactly the same to Figure 45 because the chillers do not happen to store part of the energy because, as commented, it is not typical when having a total of 5.575 MW of solar power available. On the other hand, the worst day is shown in Figure 58. It can be observed how the chillers start storing energy because the NGCC is

already operating at MO or at a lower output. The chillers increase their power capacity by a maximum of 1.69 MW in this scenario.

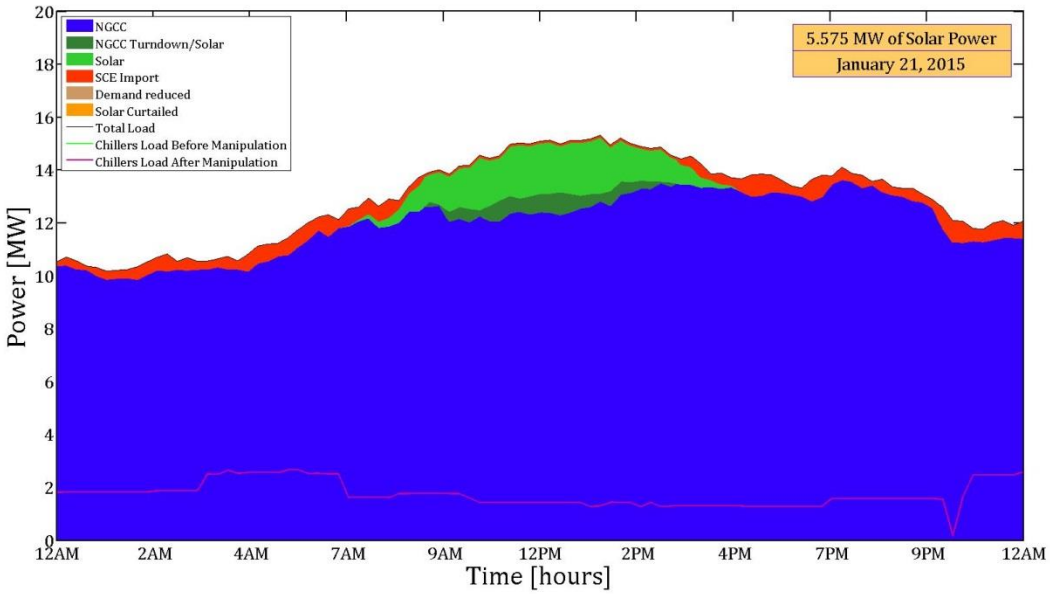

Figure 57: Typical day of the year for the hypothetical scenario where 2 extra MW are added to the 3.575 MW of solar power existent at the UCI microgrid. First, the NGCC operation is turned down when required and, second, the chiller plant operation is manipulated. Data of the year 2015 are used.

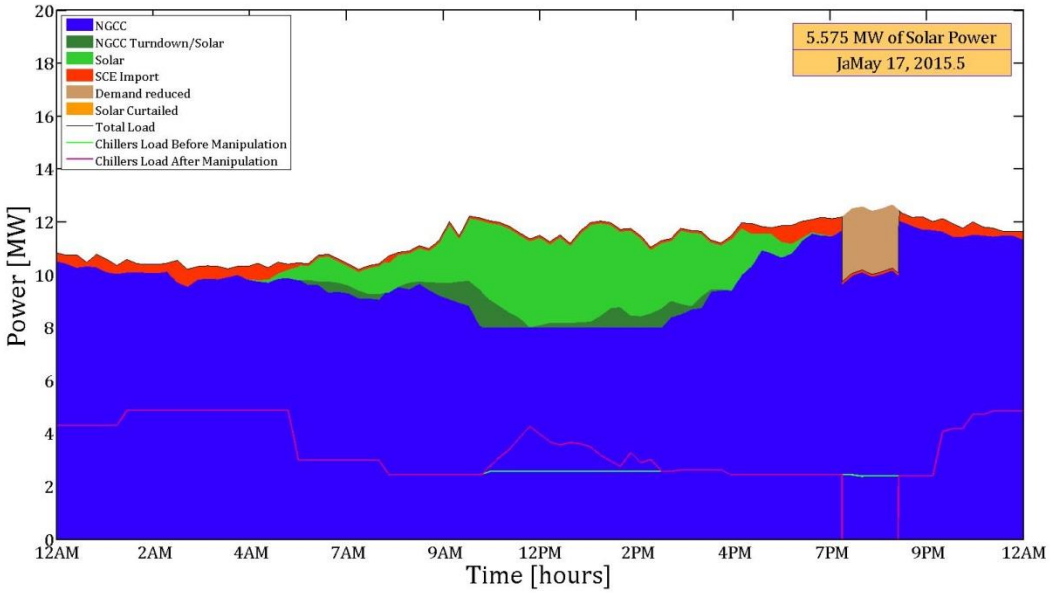

Figure 58: Worst day of the year for the hypothetical scenario where 2 extra MW are added to the 3.575 MW of solar power existent at the UCI microgrid. First, the NGCC operation is turned down when required and, second, the chiller plant operation is manipulated. Data of the year 2015 are used.

6.1.1.2. GHG Emissions Analysis

Solar GHG Emissions

With a total of 3.575 MW of solar PV power 6,151 MWh are obtained in one year. With 5.575 MW of solar PV power the energy obtained throughout the whole year is of 9,592 MWh. That is, 3,441 MWh of extra solar PV power are produced by these 2 MW of solar PV.

All the energy produced by solar PV is supposed to emit 0 GHG as Table 7 shows since the Life Cycle Analysis (LCA) of the solar panels is not considered.

Table 7: GHG emissions from solar photovoltaic power for each of the different strategies proposed for the hypothetical case where 2 MW of extra solar power are added to the 3.575 MW currently existing in the microgrid. Data of the year 2015 are used.

Chiller Plant Operation Manipulated	**NGCC Turndown**	**GHG emissions from Solar PV [tonnes of CO_2e]**
✗	✗	0
✓	✗	0
✗	✓	0
✓**(1)**	✓**(2)**	0
✓**(2)**	✓**(1)**	0

GT GHG Emissions

To compute the GT GHG emissions, first, the GT efficiency for each of the cases has been taken into account as Table 8 presents to obtain the so called 'calculated' energy input. The GT energy input is afterwards computed multiplying this 'calculated' energy input by the

higher heating value (HHV) of NG and dividing it by the lower heating value (LHV) of NG, too. The LHV and HHV of NG [63] are expressed in Equations (17) and (18).

$$LHV_{NG} = 17{,}500\ \frac{Btu}{lb} = 40.705\ \frac{MJ}{kg} = 0.0113\ \frac{MWh}{kg} \tag{17}$$

$$HHV_{NG} = 19{,}500\ \frac{Btu}{lb} = 45.360\ \frac{MJ}{kg} = 0.0125\ \frac{MWh}{kg} \tag{18}$$

Equation (19) shows how these emissions have been computed.

$$\mathrm{GHG_{GT}} = \mathrm{GT_{En.Input}}\ [\mathrm{MWh}] \cdot \frac{3.412\ [\mathrm{MMBtu}]}{[\mathrm{MWh}]} \cdot \frac{14.46\ [\mathrm{kg\ C}]}{[\mathrm{MMBtu}]} \cdot \frac{44\ [\mathrm{kg\ CO_2}]}{12\ [\mathrm{kg\ C}]} \cdot \frac{1\ [\mathrm{tonne\ CO_2}]}{1{,}000\ [\mathrm{kg\ CO_2}]} \tag{19}$$

Note that that 14.46 [kgC/MMBtu] corresponds to the average carbon coefficient of NG [64] and (44/12) makes reference to the ratio of carbon dioxide to carbon.

From the results obtained it can be inferred that, even though the GT efficiency does decrease when the NGCC operation is turned down, net carbon emissions also decrease because less fuel is inputted.

Table 8: GHG emissions from the Gas Turbine for each of the different strategies proposed for the hypothetical case where 2 MW of extra solar power are added to the 3.575 MW currently existing in the microgrid. Data of the year 2015 are used.

Chiller Plant Operation Manipulated	NGCC Turndown	Energy produced by the GT [MWh]	GT efficiency [%]	Calculated GT Energy Input [MWh]	GT Energy Input [MWh]	GHG emissions from GT [tonnes of CO_2e]
✗	✗	93,419	29.53	316,352	352,507	63,770
✓	✗	93,419	29.53	316,352	352,507	63,770
✗	✓	91,741	29.31	313,002	348,774	63,095
✓**(1)**	✓**(2)**	93,396	29.53	316,275	352,420	63,754
✓**(2)**	✓**(1)**	91,707	29.31	312,886	348,645	63,071

SCE Import GHG Emissions

Total U.S. energy-related emissions of carbon dioxide by the electric power sector in 2014 were about 38% of the total U.S. energy-related CO_2 emissions [65]. However, the GHG emissions that directly come from the electricity produced by the electricity supply companies strongly depend on the type of fuel burnt as Table 9 shows.

Table 9: Number of pounds of CO_2 produced from different fuels, the average heat rates for steam-electric generators in 2013 using those fuels, and the resulting amount of CO_2 produced per kW [66].

Type of Fuel		$\left[\frac{lb\ CO}{MMBtu}\right]$	**Heat Rate** $\left[\frac{Btu}{KWh}\right]$	$\left[\frac{lb\ CO_2}{KWh}\right]$
Coal	**Bituminous**	205.300	10,089	2.07
	Sub-bituminous	212.700	10,089	2.15
	Lignite	215.400	10,089	2.17
Natural Gas		117.080	10,334	1.21
Oil	**Distillate (No. 2)**	161.386	10,334	1.67
	Distillate (No. 6)	173.906	10,334	1.80

According to the EIA, natural gas-fired electricity generation is expected to account for 80 percent of all added electricity generation capacity by 2035 [67]. There are many reasons for this increased reliance on natural gas to generate our electricity. While coal is the cheapest fossil fuel for generating electricity, it is also the dirtiest, releasing the highest levels of pollutants into the air. The electric generation industry, in fact, has traditionally been one of the most polluting industries in the United States. Regulations surrounding the emissions of power plants have forced these electric generators to come up with new methods of generating power, while lessening environmental damage. New technology has

allowed natural gas to play an increasingly important role in the clean generation of electricity [67].

Most of the electricity the UCI microgrid imports that does not come from renewable sources comes from natural gas [56]. Thus, from Table 14, just the values of NG are taken into account for the results presented in Table 15. Also, 613.28 [lb of CO_2/MWh] is the value used by the UCI Facilities Management team when reporting the campus GHG emissions to the Climate Registry. This value is provided by the U.S. Environmental Protection Agency (EPA) [56] and it corresponds to the Western Electricity Coordinating Council (WECC) Southwest subregion total output emission rate [68]. Results from Table 15 have been obtained using this value, too. These results reflect how, when the chiller plant is being operated, the GHG emissions decrease. This trend is due to the fact that the energy demand at night is decreased by the same energy amount the chiller plant has stored previously during the day.

Table 10: GHG emissions from SCE Import for each of the different strategies proposed for the hypothetical case where 2 MW of extra solar power are added to the 3.575 MW already installed in 2015. Data of the year 2015 are used.

Chiller Plant Operation Manipulated	NGCC Turndown	Energy Imported from SCE [MWh]	GHG emissions from SCE Import [tonnes of CO_{2e}]*	GHG emissions from SCE Import [tonnes of CO_{2e}]**
✗	✗	5,082	2,789	1,414
✓	✗	4,489	2,464	1,249
✗	✓	5,082	2,789	1,414
✓**(1)**	✓**(2)**	4,489	2,464	1,249
✓**(2)**	✓**(1)**	5,059	2,777	1,407

* using 1,210 lbs of CO_{2e}/MWh from [66]: http://www.eia.gov/tools/faqs/faq.cfm?id=77&t=11
** using 613.28 lbs of CO_{2e}/MWh from [68]: http://www.epa.gov/cleanenergy/documents/egridzips/eGRID_9th_edition_V1-0_year_2010_Summary_Tables.pdf

Total GHG Emissions

Table 11 shows how just a decrease of 500 to 700 tonnes of CO_{2e} is achieved after installing 2 MW of extra solar PV power. Even though 2 MW seems to be a big fraction of a given load on a power basis, taking into account the number of MWh produced due to the capacity factor of these 2 MW and comparing them to the rest of the energy that is being self-generated or imported, it is not. That is the reason why the introduction of 2 MW of solar power roughly reduces the GHG emissions by 1% approximately.

Table 11: Total GHG emissions for each of the different strategies proposed for the hypothetical case where 2 MW of extra solar power are added to the 3.575 MW already installed in 2015. Data of the year 2015 are used.

Chiller Plant Operation Manipulated	NGCC Turndown	GHG emissions from Solar PV [tonnes of CO_{2e}]	GHG emissions from GT [tonnes of CO_{2e}]	GHG emissions from SCE Import [tonnes of CO_{2e}]**	TOTAL GHG emissions [tonnes of CO_{2e}]
✗	✗	0	63,770	1,414	65,184
✓	✗	0	63,770	1,249	65,019
✗	✓	0	63,095	1,414	64,509
✓**(1)**	✓**(2)**	0	63,754	1,249	65,003
✓**(2)**	✓**(1)**	0	63,071	1,407	64,478

** using 613.28 lbs of CO_{2e}/MWh from [68]: http://www.epa.gov/cleanenergy/documents/egridzips/eGRID_9th_edition_V1-0_year_2010_Summary_Tables.pdf

Table 11 shows that turning the NGCC down first and then modifying the chiller plant operation if required is the best approach to reduce GHG emissions. However, there is not much of a difference between the 4 different strategies. Hence, the control strategy selected to follow can be decided without significant GHG emissions impacts.

6.1.1.3. Economic Analysis

One of the most important aspects to take into account is the economic part. According to EIA, in 2014, the average price of natural gas for electric power producers in the United States was $5.19 per thousand cubic feet [69]. For the commercial sector, however, the prices of Natural Gas at the Pacific Coast were of $9.32 per thousand cubic feet in 2014 and $8.74 per thousand cubic feet ($10.28 per MMBtu) in 2015 [70].

The density of NG [63] is expressed in Equation (20). By using this parameter, the LHV of NG expressed in Equation (17), and the average price of natural gas for the commercial sector in 2015 [70], the results presented in Table 12 have been obtained.

$$\rho_{NG} = 0.049 \frac{lb}{ft^3} = 0.022 \frac{kg}{ft^3} \tag{20}$$

Table 12: Economic difference between operating the NGCC at current levels and with 2 MW of extra solar PV power. Data of the year 2015 are used.

Chiller Plant Operation manipulated	NGCC Turndown	GT Energy Input [MWh]	NG input [tonnes]	NG saved in relation to not modifying neither NGCC nor Chiller Plant Operations		
				[MWh]	[kg]	[$]
✗	✗	352,507	31,195	0	0	0
✓	✗	352,507	31,195	0	0	0
✗	✓	348,774	30,865	3,733	330,354	131,230
✓**(1)**	✓**(2)**	352,420	31,188	87	7,699	3,056
✓**(2)**	✓**(1)**	348,645	30,854	3,862	341,770	135,683

Even though the system needs more fuel to run the GT when the NGCC is turned down because of the NGCC efficiency decrease, the overall cost is substantially reduced when

doing so. Just when the chiller plant operation is manipulated the load demand during the night is decreased. Hence, just when this strategy is approached energy shifted from the night to the previous day appears. The cost of co-gen electricity produced at night is of $0.08/KWh and the cost of SCE electricity purchased at night is of $0.13/KWh [56]. The difference of $0.05/KWh needs to be thought as the maximum (upper bound) difference that it makes to shift all this amount of energy. It is just an estimate of the relative lost. In reality, not any more electricity is bought from SCE. However, less electricity is used at night at $0.08/KWh. Table 13 presents the economic effect of introducing the strategies discussed in order to accommodate the 2 MW of extra solar power.

Table 13: Economic difference between operating the NGCC at current levels and with 2 MW of solar power extra. Data of the year 2015 are used.

Chiller Plant Operation Manipulated	NGCC Turndown	Energy shifted from night to day [MWh]	Saved cost from shifted Energy [$]
✗	✗	0	0
✓	✗	547.6	27,377
✗	✓	0	0
✓**(1)**	✓**(2)**	547.6	27,377
✓**(2)**	✓**(1)**	95.6	4,780

6.2. Renewable Integration Summary

Table 14 shows the amounts of solar power the microgrid of study could handle. Results have been obtained using the equations presented in section 5.3.

Table 14: Maximum renewable integration with and without ES systems. The two strategies proposed are analyzed individually and together. Data of the year 2015 are used.

Chiller Plant Operation manipulated	NGCC Turndown	Maximum of Renewable Integration without ES		Maximum of Renewable Integration with ES	
		[%]	MW of PV	[%]	MW of PV
✓	✗	4.91	5.04	16.67	17.11
✗	✓	3.90	4.01	25.49	26.17
✓	✓	8.52	8.75	33.28	34.16

By looking at Table 14 it can be confirmed what was shown and announced in section 6.1. If just one of the strategies proposed is followed not all the solar can be utilized when adding 2 MW of extra solar PV to the current 3.575 MW of solar PV power existing on campus. For the case of just manipulating the operation of the chiller plant though, the curtailment appears less than 1% of the time when just this methodology is followed. However, as commented, the system appears to be too stressed and therefore is neither recommended nor adequate.

By combining the two strategies up to 8.75 MW can be installed at the microgrid of study. This represents 2.45 times the amount of solar power existing on campus.

Even though the solar energy produced is enough so as to satisfy the whole year demand, its production is intermittent. As Table 14 suggests, energy storage systems are completely

necessary so as to increase the renewable integration substantially. By installing those and manipulating the NGCC and chiller plant operations as discussed the campus could perfectly meet the 2020 state of California goal of having 33% of total procurement coming from renewable sources [71].

The Average Campus Load, obtained using Equation (4), for the year 2015 is of 13.00 MW. The peak of load for this year is of 18.69 MW. If 34.16 MW of solar power are to be installed on campus the solar PV peak will be 2.63 times the ACL and 1.83 times the load peak. It is evident that such an amount of power cannot be installed since the battery or electrolyzer size that would be able to store or convert into H_2 all the otherwise-curtailed energy is huge. The electrolyzer required for this scenario needs to be rated at 26.67 MW. Furthermore, the tank capacity required for daily storage is of 170.34 MWh. If an energy shifting of 30 days is desired, the tank capacity needs to be of 3,621 MWh.

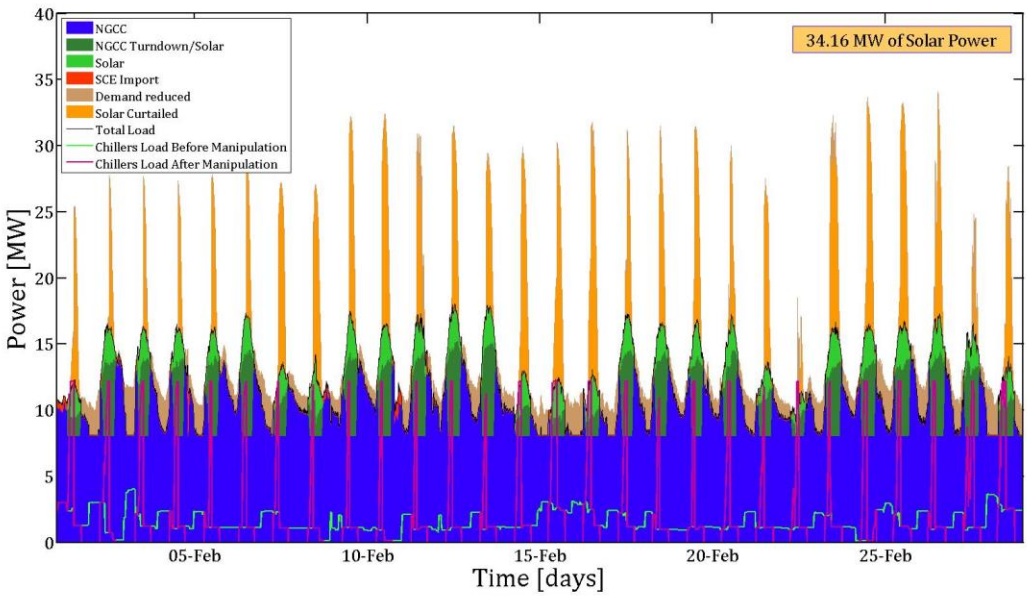

Figure 59: Hypothetical scenario where 30.585 MW extra are added to the 3.575 MW of solar power existent at the UCI microgrid for the month of February. The chillers store as much energy as possible and the NGCC is turned up to MO the whole time. Data of the year 2015 are used.

Even though the average daily storage capacity is of 72.58 MWh, the daily storage tank capacity must be able to store all the otherwise-curtailed energy of the day in which this energy is the biggest. If the microgrid was able to export, this tank capacity required could be sized much smaller.

As it can be observed in Figure 59, if 34.16 MW of solar power are installed at the microgrid of study, the NGCC operates all time at MO and the chiller store all the energy they require the following night. The NGCC operates at 30.84% efficiency though. Moreover, if no energy storage strategies are coupled with such a huge amount of solar power, a lot of curtailment is present. Figure 60 shows the hypothetical scenario where all this otherwise-curtailed power is converted into H_2 using a PEM electrolyzer and used afterwards in a 2 MW PEM FC.

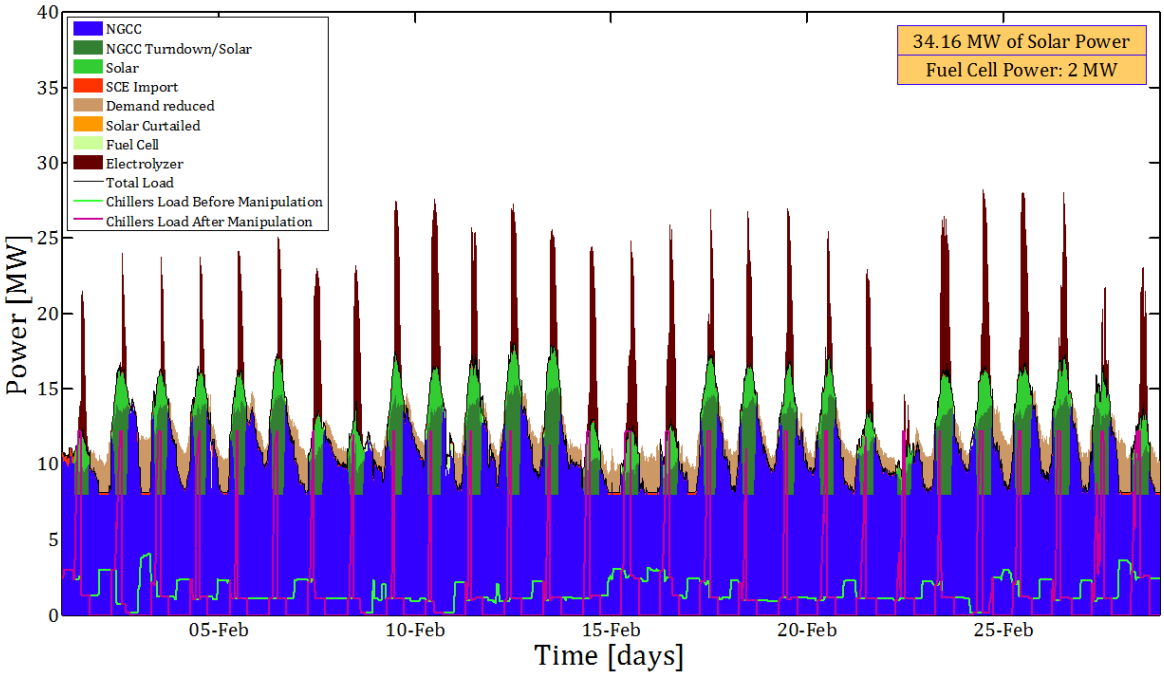

Figure 60: Hypothetical scenario where 30.585 MW extra are added to the 3.575 MW of solar power existent at the UCI microgrid for the month of February. The chillers store as much energy as possible and the NGCC is turned up to MO the whole time. The otherwise-curtailed power is converted into H_2 so as to be used afterwards to run a 2 MW PEM FC when required. Data of the year 2015 are used.

Since the NGCC is not turned down during the night most of the H_2 obtained is not used in this scenario. So as to utilize it the NGCC can be turned down and operate at lower outputs. However, if that is done, the efficiency of the co-gen cycle decreases considerably since most of the time the GT needs to be operating at MO and the ST needs to be turned off (i.e., the NGCC needs to operate at MO). Note that this energy could also be stored in a battery. However, if doing so, the advantage of having energy and power decoupled one from another would be lost.

If big amounts of solar power are installed on campus the excess of energy that can be captured in one day can be greater than the energy required for the night. Hence, the concept of seasonal shifting must be studied as well for a future scenario like the one presented in Figure 59 and Figure 60. As described in section 2.2, liquid storage and underground storage are the most recommended options for seasonal or long term storage of hydrogen [43]. Nevertheless, underground storage is not possible because of the inexistence of a salt cavern, aquifer... that can be used for such a purpose at the microgrid of study. Furthermore, liquefying the hydrogen is too expensive. Plus, the maintenance costs of liquefied hydrogen are very high in comparison to storing compressed gas [36]. Thus, in this scenario, introduction of the H_2 into the NG pipelines and into above-the-ground compressed gas storage tanks is still the best option for the UCI microgrid.

By introducing the H_2 into the NG pipeline the campus can benefit from the P2G concept. To account for the amount of hydrogen that can be introduced into the NG pipeline the lower heating value (LHV) of NG, expressed in Equation (17), and the LHV of H_2 [63], expressed in Equation (21), have been used.

$$LHV_{H_2} = 51{,}628\ \frac{Btu}{lb} = 120.087\ \frac{MJ}{kg} = 0.0334\ \frac{MWh}{kg} \tag{21}$$

The efficiency of the Gas Turbine is supposed to not vary when operating with a mixture of H_2 and Natural Gas because, as stated by Hüttenrauch et al. [72], the Wobbe index of the gas mixture just decreases by about 5%. Thus, it can be assumed that the two gases are interchangeable. Equation (22) solves for the amount of hydrogen that can be introduced into the NG pipeline.

$$m_{NG_1} \cdot LHV_{NG} = m_{NG_2} \cdot LHV_{NG} + m_{H_2} \cdot LHV_{H_2} \tag{22}$$

where m_{NG_1} is the mass of NG the GT requires in one year of operation without H_2 blended into the NG pipeline; m_{NG_2} is the mass of NG the GT requires in one year of operation with H_2 blended into the NG pipeline; and m_{H_2} is the mass of H_2 the GT requires in one year of operation when this is present into the NG pipeline blended with NG. If m_{H_2} and m_{NG_2} are expressed in terms of m_{NG_1}, Equation (22) can be rewritten as:

$$m_{NG_1} \cdot LHV_{NG} = (1 - \chi) \cdot m_{NG_1} \cdot LHV_{NG} + \chi \cdot m_{NG_1} \cdot LHV_{H_2} \tag{23}$$

where χ is the hydrogen concentration percentage in volume.

Also, since $m_{NG_1} \cdot LHV_{NG}$ is equal to the Gas Turbine total input energy, Equation (23) can be finally rewritten as:

$$m_{NG_1} = \frac{\text{GT total input energy}}{(1 - \chi) \cdot LHV_{NG} + \chi \cdot LHV_{H_2}} \tag{24}$$

And hence, m_{H_2} can be expressed as:

$$m_{H_2} = \chi \cdot \left(\frac{\text{GT total input energy}}{(1 - \chi) \cdot LHV_{NG} + \chi \cdot LHV_{H_2}} \right) \tag{25}$$

Note that all equations are computed supposing that both NG and H_2 are ideal gases. Table 15 shows the mass of H_2 that can be introduced into the NG pipelines if the NGCC is turned down and operates at MO the whole time and when no NGCC Turndown at all is allowed. These two cases represent the minimum and maximum amounts of H_2 that can be blended, respectively. Results have been computed using (17), (21), and supposing a 0.2, 5, 10, and 15% of hydrogen blended with NG into the NG pipeline. Equation (8) has been used so as to account for the efficiency of the GT in each of the two scenarios, giving an efficiency of 26.55% when the NGCC is turned down all the way down to MO and 29.53% when the NGCC is not turned down at all.

Table 15: Amount of hydrogen that can be blended with Natural Gas into the NG pipeline every month from January to June, 2015 supposing concentrations of 0.2, 5, 10, and 15% of hydrogen by volume. The maximum and minimum amounts of H_2 are presented. Data of the year 2015 are used.

	0.2% [tonnes of H_2]		**5% [tonnes of H_2]**		**10% [tonnes of H_2]**		**15% [tonnes of H_2]**	
	Max.	**Min.**	**Max.**	**Min.**	**Max.**	**Min.**	**Max.**	**Min.**
January	2.51	1.96	57.39	44.70	105.40	82.09	146.15	113.82
February	2.24	1.77	51.30	40.46	94.20	74.30	130.62	103.02
March	2.44	1.96	55.77	44.77	102.42	82.21	142.02	114.00
April	2.33	1.89	53.43	43.31	98.12	79.54	136.05	110.28
May	2.24	1.96	51.15	44.80	93.94	82.27	130.26	114.07
June	2.10	1.90	49.35	43.39	87.61	79.68	124.39	110.49
TOTAL	13.86	11.43	318.40	261.43	581.702	480.09	809.49	665.69
TOTAL (million lb.)	0.03	0.02	0.70	0.58	1.28	1.06	1.78	1.47

The results obtained in Table 15 can be well represented in a plot, as Figure 61 shows:

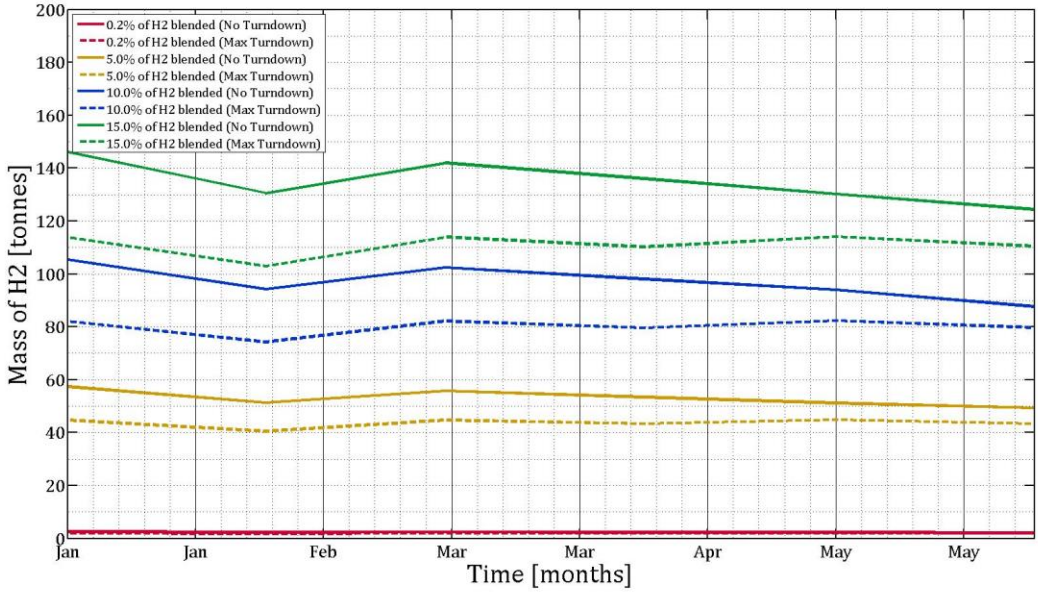

Figure 61: Amount of H_2 that can be blended with Natural Gas into the NG pipeline.

Figure 61 shows that the months of winter are more challenging for the NGCC than the summer months. That is because the chiller can store more energy during the day in summer months than in winter months because the overall campus cooling load is higher during summer.

By following this approach a $(\chi \cdot 100)\%$ of the gas used to operate the GT can be considered renewable. Hence, it does contribute to the overall renewable penetration. Table 16 presents it.

Table 16: Overall demand renewable energy contribution when blending a 0.2, 5, 10, and 15% of hydrogen by volume into the natural gas pipeline system. Data of the year 2015 are used.

	Maximum Renewable Energy Contribution		Minimum Renewable Energy Contribution	
	[MWh] (1/2 year)	[%]	[MWh] (1/2 year)	[%]
0.2% of hydrogen by volume	93.93	0.17	69.50	0.12
5% of hydrogen by volume	2,348.30	4.16	1,737.60	3.08
10% of hydrogen by volume	4,696.60	8.31	3,475.20	6.16
15% of hydrogen by volume	7,044.90	12.47	5,212.80	9.23

Results prove that by feeding the GT with 15% of renewable gas after turning the NGCC to MO the whole time (i.e., ST turned off), the overall renewable energy contribution can increase by 9.23%. Furthermore, if the NGCC is not turned down at all, 12.47% of the total energy produced by the GT can be considered renewable energy.

Figure 62 shows how all the energy that was otherwise-curtailed is now utilized by injecting it into the NG pipeline. Even though the SCE Import is pretty low, it is not completely constant. This trend can be easily observed by looking at Figure 63, which shows the operation for the 11th of February.

By following this approach the energy storage requirement decreases since a big amount of the H_2 produced is directly introduced into the NG pipeline. However, as Figure 62 shows, not all the H_2 produced at one moment can be directly injected. It must be assured that the blending meets specific percentages of H_2 and NG, respectively. For the blending of the scenario described to be feasible, a storage capacity of 25.48 MWh is required.

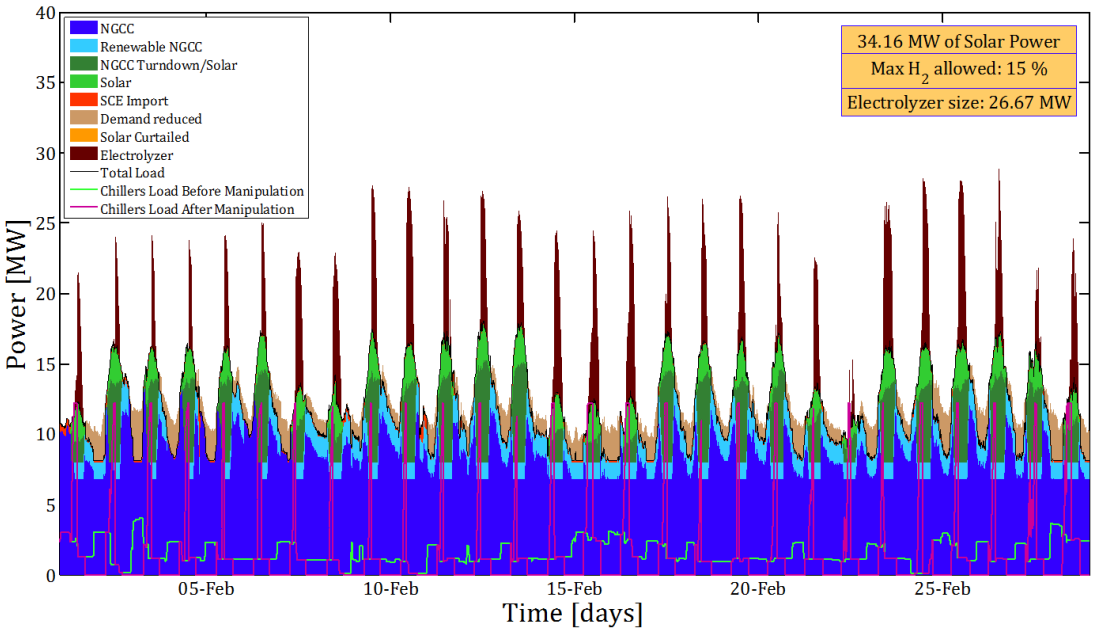

Figure 62: Hypothetical scenario where 30.585 MW extra are added to the 3.575 MW of solar power existent at the UCI microgrid for the month of February. The chillers store as much energy as possible and the NGCC is turned down up to MO the whole time. The otherwise-curtailed power is converted into H_2 and injected intoto the NG pipeline that feeds the GT. Data of the year 2015 are used.

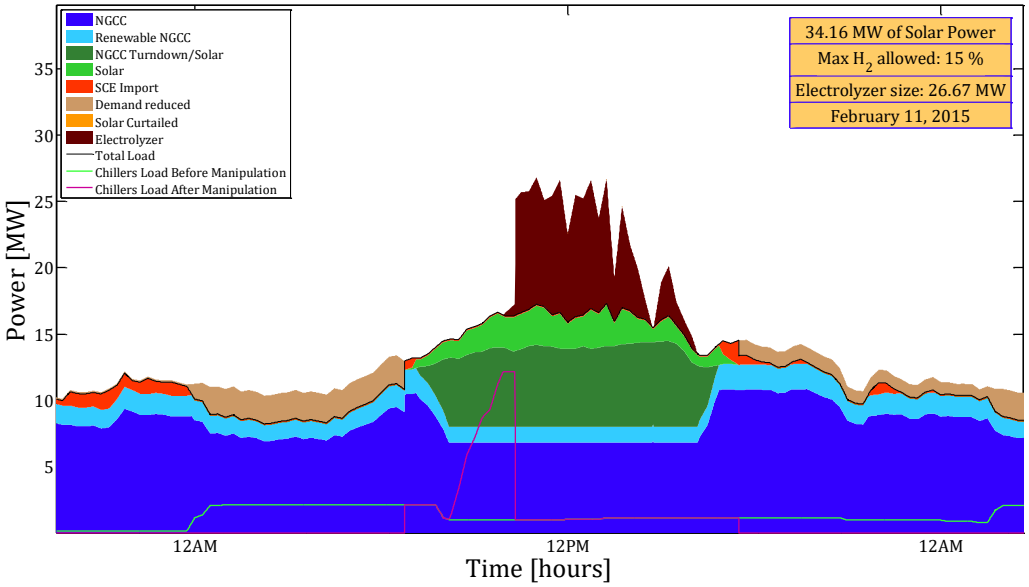

Figure 63: 11th of February of the hypothetical scenario where 30.585 MW extra are added to the 3.575 MW of solar power existent at the UCI microgrid. The chillers store as much energy as possible and the NGCC is turned down up to MO the whole time. The otherwise-curtailed power is converted into H_2 and injected into the NG pipeline that feeds the GT. Data of the year 2015 are used.

To smooth the SCE Import, a fuel cell (FC) can be used. When the power generated by the solar panels exceeds the load on the microgrid, the excess solar power is diverted to produce hydrogen as described. If the solar power is insufficient to meet the load, the energy in storage is released to a PEM FC to meet the demand. However, in this scenario, less hydrogen is blended with NG into the NG pipeline as Figure 64 shows. Figure 65 zooms in one of the days again so as to show better the tendency described. It can be observed how the SCE Import is kept constant at 100 KW. By following this approach, a 36.40% of all the energy produced or imported is renewable. Thus, the campus can meet the 2020 state of California goal of having 33% of total procurement coming from renewable sources if this approach is followed.

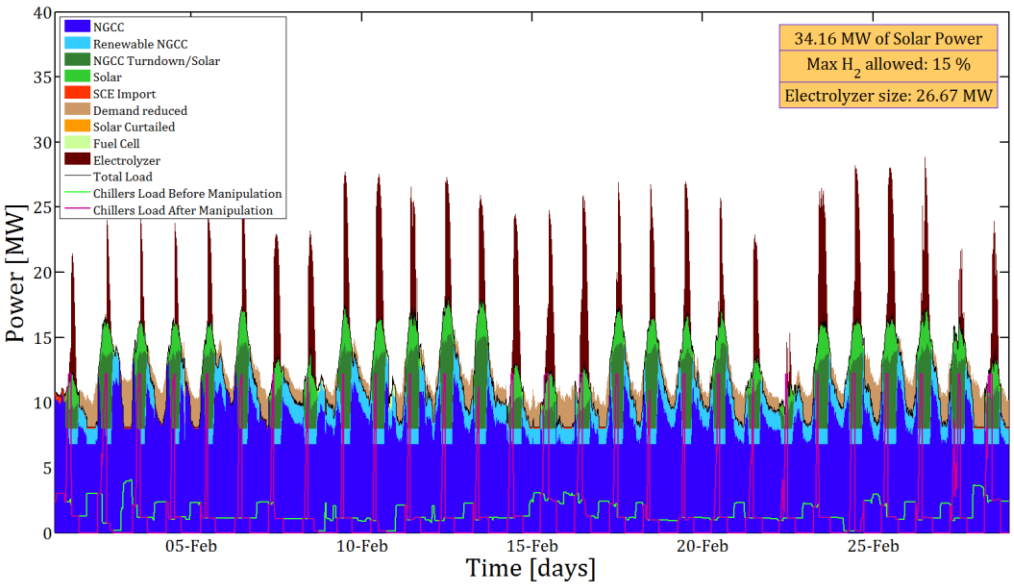

Figure 64: Hypothetical scenario where 30.585 MW extra are added to the 3.575 MW of solar power existent at the UCI microgrid for the month of February. The chillers store as much energy as possible and the NGCC is turned down up to MO the whole time. The otherwise-curtailed power is converted into H_2 and used afterwards to run a PEM FC and smooth the imported electricity. The remaining H_2 is injected into the NG pipeline that feeds the GT. Data of the year 2015 are used.

Even though the FC should not be used just for a couple of hours a day, the results presented in Figure 64 and Figure 65 basically show how the SCE Import can be smoothed by using this excess of solar power. A battery could be used for the same purposes.

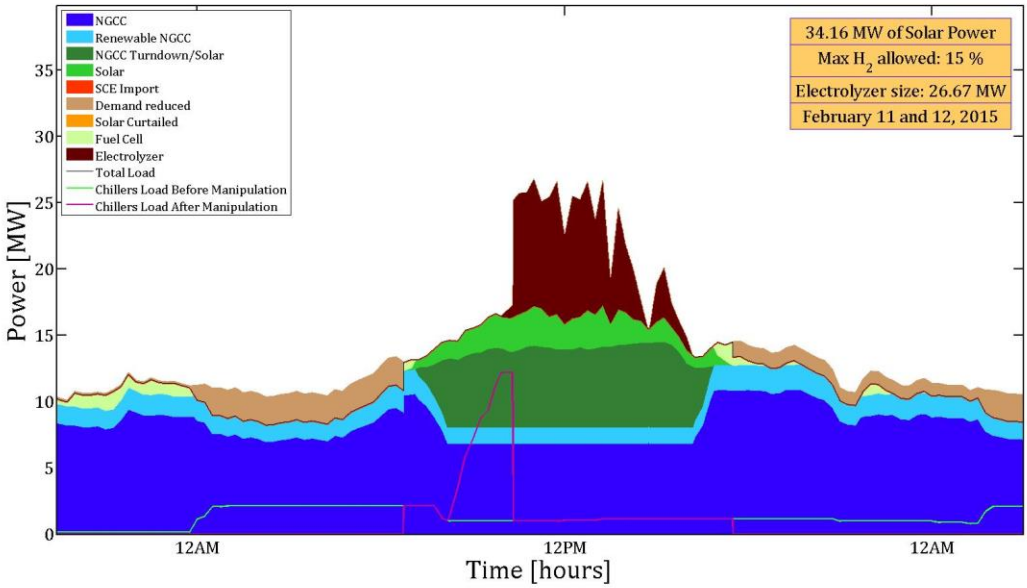

Figure 65: 11th of February of the hypothetical scenario where 30.585 MW extra are added to the 3.575 MW of solar power existent at the UCI microgrid. The chillers store as much energy as possible and the NGCC is turned down up to MO the whole time. The otherwise-curtailed power is converted into H_2 and used afterwards to run a PEM FC and smooth the imported electricity. The remaining H_2 is injected into the NG pipeline that feeds the GT. Data of the year 2015 are used.

For the scenario of 34.16 MW of solar power installed, after manipulating the operations of the NGCC and the chiller plant, 78,278 MWh of energy are still produced by the GT at the end of the year. With 34.16 MW of solar power the NGCC renewable power obtained throughout the year represents a 14.66% of the total power used. Thus, 66,802 MWh are still being produced using NG. The GT efficiency when operating the NGCC as described is of 27.41%.

7. Summary and Conclusions

7.1. Summary

The main goals and objectives outlined in sections 1.2.1 and 1.2.2 were achieved. 15-minute resolution experimental data from Melrok®, SunEdison®, and AlsoEnergy® were obtained. These data provided the initial necessary inputs to develop the Matlab/ Simulink® dynamical physical model of the University of California, Irvine microgrid operation control. Afterwards, once the model was created, different case scenarios were tested applying the model to parametric variations in order to utilize as much of the otherwise-curtailed power that the solar PV arrays existing on campus would generate if their capacities were to be increased. Finally, new ways of operating the microgrid in order to increase its renewable energy penetration and mitigate the power intermittency associated with a high-penetration of renewable photovoltaic resources have been proposed and studied (i.e., use of RFC and P2G).

7.2. Conclusions

- When solar energy or any other renewable energy is introduced into a microgrid, intermittencies and fluctuations of the energy input increase and become more and more difficult to manage as renewable power penetration is increased.

  This trend will also appear in the larger utility grid network in the following years due to a rising share of renewable power sources being used throughout the electric grid. By using energy storage systems the problem can be alleviated since

these systems can provide a controllable, flexible, and bi-directional flow of clean energy to manage the intermittencies of renewable energy output power.

- By manipulating the way the chiller plant operates together with the power output of the NGCC (i.e., combining the two strategies) the renewable integration of the UCI microgrid (and other similar grids) can be substantially increased

  In the case of the UCI Microgrid, two major strategies for managing the increased use of solar power without adding energy storage are proposed: (1) manipulating chiller plant operations, and (2) manipulating NGCC operations. If just one of these strategies proposed is followed, the system is stressed and the amount of renewable power integration can barely be increased. By manipulating both of them though, this overall renewable integration is more than doubled.

  It has been shown that in the case of the UCI microgrid the renewable integration could be increased from the current 3.48% to a total of 8.52% of all delivered energy without energy storage. That is, up to 5.175 MW of solar power could be added to the existing 3.575 MW. Hence, prior to installing energy storage systems it is important to analyze how to operate the available devices of a microgrid in the most efficient way.

- The P2G strategy of introducing H_2 produced from the otherwise-curtailed renewable power and blending it with NG into the NG pipeline appears to be a highly effective way of integrating renewables into a microgrid.

P2G is a feasible way of storing excess energy for the long term. Moreover, the impact associated with implementing this strategy is not very big since the pipelines used are the ones currently used only for natural gas.

- The use of an RFC also helps to overcome the intermittent output and input fluctuations as well as to smooth the power imported from the regional electric utility that feeds the microgrid. Furthermore, it supports grid stability by providing another controllable (dispatchable) generator.

- The UCI Microgrid can achieve the 2020 state of California goal of having 33% of total electric energy procurement coming from renewable sources.

Results have shown that the by manipulating both the chiller plant and the NGCC operations to their maximum capacities, and then through P2G the NGCC is fed by the NG pipeline that contains the H_2 previously injected.

8. Recommendations

- Follow-on research to investigate the potential of integrating microgrids with the current grid is recommended. The way to further this is none other than making this grid smart. If people were able to share the renewable energy produced with their neighbors a greater and bigger flexibility of the overall system would be accomplished since less energy storage capacity would be required.

- Biogas can also be used to increase the renewable penetration of a microgrid and decrease the overall GHG emissions. Hence, follow-on research is also recommended to the use biogas as a non-polluting renewable source of energy to feed the GT of a given microgrid. However, it is important to note that in order to benefit from this strategy system modifications are required due to the low Wobbe index of biogas in comparison to the one of NG.

9. Bibliography

[1] R. J. Yinger and A. E. Kamiab, "Good Vibrations," *IEEE power & energy magazine,* pp. 1,2, september/october 2011.

[2] J. Auer and J. Keil, "State-of-the-art electricity storage systems: Indispensable elements of the energy revolution," Deutsche Bank, 8 March 2012. [Online].

[3] X. Tan, Q. Li and H. Wanga, "Advances and trends of energy storage technology in Microgrid," *Electrical Power and Energy Systems 44,* pp. 179-191, 5 July 2012.

[4] "Energy Storage for Microgrids," Navigant Research, [Online]. Available: https://www.navigantresearch.com/research/energy-storage-for-microgrids.

[5] E. a. M. The National Academies of Sciences, What You Need to Know About Energy, Wahington, D.C., 2015.

[6] J.-P. Maton, L. Zhao and J. Brouwer, "Dynamic modeling of compressed gas energy storage to complement renewable wind power intermittency," *Elsevier,* vol. 38, pp. 7867-7880, 2013.

[7] D. Akinyele and R. Rayudu, "Review of energy storage technologies for sustainable power networks," *Sustainable Energy Technologies and Assessments,* vol. 8, pp. 74-91, 2014.

[8] A. Etxeberria, I. Vechiu, H. Camblong and J. Vinassa, "Hybrid Energy Storage Systems for Renewable Energy Sources Integration in Microgrids: A Review," *IEEE,* Vols. 978-1-4244-7398-4/10, pp. 532-537, 2010.

[9] J. I. San-Martín, I. Zamora, J. J. San-Martín, V. Aperribay and P. Eguia, "Hybrid fuel cells technologies for electrical microgrids," *Elsevier - Electric Power Systems Research,* vol. 80, pp. 993-1005, 2010.

[10] M. Madou, *Engineering Electrochemistry,* University of California, Irvine, 2015.

[11] Altairnano, "Applications for Advanced Batteries in Microgrid Environments," 12 12 2012. [Online]. Available: http://www.altairnano.com/wp-content/uploads/2013/01/ApplicationsForAdvancedBatteriesWP.pdf. [Accessed 14 01 2015].

[12] E. Hittinger, T. Wiley, J. Kluza and J. Whitacre, "Evaluating the value of batteries in microgrid electricity systems using an improved Energy Systems Model," *Elsevier - Energy Conversion and Management,* vol. 89, pp. 458-472, 2015.

[13] X. Dou, X. Quan, Z. Wu, Z. Wu, M. Hu, J. Sun, K. Yang and M. Xu, "Improved Control Strategy for Microgrid Ultracapacitor Energy Storage Systems," *Energies,* vol. 7, pp. 8095-8115, 2 December 2014.

[14] "Ultracapacitor & Supercapacitor," Tecate Group, [Online]. Available: http://www.tecategroup.com/ultracapacitors-supercapacitors/ultracapacitor-FAQ.php. [Accessed 21 01 2015].

[15] S. Teleke, "Energy storage overview: applications, technologies and economical," Quanta Technology, Raleigh, NC, 2011.

[16] M. S. Whittingham, "History, Evolution, and Future Status of Energy Storage," *IEEE,* pp. 1527-1532, 13 May 2012.

[17] J. A. Turner, "Sustainable Hydrogen Production," *Science,* vol. 305, no. 5686, pp. 972-974, 2014.

[18] G. Kyriakarakos, A. I. Dounis, S. Rozakis, K. G. Arvanitis and G. Papadakis, "Polygeneration microgrids: A viable solution in remote areas for supplying power, potable water and hydrogen as transportation fuel," *Elsevier,* vol. 88, no. 12, pp. 4517-4526, 2011.

[19] S. C. Singhal and K. Kendall, "High-temperature Solid Oxide Fuel Cells: Fundamentals Design and Applications," *Elsevier,* 2003.

[20] R. Lasseter and P. Paigi, "Microgrid: a conceptual solution," in *Power Electronics Specialists Conference*, 2004.

[21] M. El-Sharkh, A. Rahman and M. Alam, "Short term scheduling of multiple grid-parallel PEM fuel cells for microgrid applications," *Elsevier - International ournal of Hydrogen Energy,* vol. 35, pp. 11099-11106, 2010.

[22] "Stationary fuel cells," Navigant Research, 2014.

[23] S. Schiebahn, T. Grube, M. Robinius, L. Zhao, A. Otto, B. Kumar, M. Weber and D. Stolten, "Power to Gas," in *Transition to Renewable Energy Systems*, D. Stolten and V. Scherer, Eds., Wiley-VCH Verlag GmbH & Co. KGaA, 2013, pp. 813-848.

[24] J. Maclay, J. Brouwer and G. S. Samuelsen, "Dynamic analyses of regenerative fuel cell power for potential use in renewable residential applications," *International Journal of Hydrogen Energy,* vol. 31, pp. 994-1009, 2006.

[25] A. Carmona, "Dynamic modeling of compressed hydrogen energy storage and dispatch coupled to variable renewable power," University of California, Irvine, 2014.

[26] J. D. Maclay, Solar Hydrogen Production and reversible fuel cells for resdential power, Master's Thesis, 2006.

[27] P. Denholm and R. M. Margolis, "Evaluating the limits of solar photovoltaics (PV) in electric power systems utilizing energy storage and other enabling technologies," *Energy Policy,* vol. 35, pp. 4424-4433, 2007.

[28] C. Jørgensen and S. Ropenus, "Production price of hydrogen from grid connected electrolysis in a power market with high wind penetration," *International Journal of Hydrogen Energy,* vol. 33, pp. 5335-5334, 2008.

[29] T. L. Gibson and N. A. Kelly, "Optimization of solar powered hydrogen production using photovoltaic electrolysis devices," *Elsevier,* vol. 33, pp. 5931-5940, 2008.

[30] D. Stolten and D. Krieg, "Alkaline electrolysis–introduction and overview," in *Hydrogen and Fuel Cells*, D. Stolten, Ed., Weinheim, Wiley-VCH Verlag GmbH, 2010.

[31] S. Andrea, Tecnologia dell' idrogeno, Torino: Politecnico di Torino, 2012.

[32] T. Flynn, Liquification of Gases, M. E. o. S. &. Technology, Ed., New York: McGraw-Hill, 1992, pp. 106-109.

[33] L. Noganow, Hydrogen, vol. 8, M. E. o. S. &. Technology, Ed., New York: McGraw-Hill, 1992, pp. 581-588.

[34] C. Timmerhaus and T. Flynn, "Plenum Press," in *Cryogenic Engineering*, New York, 1989.

[35] D. Hart, "Hydrogen Power: The Commercial Future of the Ultimate Fuel," *Financial Times Energy Publishing,* 1997.

[36] W. A. Amos, "Costs of Storing and Transporting Hydrogen," National Renewable Energy Laboratory, Golden, Colorado, 1998.

[37] W. Zittel and R. Wurster, Hydrogen in the Energy Sector.

[38] A. T-Raissi and A. Sadhu, "System Study of Metal Hydride Storage Requirements," in *Proceedings of 1994 DOE/NREL Hydrogen Program Review*, Livermore, CA, 1994.

[39] S. Sherifa, F. Barbirb and T. Vezirogluc, "Wind energy and the hydrogen economy—review of the technology," *Elsevier - Solar Energy,* vol. 78, no. 5, pp. 647-660, 2005.

[40] J. Schwarz and K. Amonkwah, "Hydrogen Storage Systems," U.S. Geological Survey, Washington, D.C., 1993.

[41] J. Taylor, J. Alderson, K. Kalyanam, A. Lyle and L. Phillips, "ATechnical and Economic Assessment of Methods for the Storage of Large Quantities of Hydrogen," *International Journal of Hydrogen Energy,* vol. 11, no. 1, pp. 5-22, 1986.

[42] A. Lord, P. Kobos, G. Klise and D. Borns, "A life cycle cost analysis framework for geologic storage of hydrogen: a user's tool," Albuquerque, NM, 2011.

[43] C. Carpetis, Technology and Costs of Hydrogen Storage, vol. 1, TERI Information Digest on Energy, 1994, pp. 1-13.

[44] N. Oy, "New Hydrogen Technologies Project Report: Evaluation of Techniques," 1992.

[45] S. G. Solomon and D. C. Whitman, "Above-ground storage system". Patent US4890983 A, 17 August 1988.

[46] A. Mustafa and Al-Refai, "Matlab/Simulink Simulation of Solar Energy Storage System," *International Journal of Electrical, Computer, Electronics and Communication Engineering,* vol. 8, no. 2, pp. 293-298, 2014.

[47] M. Sterner, M. Jentsch and U. Holzhammer, "Energiewirtschaftliche und ökologische Bewertung," Fraunhofer IWES, Kassel, 2011.

[48] M. Melaina, O. Antonia and M. Penev, "Blending Hydrogen into Natural Gas Pipeline Networks: A Review of Key Issues," NREL, Golden, CO, 2013.

[49] U. E. I. Administration, "About U.S. Natural Gas Pipelines," 2007.

[50] O. Florisson, "Preparing for the Hydrogen Economy by Using the Existing Natural Gas System as a Catalyst," NaturalHy project Report SES6/CT/2004/502661, 2010.

[51] TGC, "Hawai'i Gas: The clean energy company," The Gas Company, 2012. [Online]. Available: http://www.hawaiigas.com/.

[52] F. Öney, T. Veziroğlu and Z. Dülger, "Evaluation of pipeline Transportation of hydrogen and natural gas mixtures," *International Journal of Hydrogen Energy,* vol. 19, no. 10, pp. 813-822, 1994.

[53] M. Gudorf, *Energy Management,* University of California, Irvine.

[54] D. McLarty, C. Civit Sabaté, J. Brouwer and F. Jabbari, "Micro-grid energy dispatch optimization and predictive control algorithms; A UC Irvine case study," *Elsevier: Electrical Power and Energy Systems,* vol. 65, pp. 179-190, 2015.

[55] B. P. Shaffer, "UCI Microgrid," Advanced Power and Energy Program, Irvine.

[56] A. Jazayeri, "Generating facility interconnection agreement (inadvertent-export). Form 14-745," Southern California Edison, 2012.

[57] B. P. Shaffer and D. Mclarty, "UCI Microgrid, ppt presentation," in *Advanced Power and Energy Program*, Irvine, 2014.

[58] J. B. S. S. Anh-Tuan Vu Do, Performance and Controls of Gas Turbine-Driven Combined with Cooling, Heating, and Power Systems for Economyc Dispatch, University of California, Irvine, 2010.

[59] F. Barbir, "PEM electrolysis for production of hydrogen from renewable energy sources," *Elsevier,* vol. 78, no. Solar Energy, pp. 661-669, 2005.

[60] R. O'hayre, S.-W. Cha, W. Colella and F. B. Prinz, Fuel Cell Fundamentals, New York: John Wiley & Sons, 2009.

[61] T. G. F. Barbir, "Efficiency and economics of proton exchange membrane (PEM) fuel cells," *International Journal of Hydrogen,* vol. 22, no. 10/11, pp. 1027 - 1037, 1997.

[62] F. Gonzatti, V. N. Kuhn, F. Z. Ferrigolo, M. Miotto and F. A. Farret, "Theoretical and practical analysis of the fuel cell integration of an energy storage plant using hydrogen," in *Industry Applications (INDUSCON)*, Juiz de Fora, Brasil, 2014.

[63] "The Engineering Toolbox," [Online]. Available: http://www.engineeringtoolbox.com/heating-values-fuel-gases-d_823.html. [Accessed 22 May 2015].

[64] U. E. P. Agency, "Inventory of U.S. GHG emissions and Sinks: 1990-2011. Annex 2, table A-36 (Methodology for estimating CO_2 emissions from fossil fuel combustion)," Washington, DC.

[65] U.S. Energy Information Administration, [Online]. Available: http://www.eia.gov/tools/faqs/faq.cfm?id=77&t=11. [Accessed 23 July 2015].

[66] U.S. Energy Information Administration, [Online]. Available: http://www.eia.gov/tools/faqs/faq.cfm?id=74&t=11.

[67] NaturalGas.org. [Online]. Available: http://naturalgas.org/overview/uses-electrical/. [Accessed 3 August 2015].

[68] "eGRID 9th edition Version 1.0 Year 2010 Summary Tables," Environmental Protection Agency (EPA), 2014.

[69] U.S. Energy Information Administration, [Online]. Available: http://www.eia.gov/tools/faqs/faq.cfm?id=51&t=8. [Accessed 3 August 2015].

[70] U. E. I. A. (EIA), "Short-term energy outlook; Table 5b : U.S. Regional Natural Gas Prices (Dollars per Thousand Cubic Feet)," U.S. Department of Energy, Washington, D.C., 2015.

[71] "California Renewables Portfolio Standard (RPS)".

[72] J. Hüttenrauch and G. Müller-Syring, "Zumischung von Wasserstoff zum Erdgas," *Energie Wasser-Praxis,* vol. 61, no. 10, pp. 68-71, 2010.

[73] J. Worf, Metal Hydrides, 7 ed., vol. 11, M. E. o. S. &. Technology, Ed., New York: McGraw-Hill, 1992.

[74] M. Au, C. Chen, Z. Ye, T. Fong, J. Wu and O. Wang, "AThe Recovery, Purification, Storage and Transport of Hydrogen Separated from Industrial Purge Gas by Means of Mobile Hydride Containers," *International Journal of Energy,* vol. 12, no. 1, pp. 33-37, 1996.

[75] S. G. C. AB, "Basic data on Biogas," Malmö, Sweden, 2012.